

8. Applications



How use ICA and other BSS methods?

Panorama of selected applications

IC relevance: Hyperspectral images

Priors and independent subspace: ECG extraction

Nonlinear mixtures: chemical sensor array and scanned images



8.1. Introduction

What applications ?

- Biomedical signals : EEG, ECG, MEG, RMIf
 - techniques non invasives, localisation, élimination d'artefacts
- Communications et antenna processing
 - sonar, radar, mobile phones,
- Monitoring
- Parsimonial images coding
- Classification
- Smart sensor design



8.1. Introduction.

How to use ICA...?

- ICA is now a usual method for solving blind source separation problems
- ICA is an estimation method, which requires:
 - a separating model, suitable to the mixing model,
 - an independence criterion,
 - an optimisation algorithm.
- When running ICA algorithm, one obtains a solution, which is the best one under the above constraints.

Are the Independent Components (IC) relevant ?



8.1. Introduction

How to use ICA...?

- Relevance requires:
 - a good model,
 - the sources satisfy the independence assumption,
 - the optimisation algorithm does not stop in a bad local minima.
- With actual problems, basically, the relevance is not sure since:
 - the model is often an approximation of the physical system
 - we don't know the sources (and their number), consequently source independence assumption is not sure



8.1. Introduction.

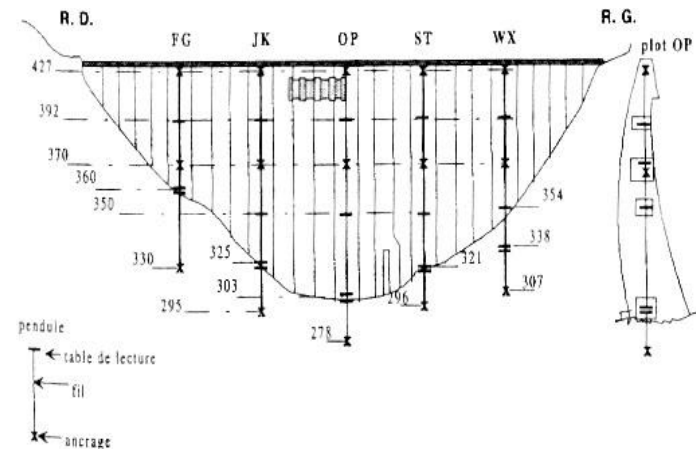
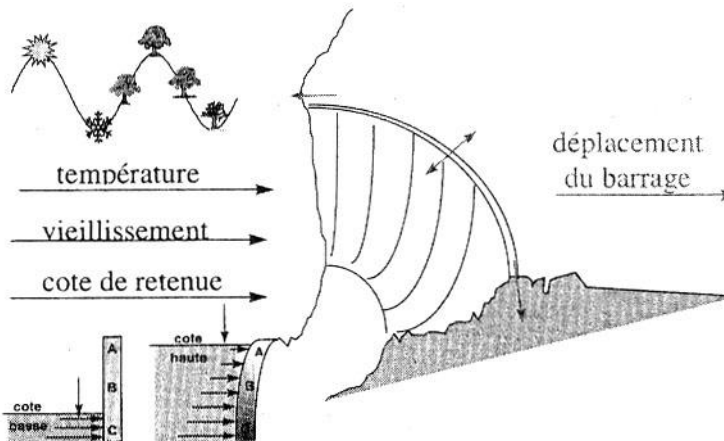
How to use ICA and beyond ?

- **All possible priors have to be used**
 - Positivity, sparsity, temporal dependance, periodicity or cyclostationnarity, discrete-valued data, etc.
 - Priors can lead to better criteria than independence
- **Careful modelization of observations, i.e. of how the physical system provides the observations**
 - Modelization leads to a mixing model, and hence to a suited model of separating structure
 - Modelization is important for showing what should be the estimated sources
 - Physics of the system is important for component interpretation
- **Choose the best representation domain for applying BSS**

8.2. A few examples

8.2.1. Dam monitoring

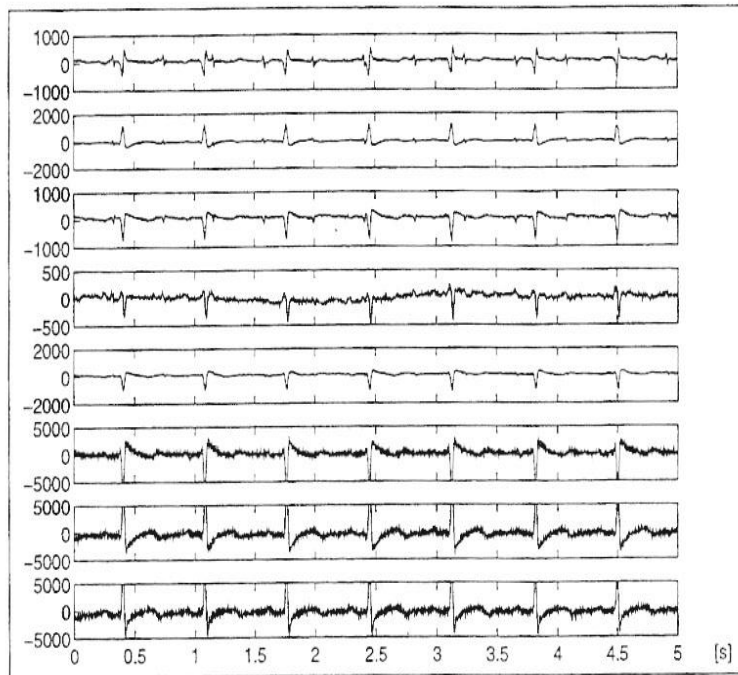
- The dam wall moves according to the water level, the temperature, etc.
- Simple pendular are hung on the wall, at different locations: the pendular deviations measure the wall motions, with different sensitivities for the water level or the temperature, etc.



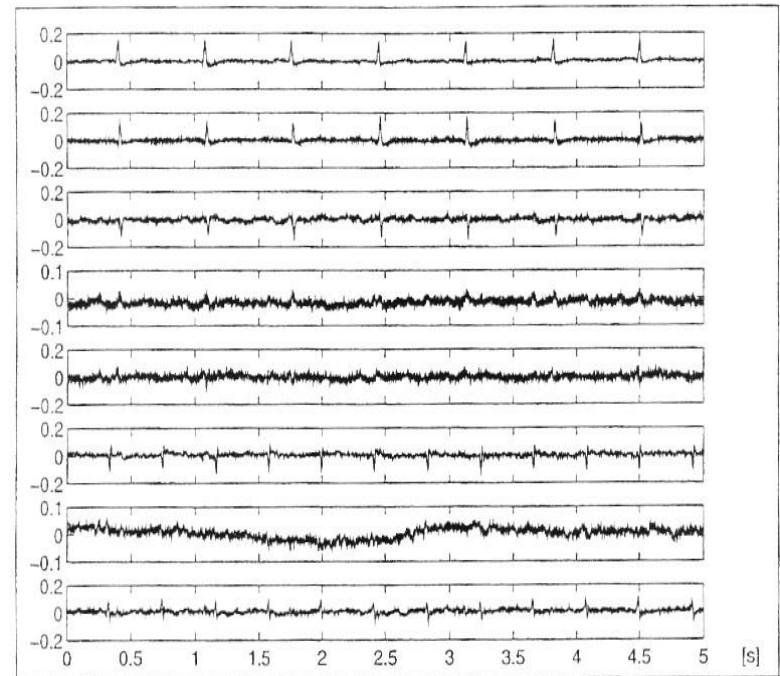
G. d'Urso *et al.*, Modélisation des déplacements de barrages, GRETSI 1997, Grenoble (France), 215-218.

A few examples

8.2.2. Fetal ECG Extraction



Observations

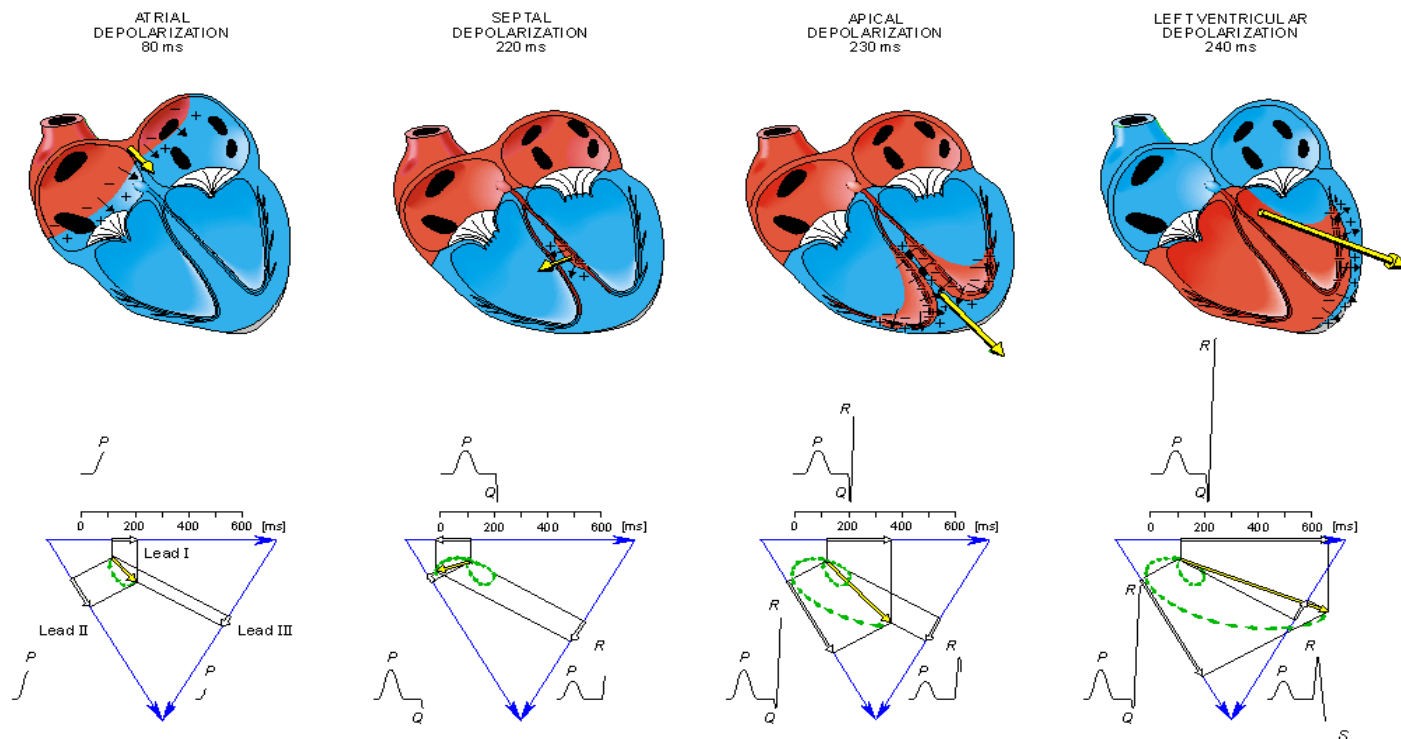


estimated sources

- L. De Lathauwer, B. De Moor, J. Vanderwalle, Fetal electrocardiogram extraction by blind subspace separation, IEEE Trans. on BME, 47(5):567-572, 2000
- V. Zarsoso et al., IEEE Trans. on BME, 2003 (?)
- Current works on ICA, ECG and VCG: R. Sameni, M. Shamsollahi, C. Jutten

Noninvasive extraction of fECG: The electrical heart activity

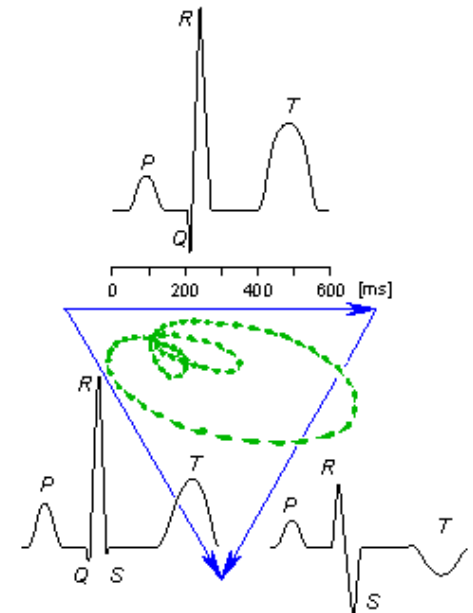
The contraction of the heart muscle is due to the periodic stimulation of the cardiac nervous system.



Noninvasive extraction of fECG:

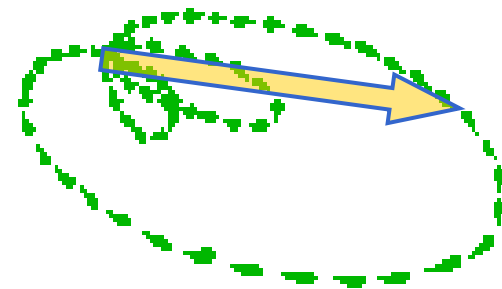
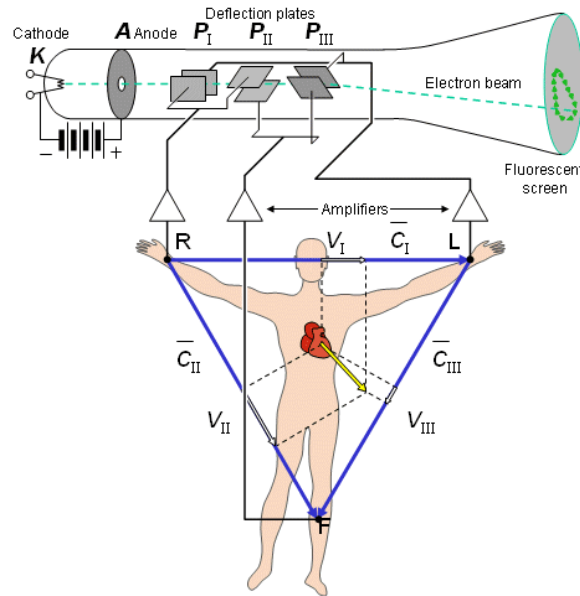
What is the ECG ?

- The Electrocardiogram (ECG) is the overall electrical activity of the heart recorded from the body surface.



Noninvasive extraction of fECG: What is the VCG ?

- The **V**ector**c**ardiogram (VCG) is a 3-D representation of 3 orthogonal ECG leads.

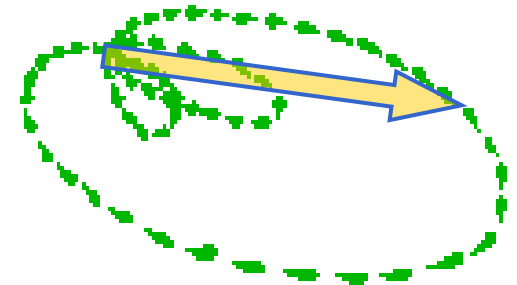


*VCG under single
dipole assumption*

Noninvasive extraction of fECG:

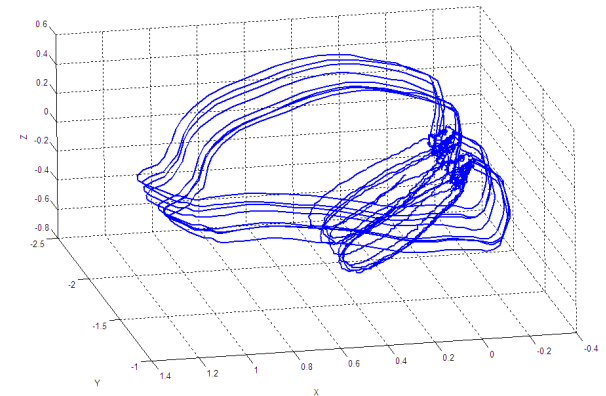
What is the VCG ?

- The VCG loop is a phase representation of the ECG signal.
- The **orientation**, **surface**, and **angles** between the VCG loop components convey physiological information.
- ECG noises cause the VCG loop **become noisy** around its mean, **move**, **rotate**, or **scale**.



Noninvasive extraction of fECG: VCG facts

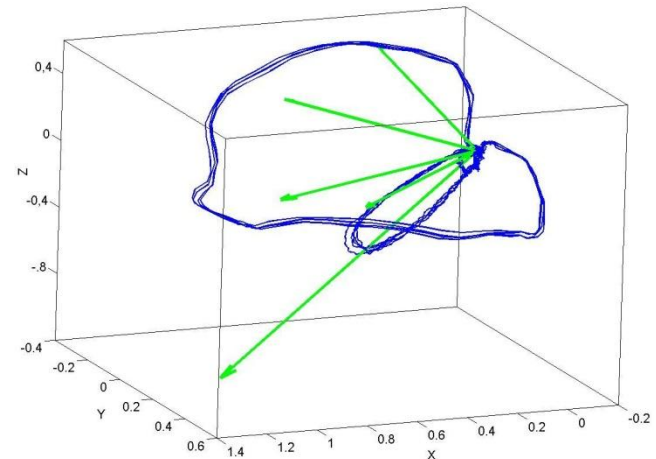
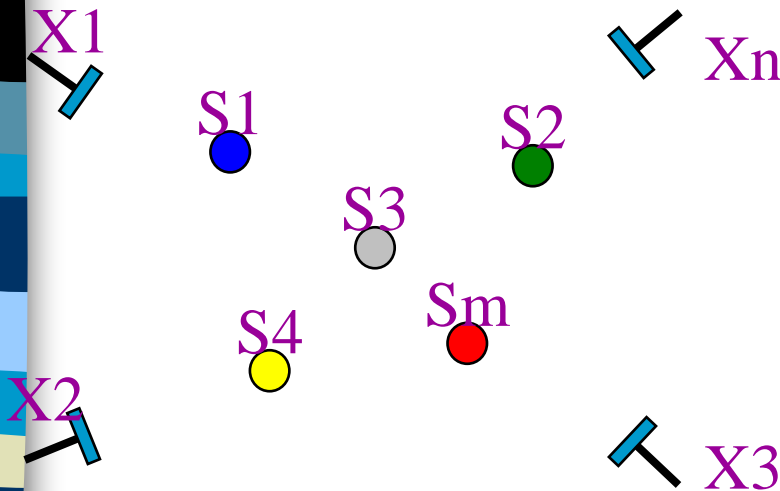
- The VCG loop may be assumed as a quasi-periodic loop.
- The VCG loop is very sparse.
- The VCG is not symmetric around its mean.
- The mean of the VCG representation is not equal to the **isoelectric** point of the VCG.



All these remarks cause problems in estimating relevant ICs.

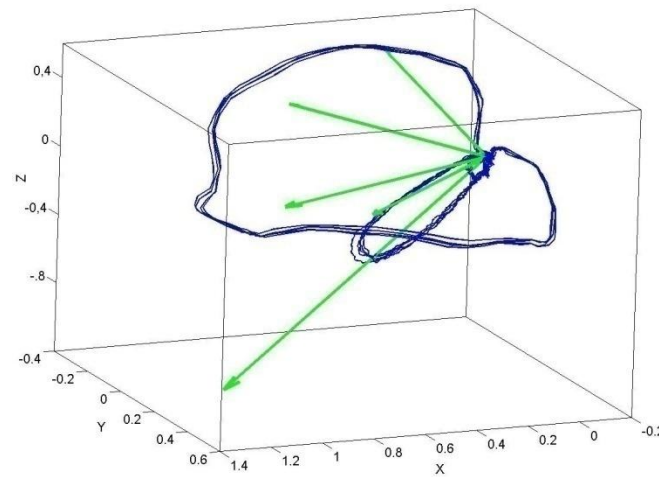
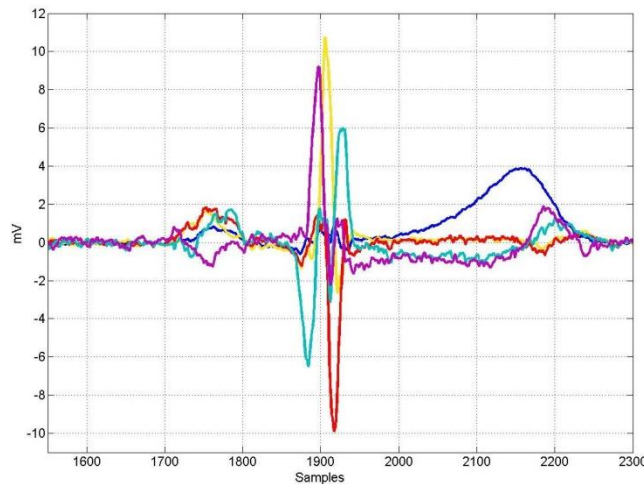
Noninvasive extraction of fECG: Applying ICA

- There are evidences that linear mixture holds in first approximation. We can use simple ICA...
- The VCG loop representation of the ECG can be used for the study and interpretation of the ICs extracted from ECG signals.



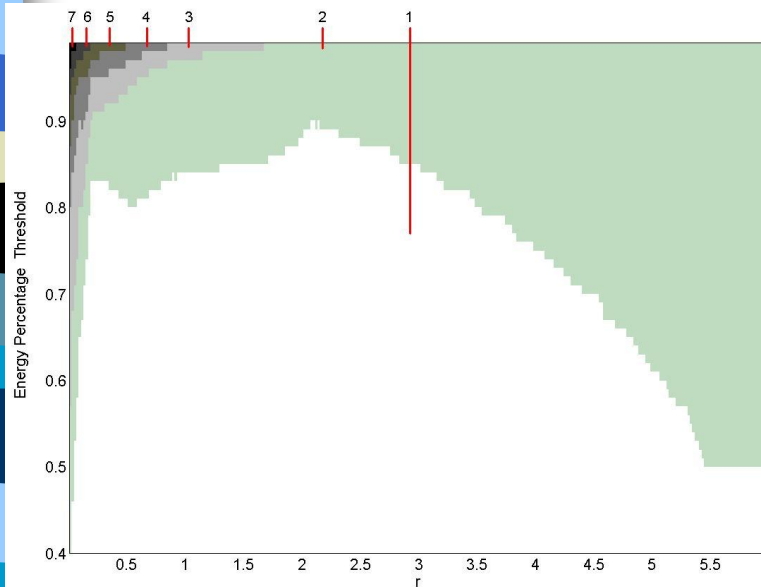
Noninvasive extraction of fECG: ECG dimensionality

- From the VCG representation, we can assume ECG dimensionality is equal to 3, *i.e.* 3 ICs. In fact, **these ICs are not independent !**
- Previous works (De Lathauwer *et al.*, Zarsoso *et al.*) claimed 3 for mother ECG and 1 or 2 for fetal ECG on the DAISY database.
- Experimentally (MIT-BIH PTB), adult ECG signals have 5-6 dim., meaning that up to 5-6 robust ICs can be extracted from these signals.

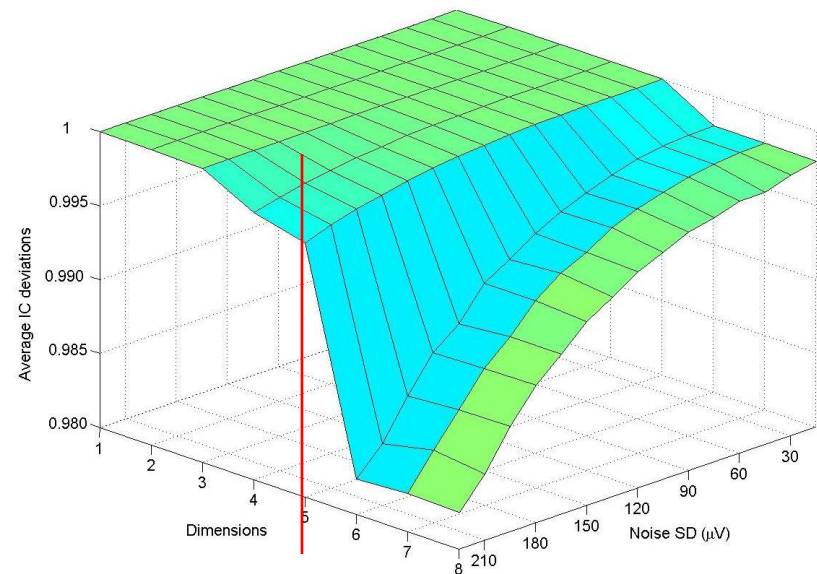


Noninvasive extraction of fECG: ECG dimensionality

Looking for energy preservation and reliability of ICs



**Required dimensions for
signal power preservation**

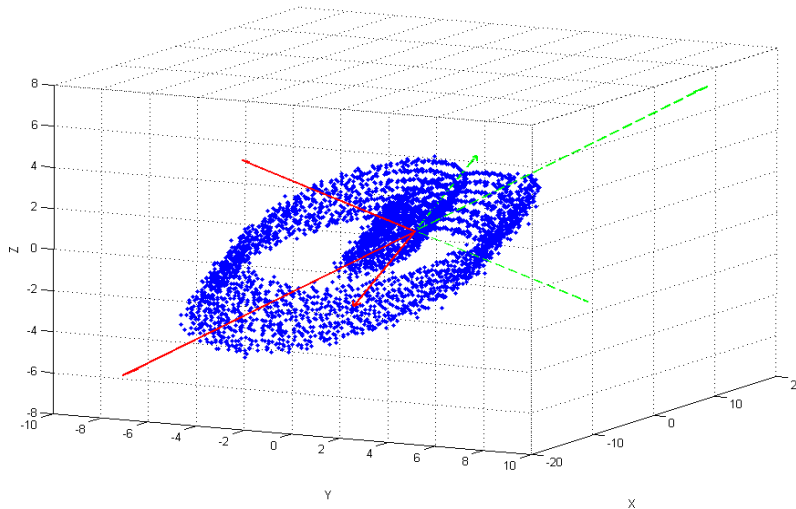


**Robustness of ICs to
noise**

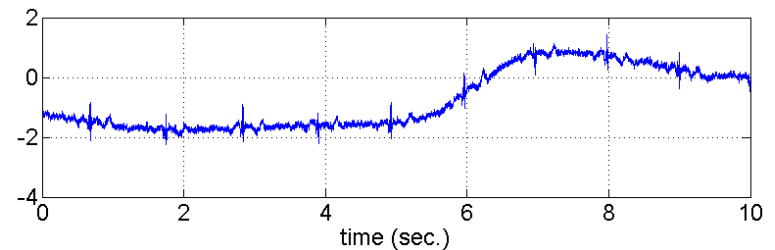
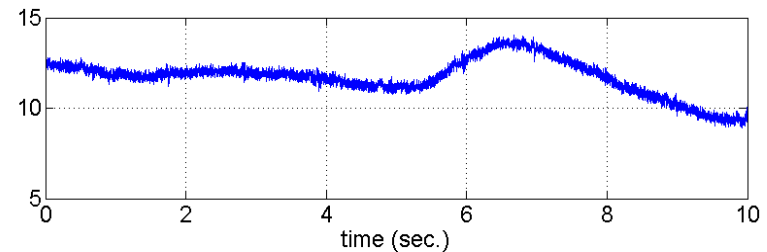
Noninvasive extraction of fECG:

Importance of baseline-wander removal

- Baseline wander is due, for instance, to impedance changes with respiration. It implies low frequency superposition to the ECG signal and shift in the VCG loop.



Synthetic VCG loop

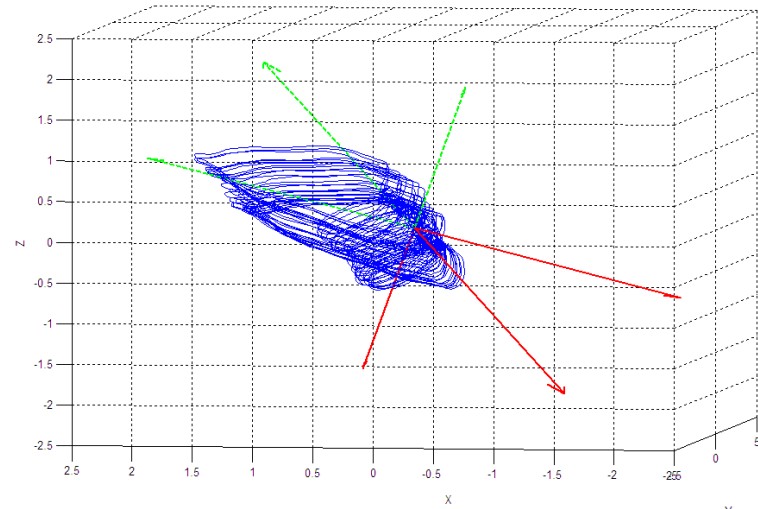


ICs / 2 diff. b.-w. directions

Noninvasive extraction of fECG:

Importance of baseline-wander removal

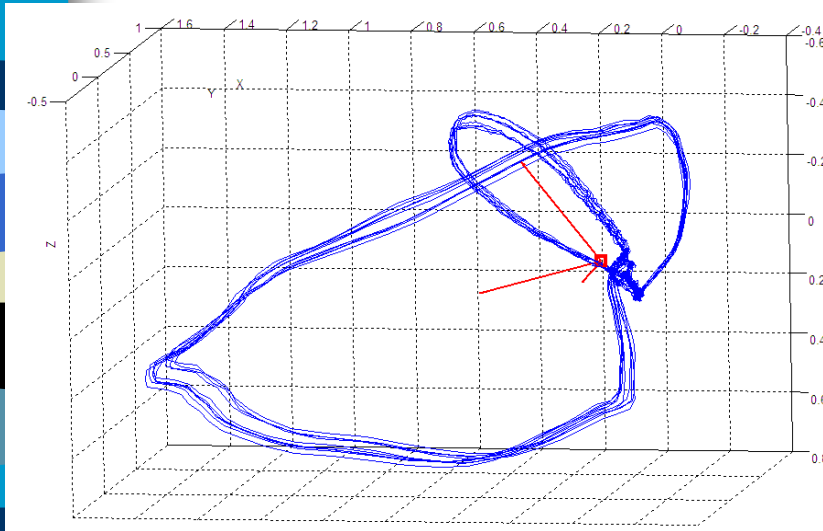
- ICs are very sensitive to the reference point (isoelectric point).
- Estimation of this point requires an accurate baseline-wander removal.
- A wrong reference point leads to wrong ICs.



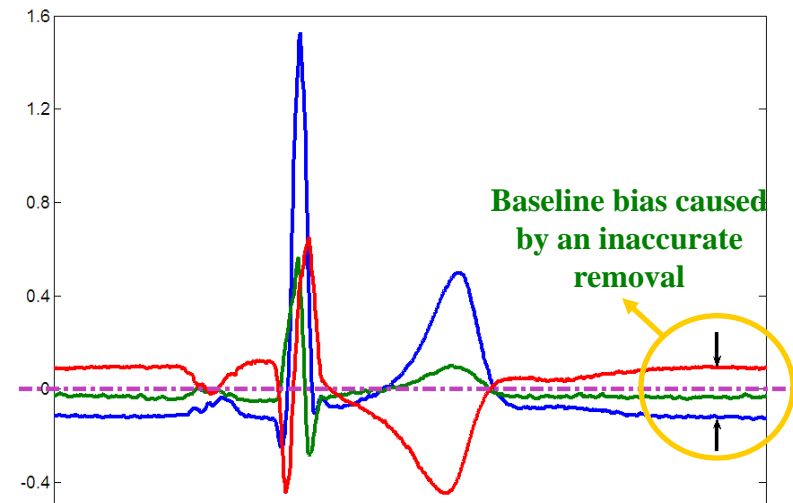
Typical VCG loop

Noninvasive extraction of fECG:

Importance of baseline-wander removal



Typical VCG loop
(DAISY)

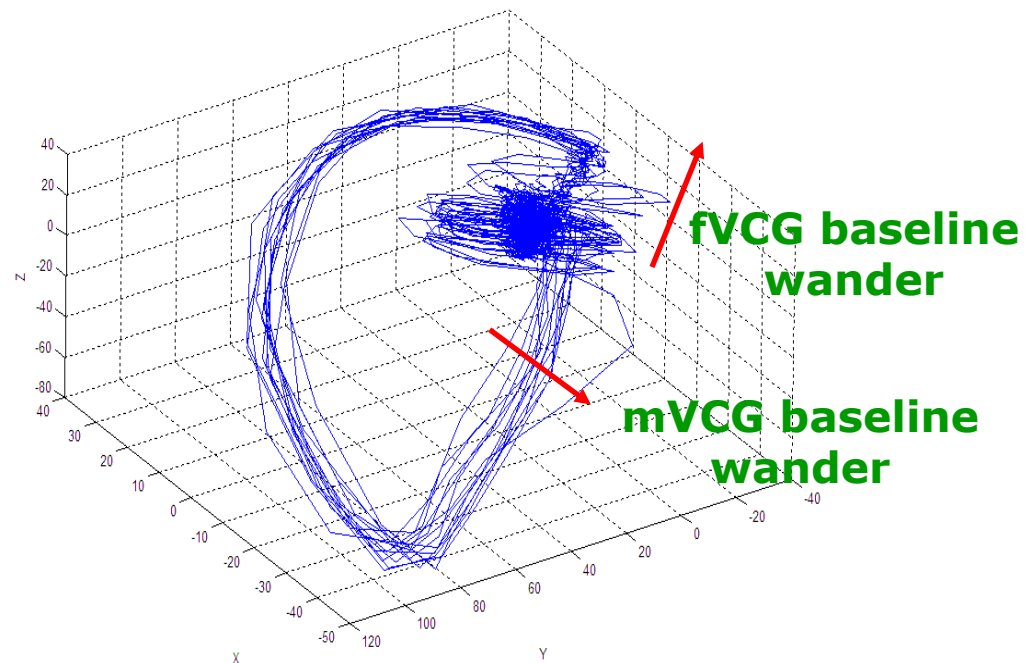


ICs with poor ref. point

Noninvasive extraction of fECG:

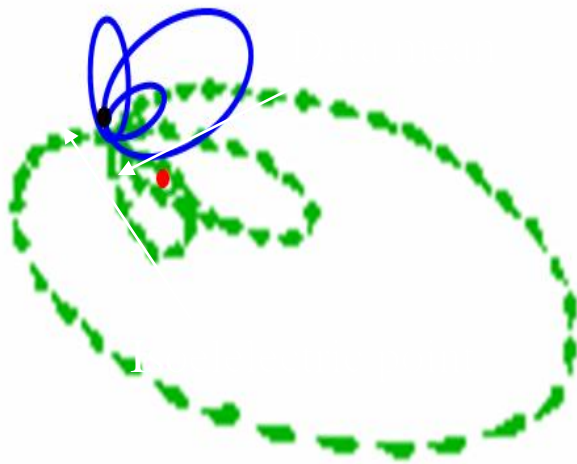
Importance of baseline-wander removal

- ICs are very sensitive to the reference point (isoelectric point).
- This is especially true for estimating ICs related to the fECG, since the fVCG loop is very small.

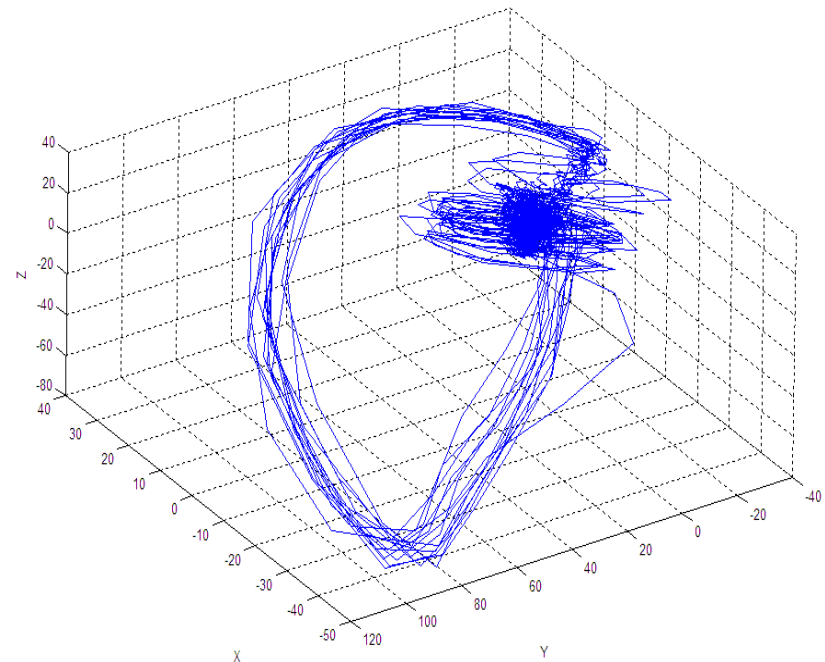


Noninvasive extraction of fECG: Importance of baseline-wander removal

Fetus VCG loop



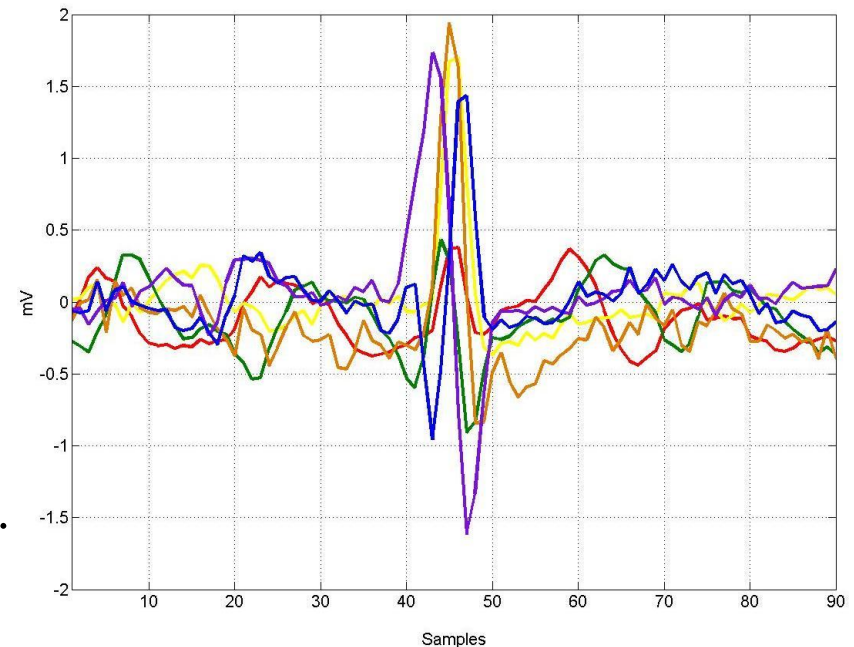
Mother VCG loop



Noninvasive extraction of fECG:

Importance of baseline-wander removal

- **Experiment:** on DAISY database, with accurate baseline-wander removal and isoelectric point estimation one recovers 4 ICs for mECG, 2 for fECG and 2 for noise (?).
- **Assumption:** according to relative positions, fECG components could be hidden in the mother components.
- **In fact,** after synchronisation on R-peaks of fECG and synchronous averaging of all ICs, one can find 6 fetal ICs !



8.2.3. Artefacts removal in MEG (1/2)

R. Vigário, E. Oja / Neural Networks 13 (2000) 891–907

897

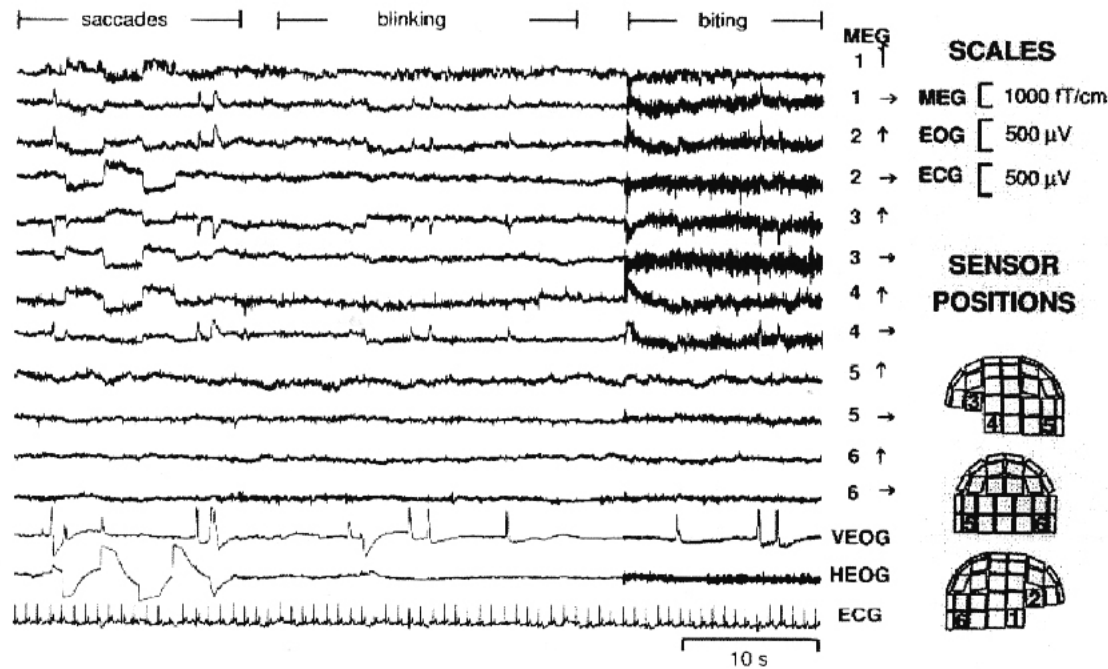


Fig. 6. A subset of 12 spontaneous MEG signals from the frontal, temporal and occipital areas. The data contain several types of artifacts, including ocular and muscle activity, the cardiac cycle, and environmental magnetic disturbances. Adapted from Vigário, Jousmäki et al. (1998).

8.2. A few examples

8.2. 3. Artefacts removal in MEG (2/2)

898

R. Vigário, E. Oja / Neural Networks 13 (2000) 891–907

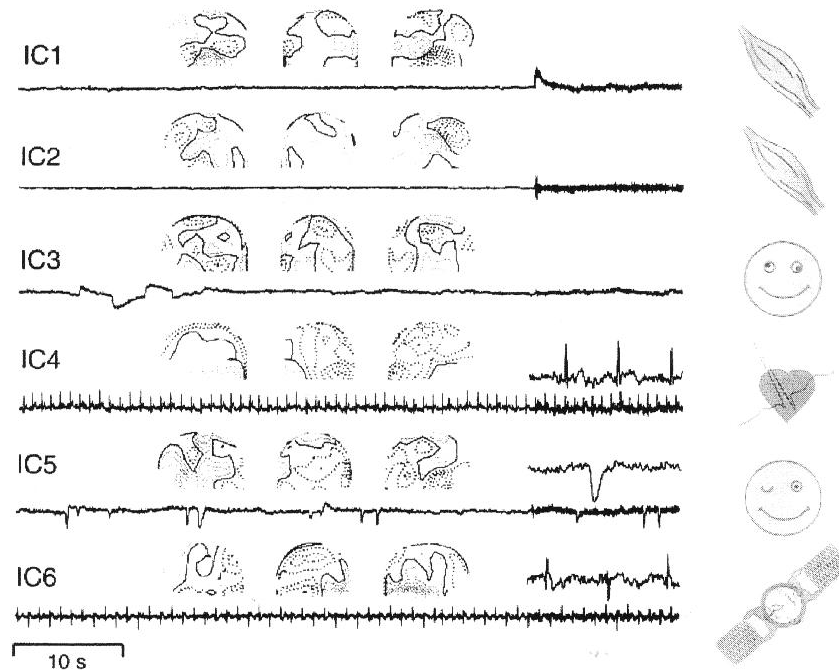


Fig. 7. Artifacts found from MEG data, using the FastICA algorithm. Three views of the field patterns generated by each independent component are plotted on top of the respective signal. Full lines correspond to magnetic flux exiting the head, whereas the dashed lines correspond to the flux inwards. Adapted from Vigário, Jousmäki et al. (1998).

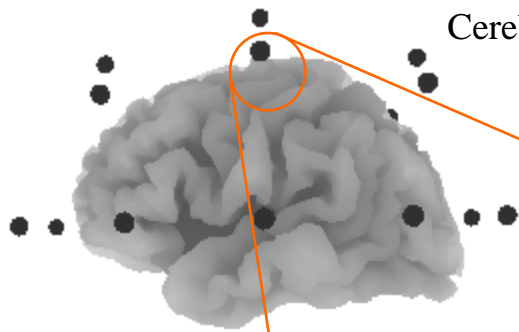


8.2. A few examples

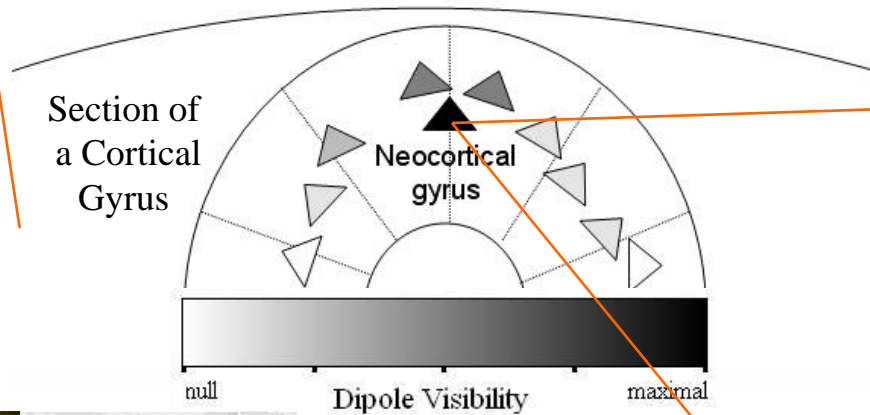
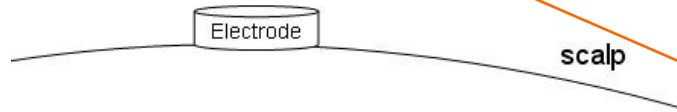
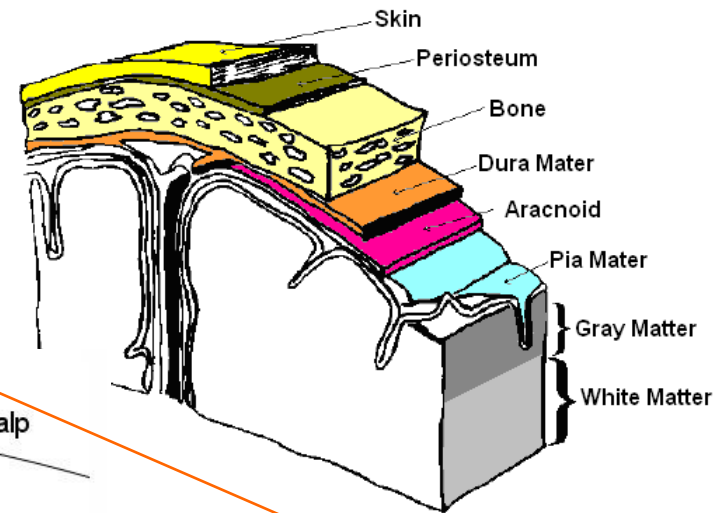
8.2. 4. EEG spatial filtering with ICA...

- EEG processing, in different frequency bands
- Preprocessing for providing features in BCI

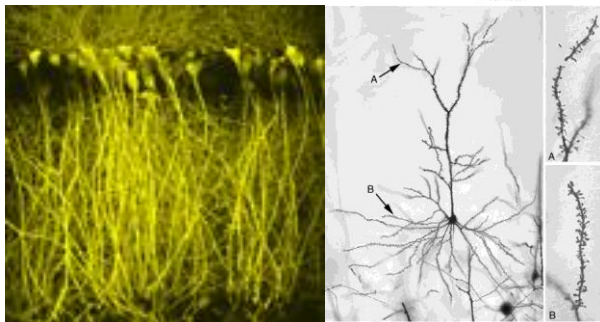
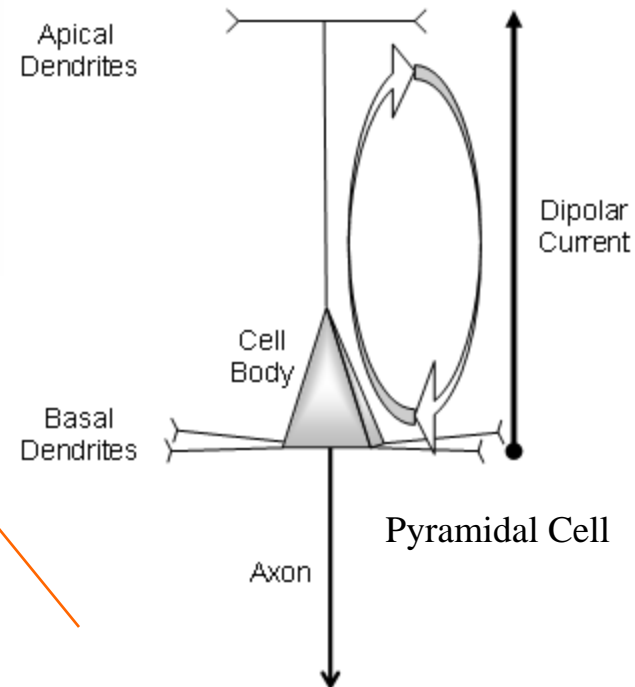
Slides designed by Dr. Cédric Gouy-Pailler, PhD in BCI, GIPSA-lab, Grenoble, October 2009



Cerebral Cortex

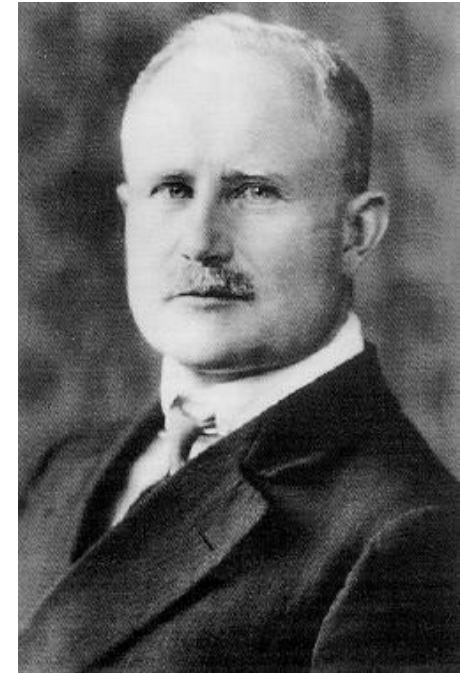
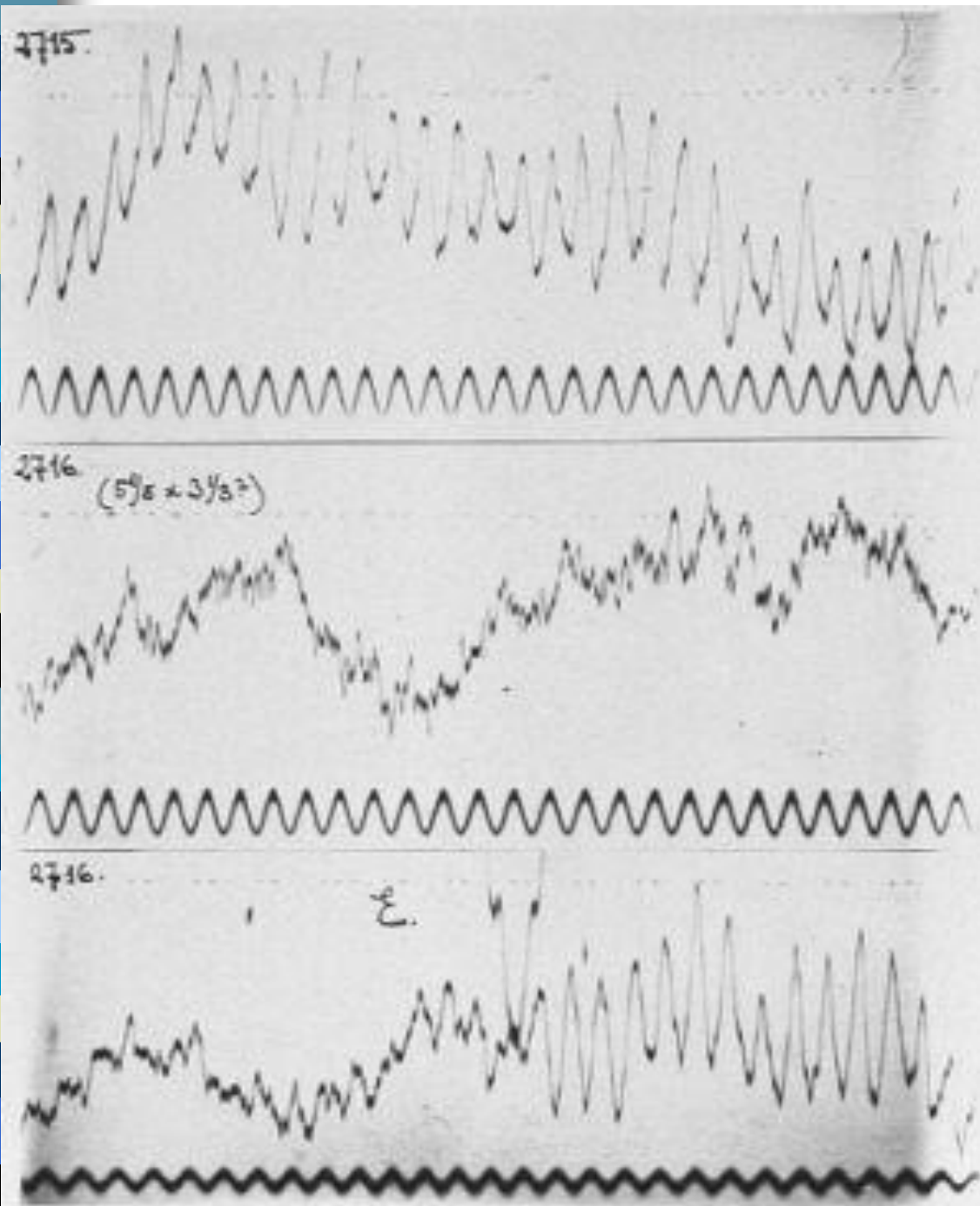


Section of a Cortical Gyrus



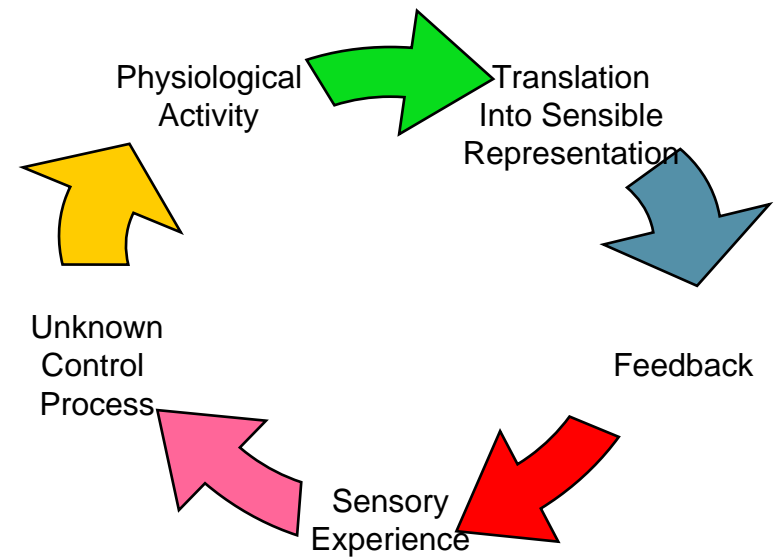
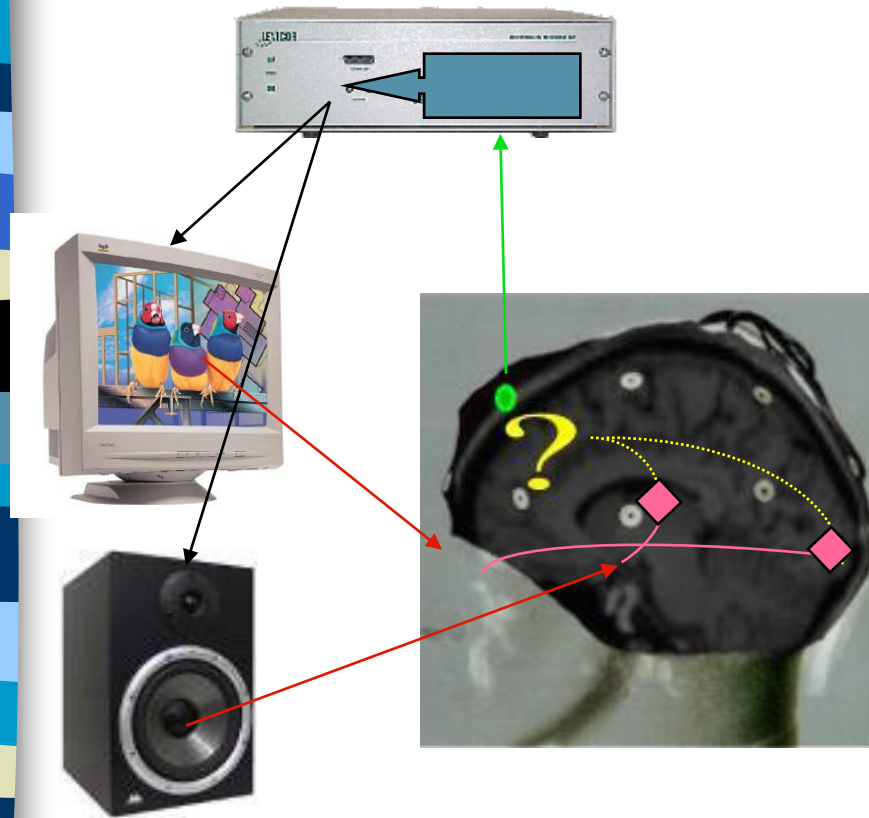
Pyramidal cell assembly in the hippocampus

Pyramidal cell



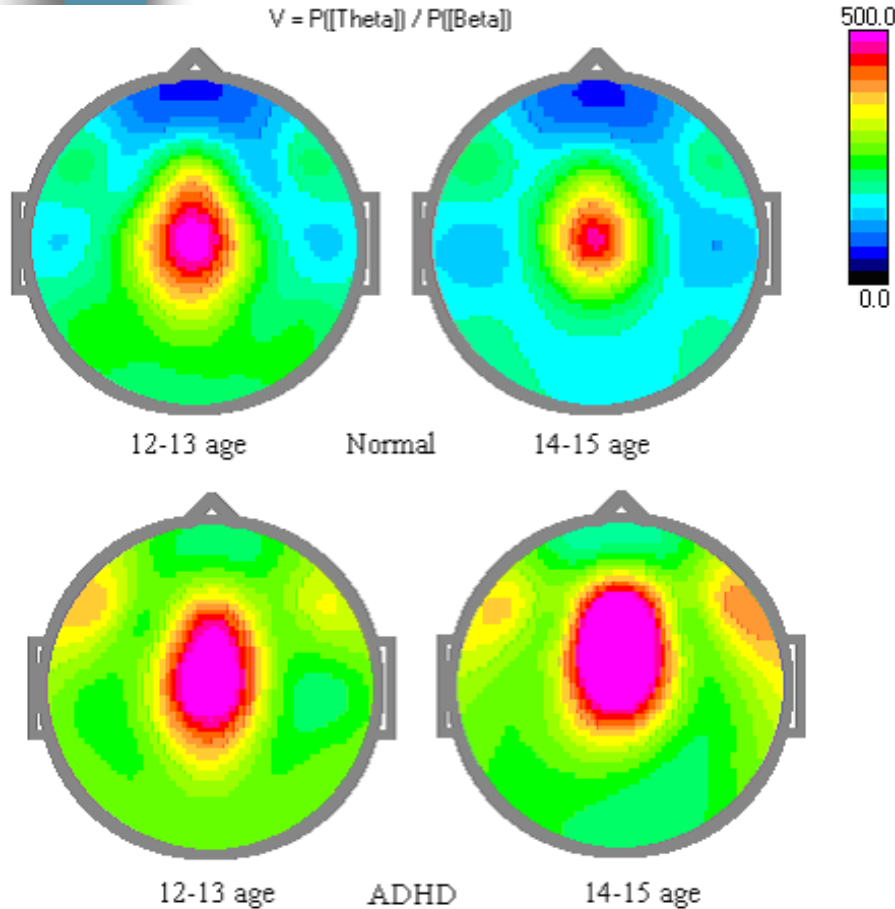
Hans Berger
(1928)

Neurofeedback



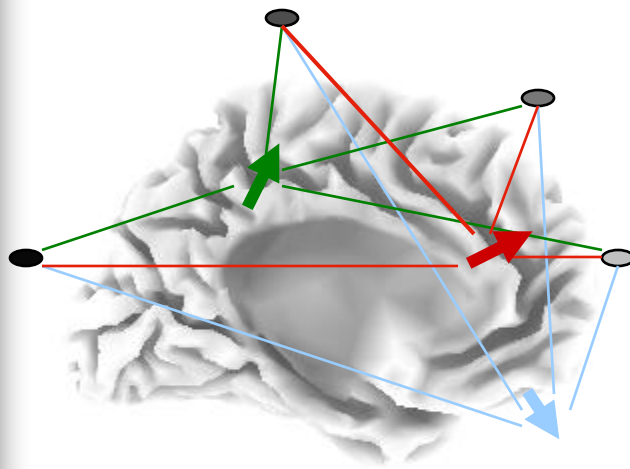
Example of clinical Application: the Theta/Beta power ratio as inattention index

$$V = P[\text{Theta}] / P[\text{Beta}]$$



- The maps of theta/beta ratio in normal children (N=64 and 63).
- Increase of this ratio in ADHD children (N=20 and 10).

Independent Component Analysis for EEG



Input (\mathbf{x}): sensor measurements ● ● ● ●

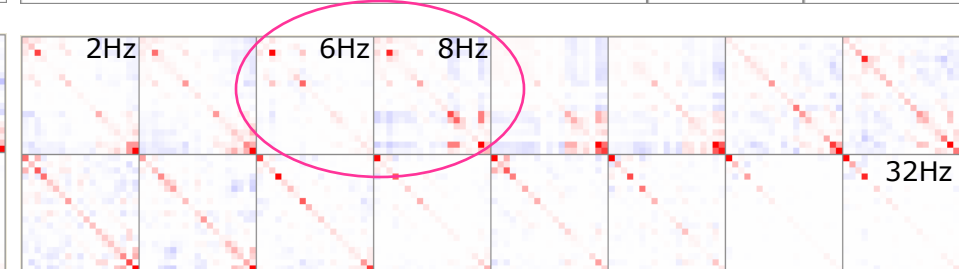
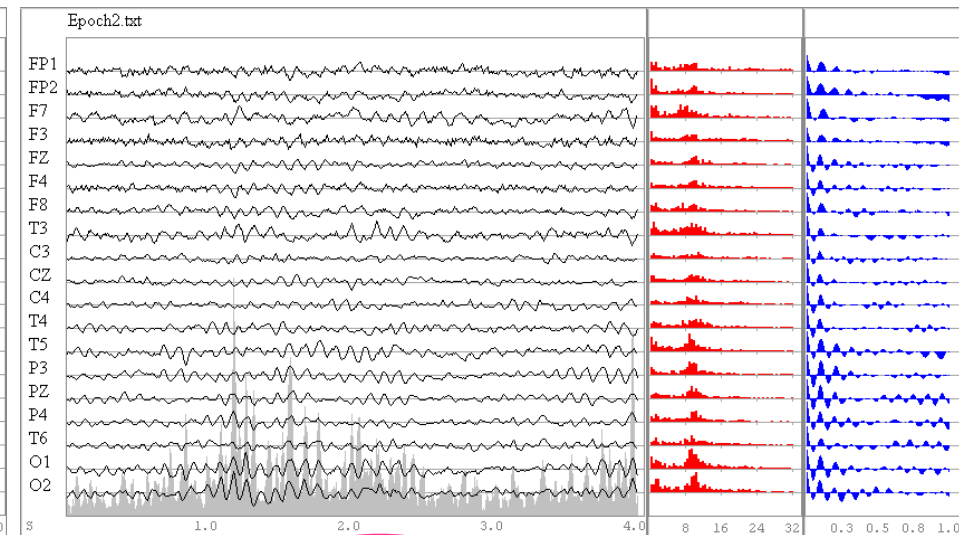
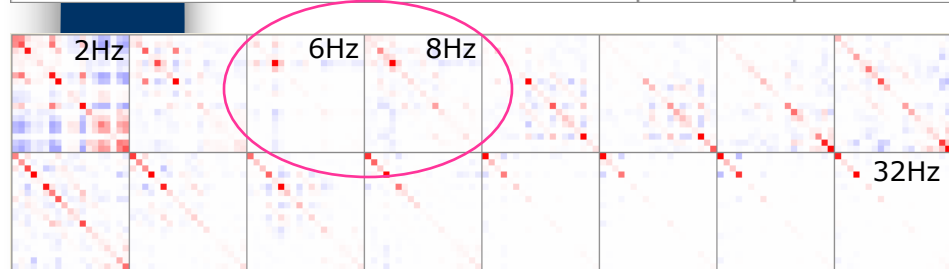
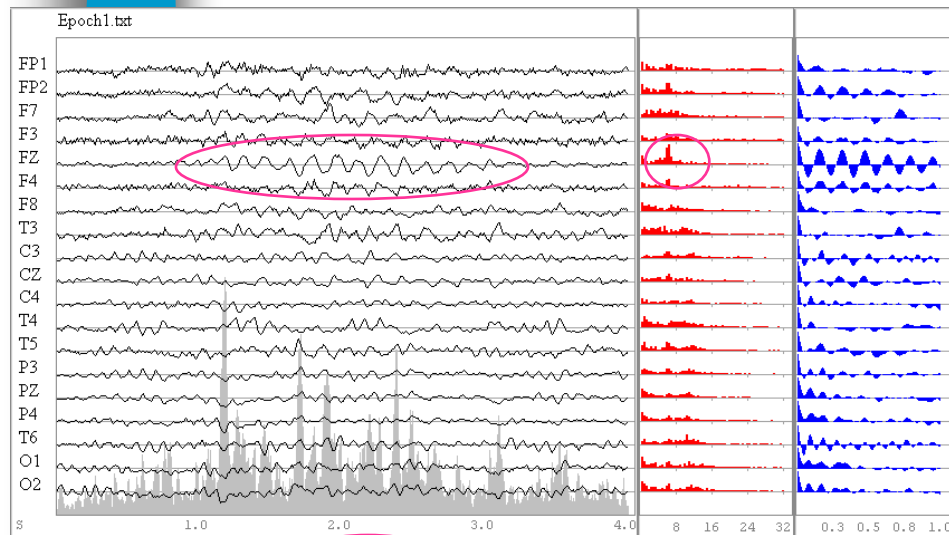
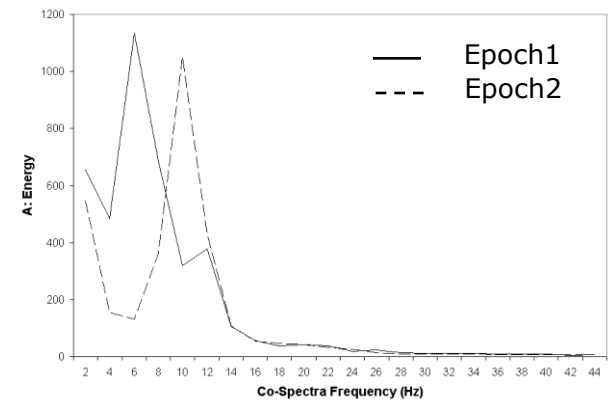
Seek Maximal « Independence »

Output (\mathbf{s}): source dipolar fields   

Linear Instantaneous Model

$$\mathbf{x}(t) = \mathbf{A}\mathbf{s}(t)$$

ICA by Approximate Joint Diagonalization

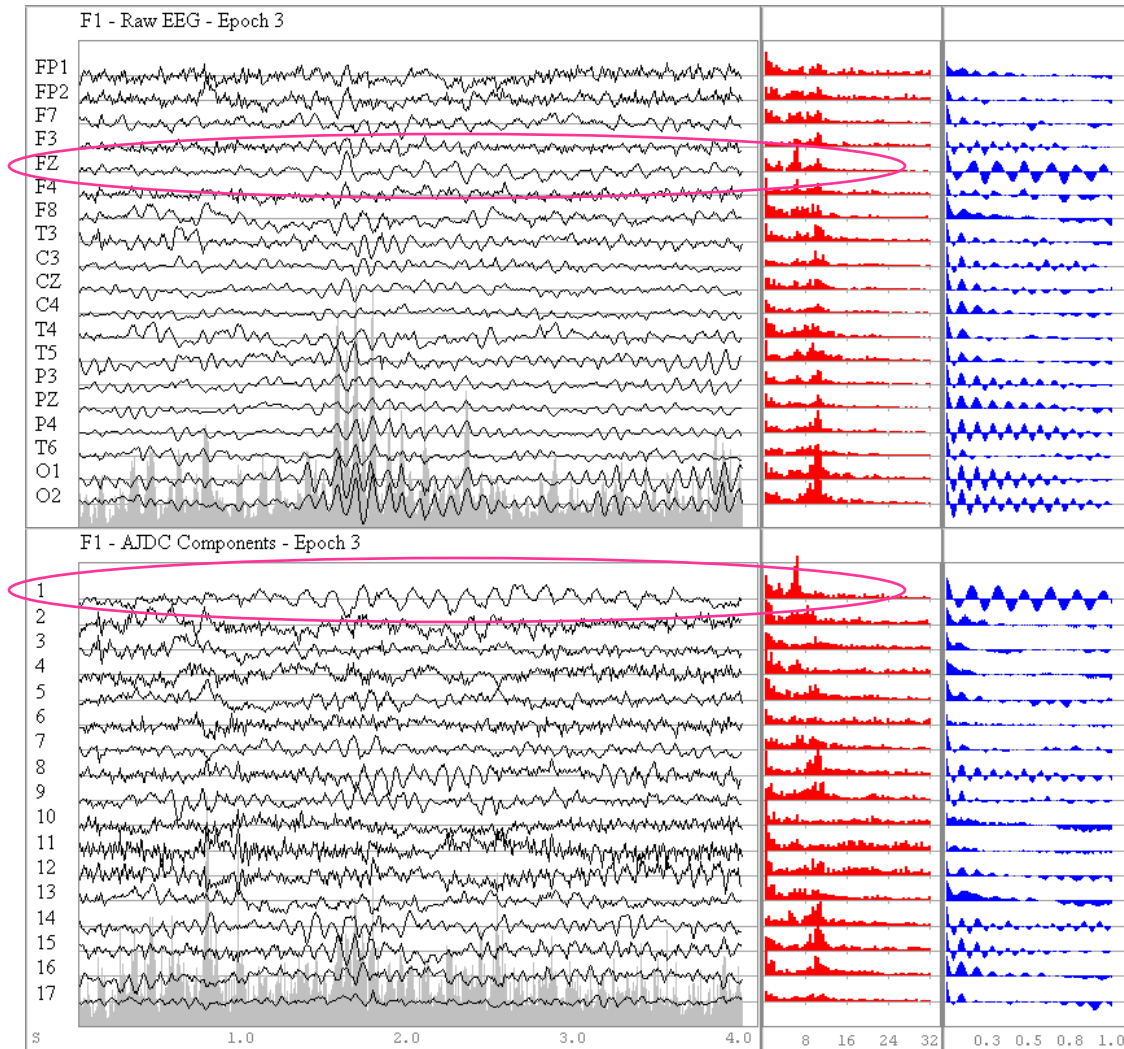


16 y.o. female with a diagnosis of ADHD (attention deficit hyperactivity disorder)

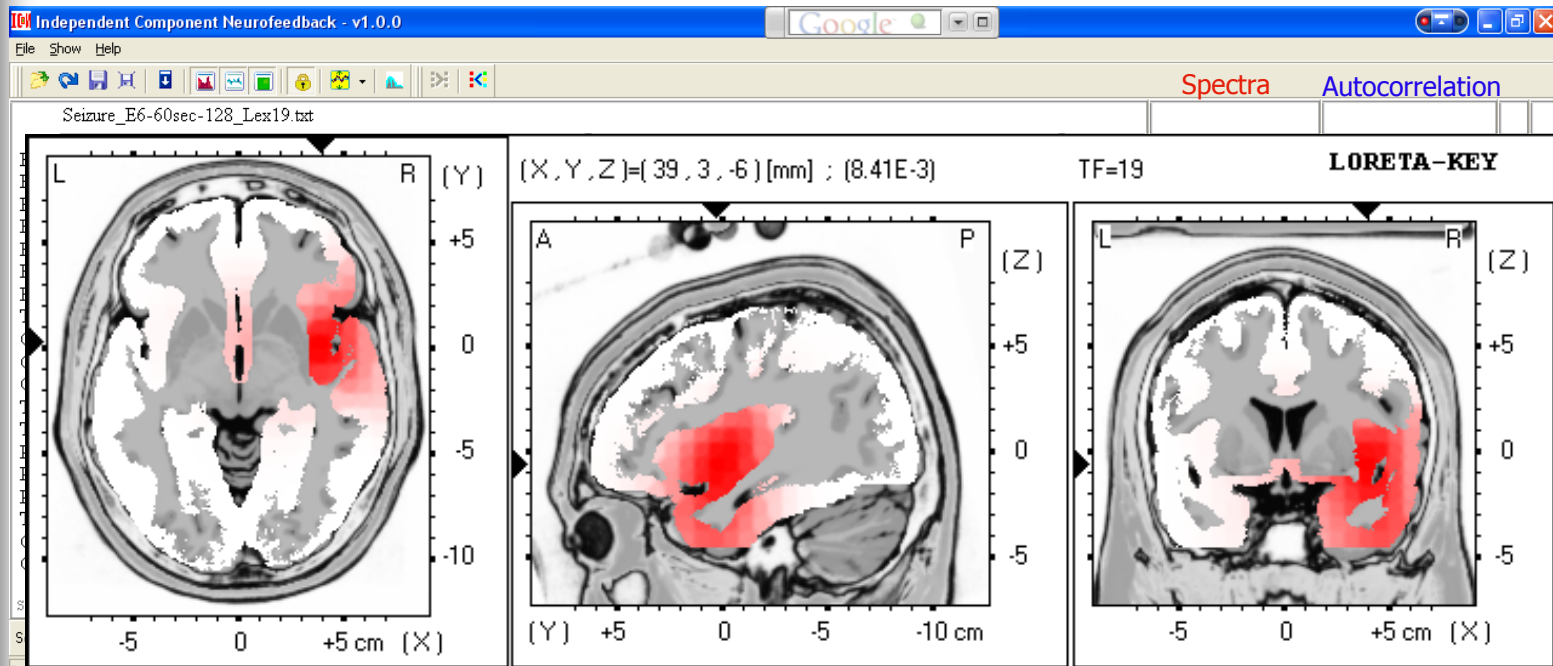
Extraction of Frontal Theta Rhythm from an unknown epoch

Mixture of Theta and Alpha at CZ

Extracted Theta Source



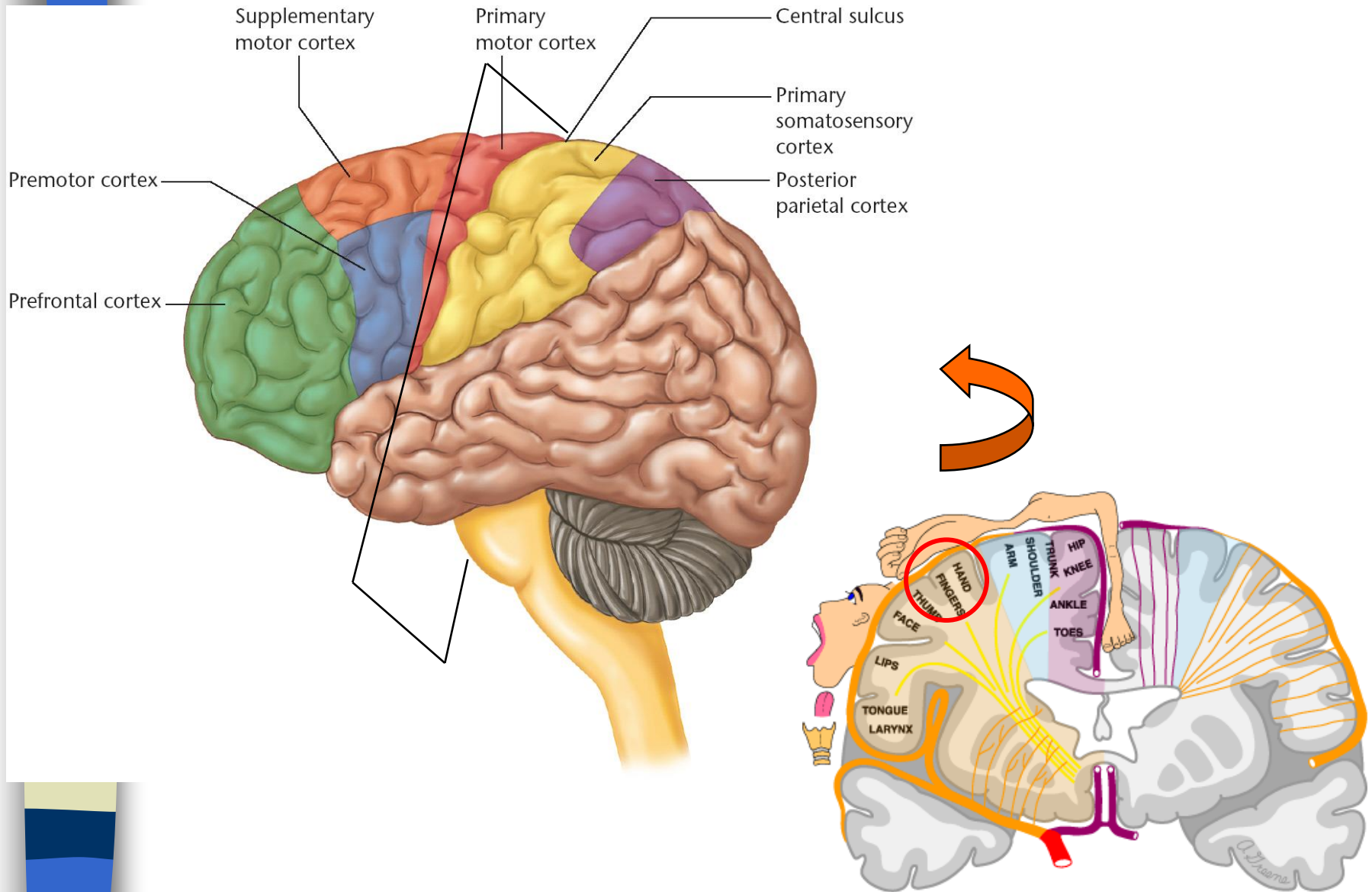
Male 34 y.o. Epileptic Patient



localization of the 19th mixing component

(x=39; y=3, z=-6), BA 13, Right Temporal lobe, Insula

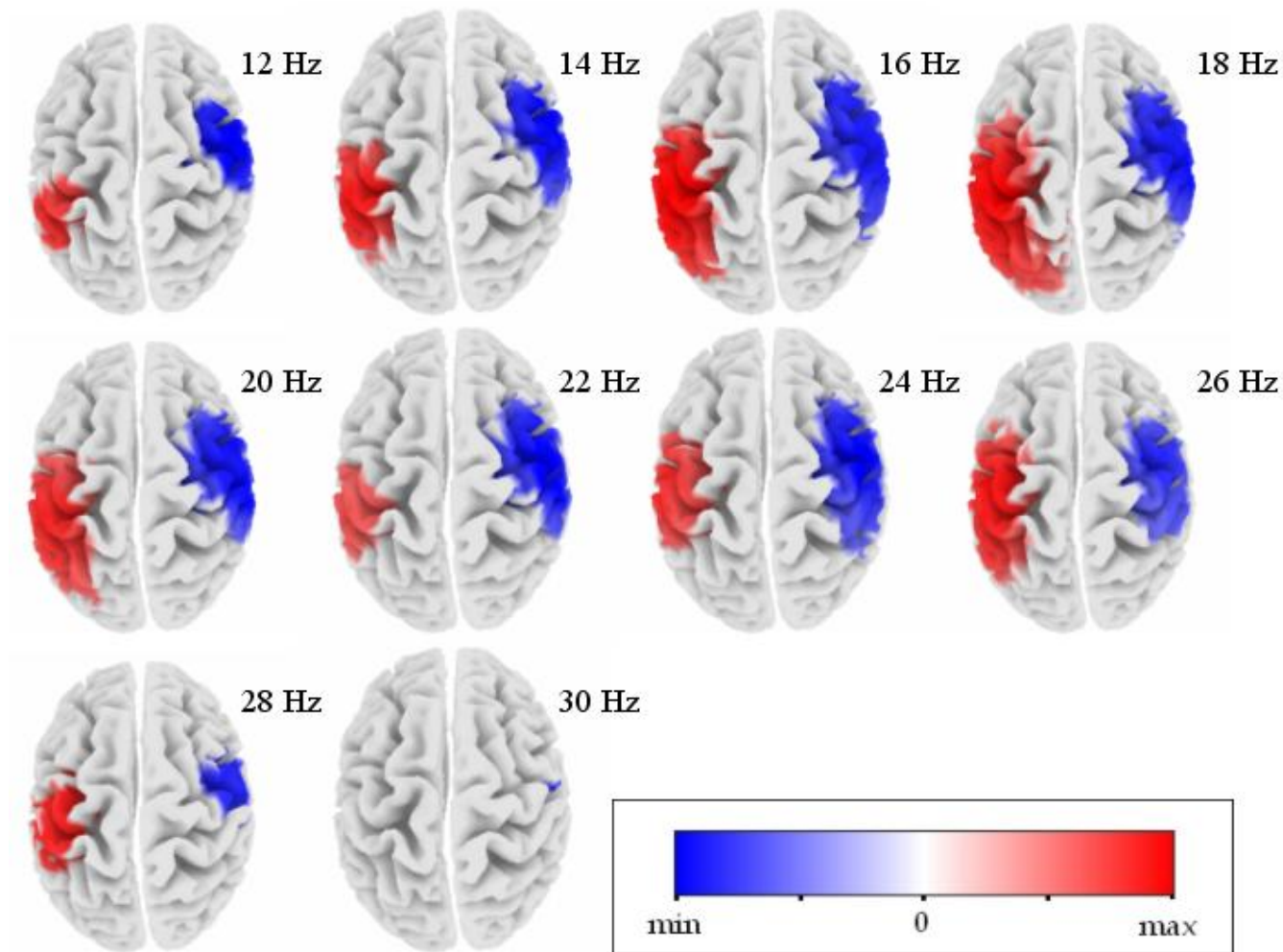
Brain-Computer Interface



The Motor "Homunculus"



Inverse solution

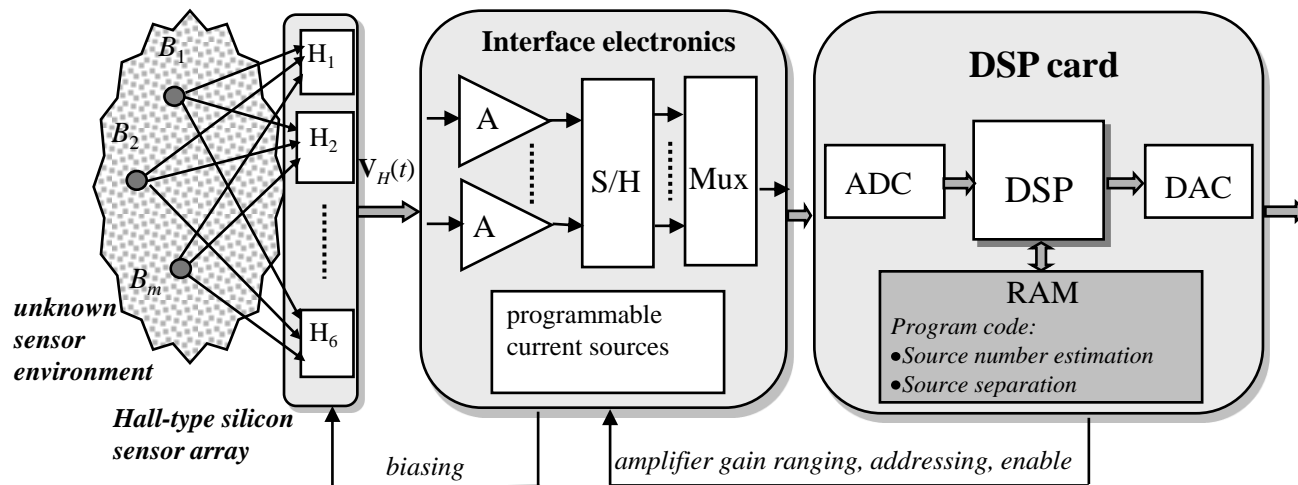


T-tests of Left vs. Right Finger Movement Intention
(N= 159 Left Fingers trials + 157 Right Fingers trials.)

8.2. A few examples

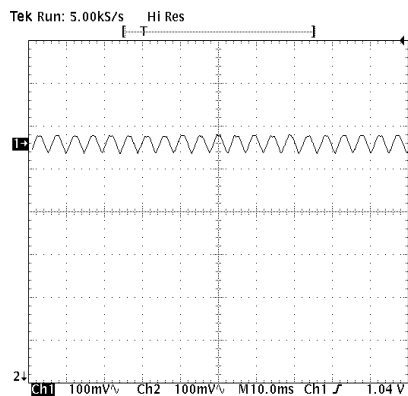
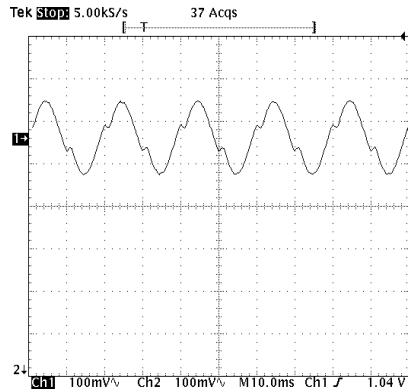
8.2. 5. Smart sensor arrays (1/2)

- Smart sensor arrays based on low cost sensors
 - unknown source number: it must be estimated,
 - sensors are very close ($200\text{ }\mu\text{m}$): very weak spatial diversity(Paraschiv-Ionescu, Jutten, Bouvier, *IEEE Sensors Journal*, Dec. 2002)

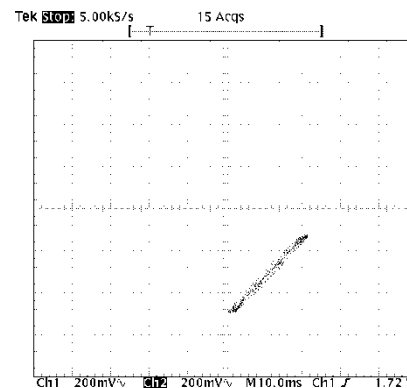
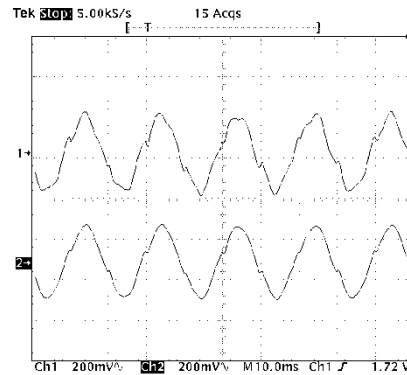


8.2. A few examples

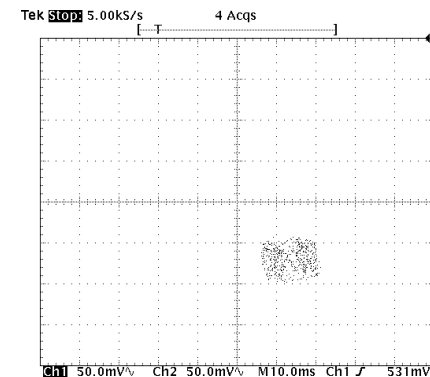
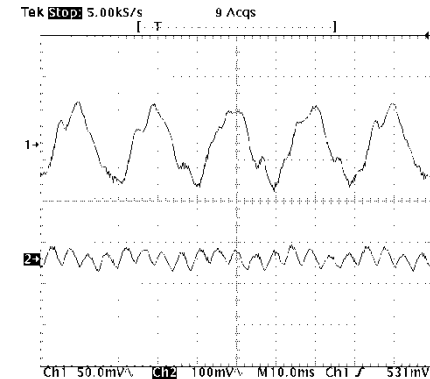
8.2.5. Smart sensor arrays (2/2)



Sources



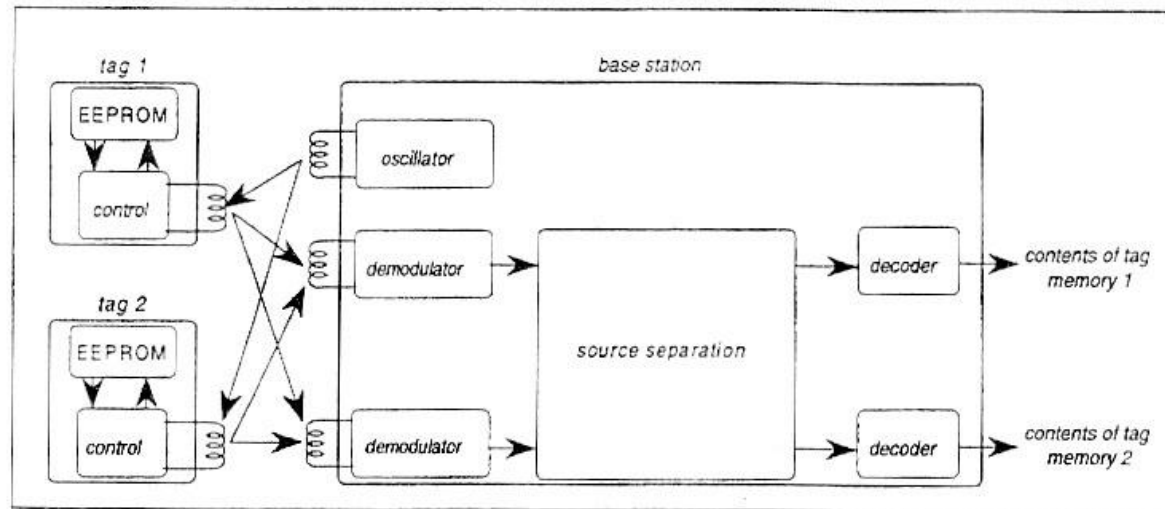
Mixtures



Estimated sources

8.2. A few examples

8.2.6. Multi-user access control



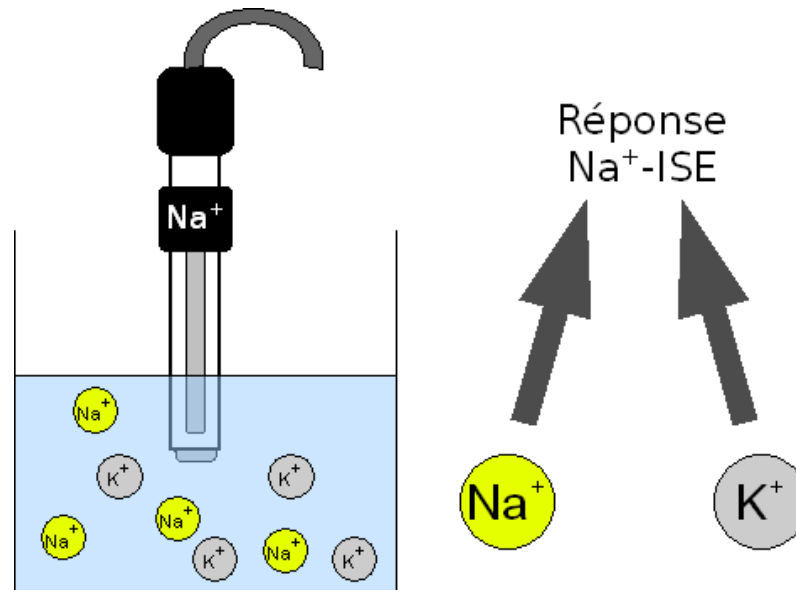
Y. Deville, L. Andry, Application of blind source separation techniques for multi-tag contactless identification systems (NOLTA 95; IEICE Trans. On Fundamentals of Electronics, 1996; French patent Sept. 1995 subsequently extended)

8.2.7. Chemical sensor arrays

Sensors: Ion Sensitive Electrode (ISE, ISFET)

Interest: water quality monitoring, biological analysis (blood, etc.)

Problem: ion cross-sensitivity !

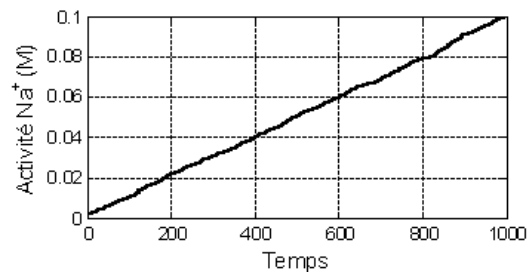
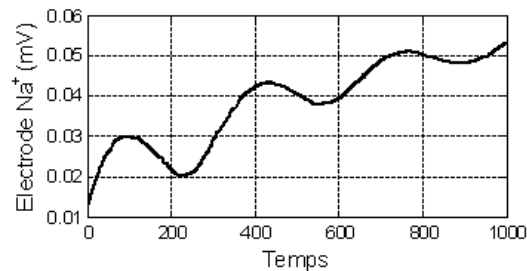


Ph.D. L. Duarte ; cooperation UPC Barcelona (Espagne), LAAS Toulouse, Univ. Campinas (Brazil)

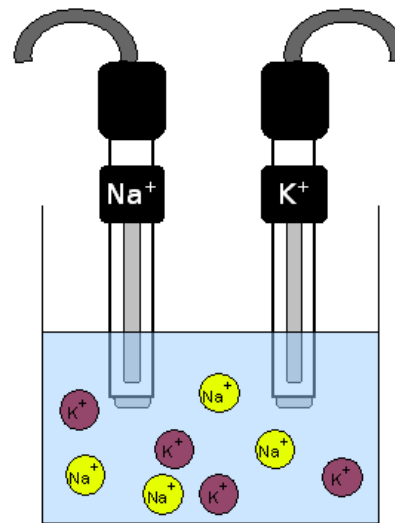
8.2.7. Chemical sensor arrays

Solution : **diversity** with different kinds of electrodes

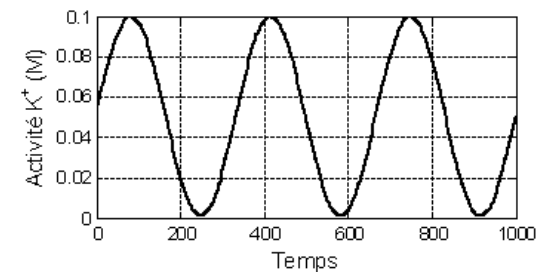
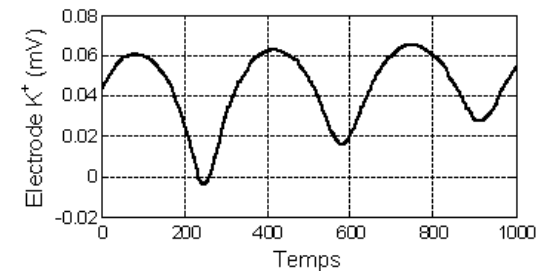
Mélange 1 : Na^+ -ISE



Source 1 : Activité Na^+



Mélange 2 : K^+ -ISE



Source 2 : Activité K^+

Ph.D. L. Duarte ; cooperation UPC Barcelona (Espagne), LAAS Toulouse, Univ. Campinas (Brazil)

8.2.7. Chemical sensor arrays

Nicolski-Eisenman Model

$$\begin{cases} x_{Na}(n) = e_{Na} + d_{Na} \log \left(s_{Na}(n) + a_{Na,K} s_K^{z_{Na}/z_K}(n) \right) \\ x_K(n) = e_K + d_K \log \left(s_K(n) + a_{K,Na} s_{Na}^{z_K/z_{Na}}(n) \right) \end{cases}$$

$s_{Na}(n), s_K(n)$: activities of Na and K, to estimate

e_{Na}, e_K, d_{Na}, d_K : unknown parameters

$a_{Na,K}, a_{K,Na}$: unknown cross - sensitivities

One can estimate activities with statistical methods based on:

- Activity and mixture coefficient **positivity**,
- activity **independence** ,
- **Temporal invariance** of ionic activity.

Ph.D. L. Duarte ; cooperation UPC Barcelona (Espagne), LAAS Toulouse, Univ. Campinas (Brazil)

8.2. A few examples

8.2.8. Pre-processing for classification

- Bayesian classification requires conditional densities $p(\mathbf{r} / H_i)$
Multivariate density estimation (sparse sample, complexity)

- Idea: transform observations \mathbf{r} to \mathbf{r}^* by ICA

Then, if ICA provides independent enough variables:

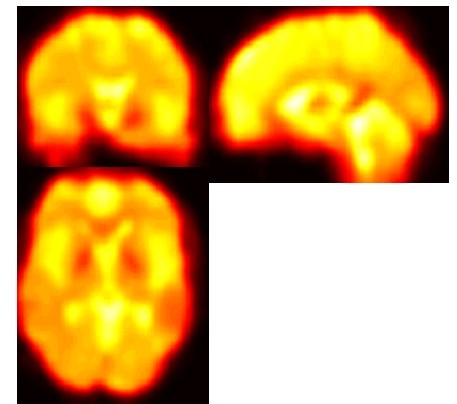
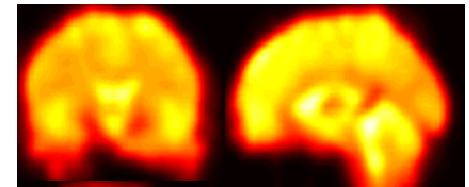
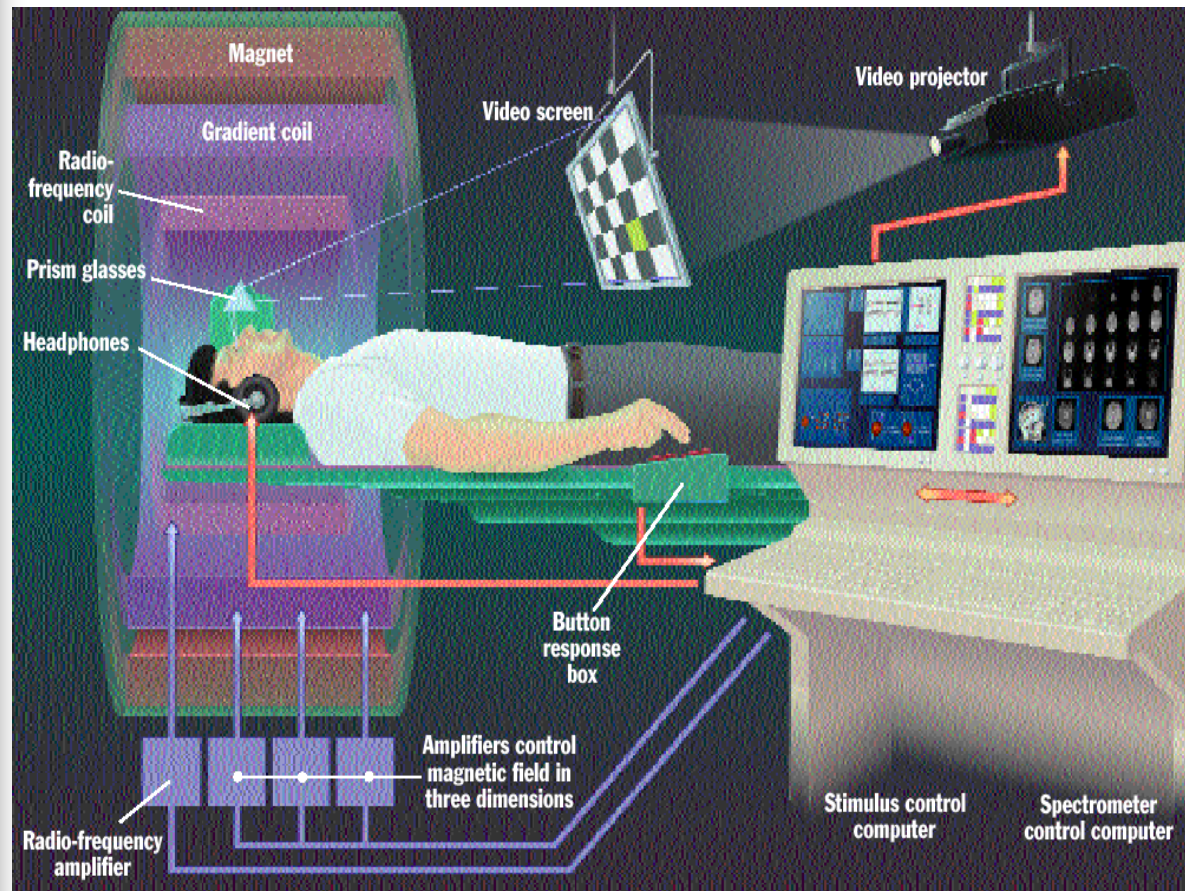
$$p(\mathbf{r}^* / H_i) \approx \prod_j p(r_j^* / H_i)$$

- The method replaces 1 multivariate (size N) density estimation by N scalar density estimations

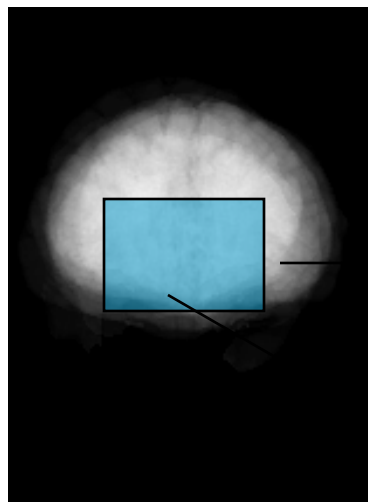
Reference: U. Amato, A. Antoniadis, G. Grégoire, Independent Component discriminant analysis , Int. Math. J. 3 (2003), no. 7, 735 - 753.

8.2. A few examples

8.2.9. Pre-processing for classification



MRI recording



→ Observation 1

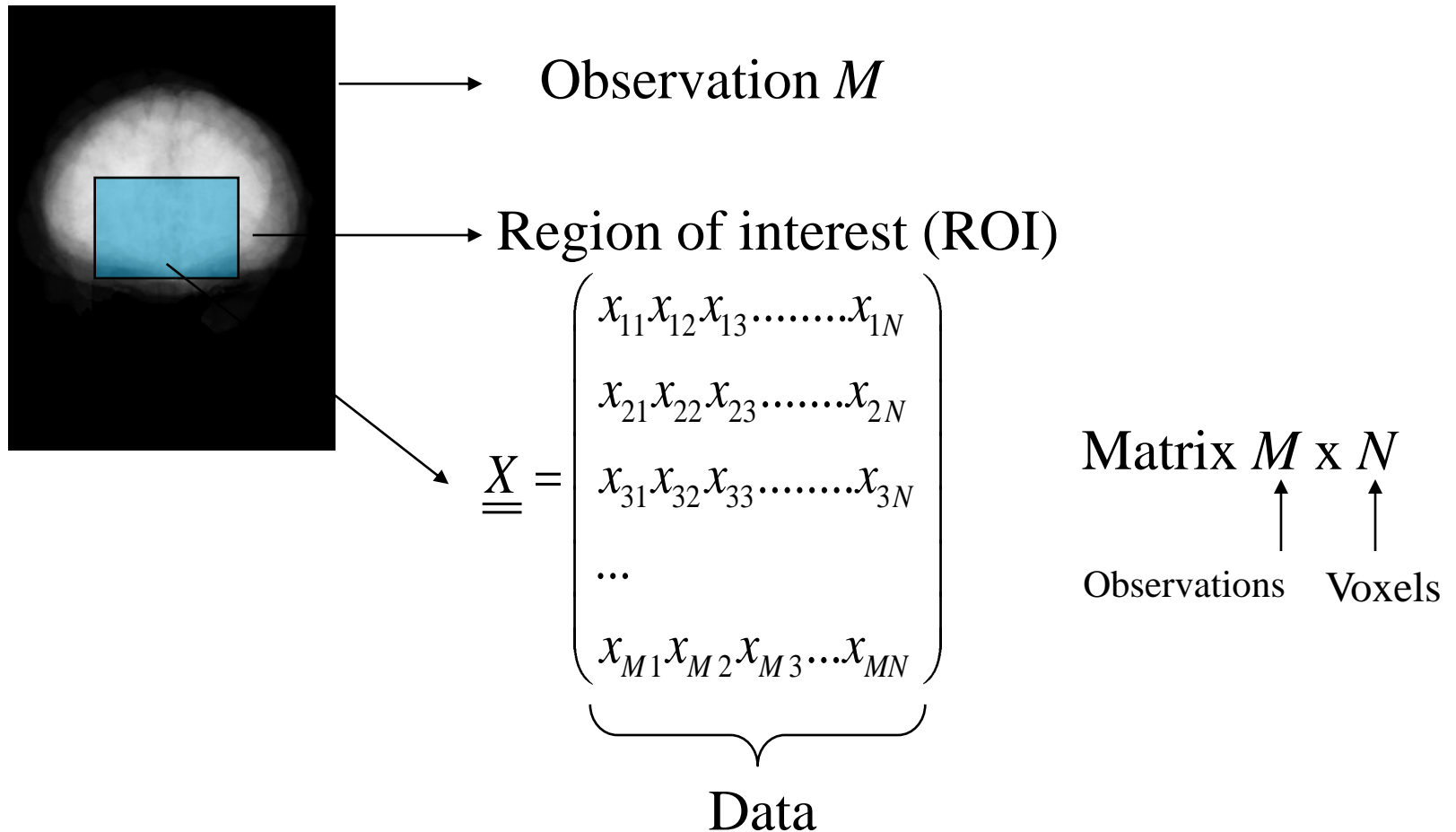
→ Region of interest (ROI)

$$\underline{\underline{X}} = \begin{pmatrix} x_{11} & x_{12} & x_{13} & \dots & x_{1N} \\ x_{21} & x_{22} & x_{23} & \dots & x_{2N} \end{pmatrix}$$

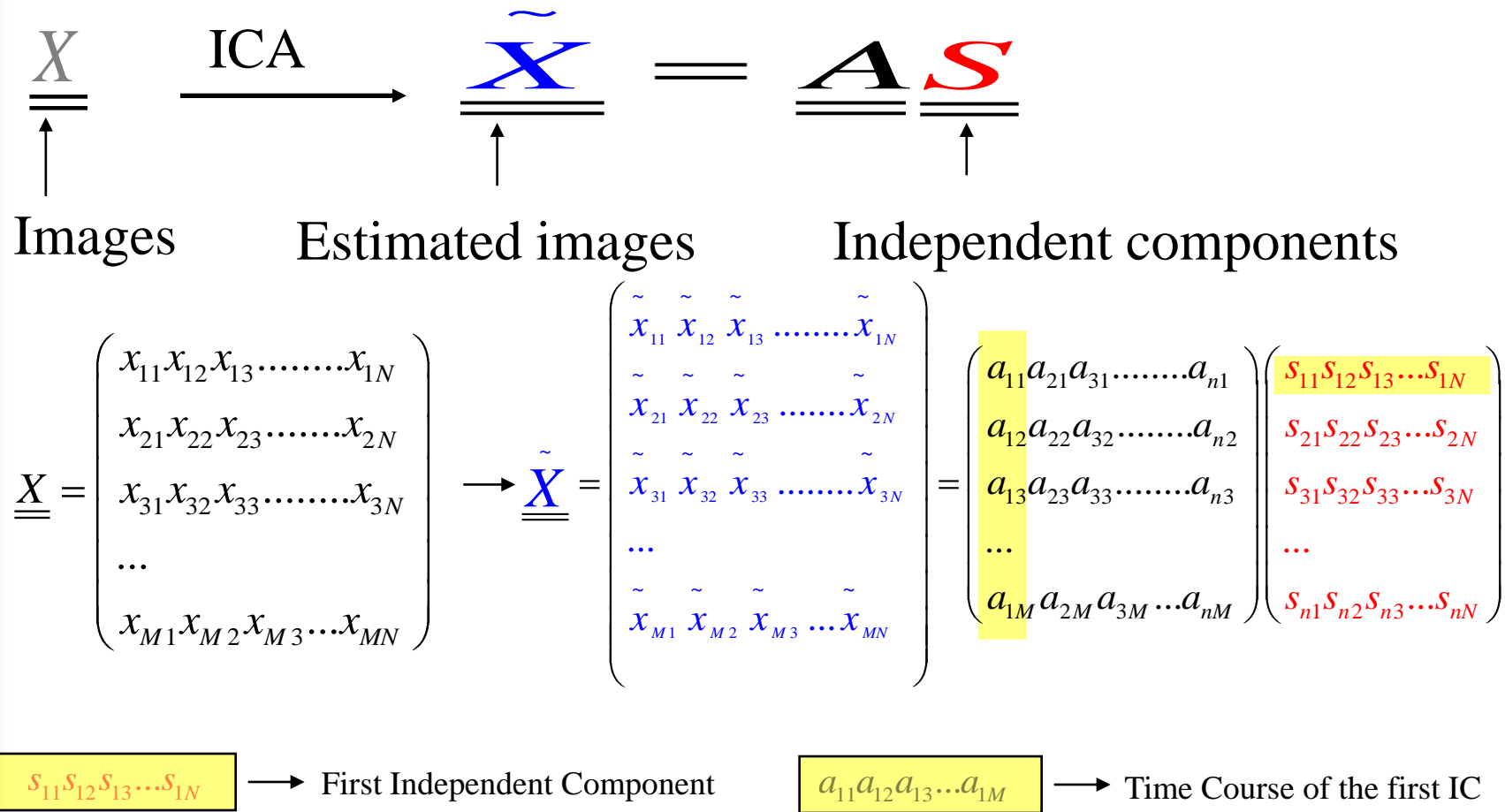
Data (Observation 1, N voxels)

Data (2 Observations, N voxels for each observation)

MRI recording



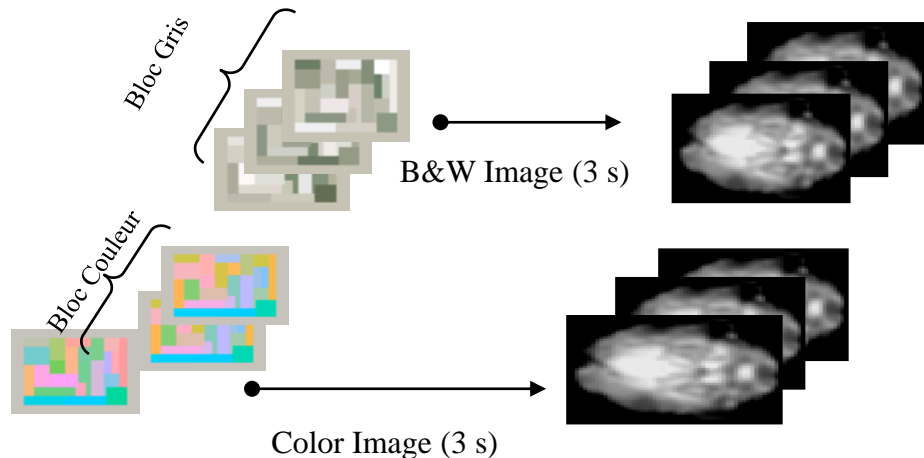
Spatial ICA model



Functional MRI Experiment

Experiment (Bloc design 801):

- **Color Bloc (BC)/B&W Bloc(BG)**
12 observations for each bloc of color images or B&W images, 3 s for each observation.
- BC BG BC BG BC BG BC BG BC BG
BC BG
- **Total: 144 observations**
- **Region of Interest (ROI)**

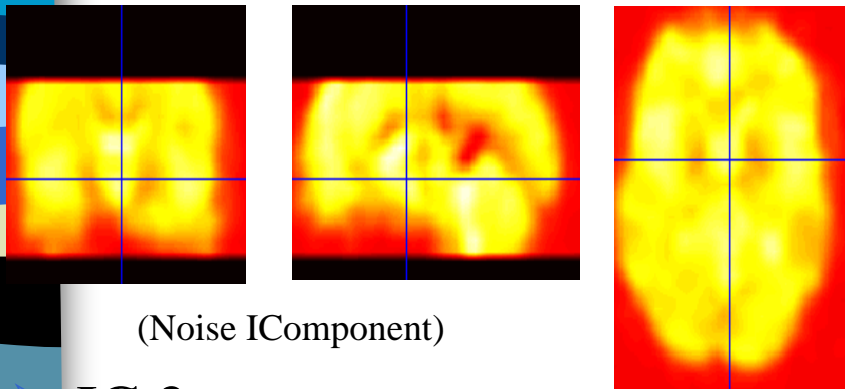


Region on study
Visual Cortex

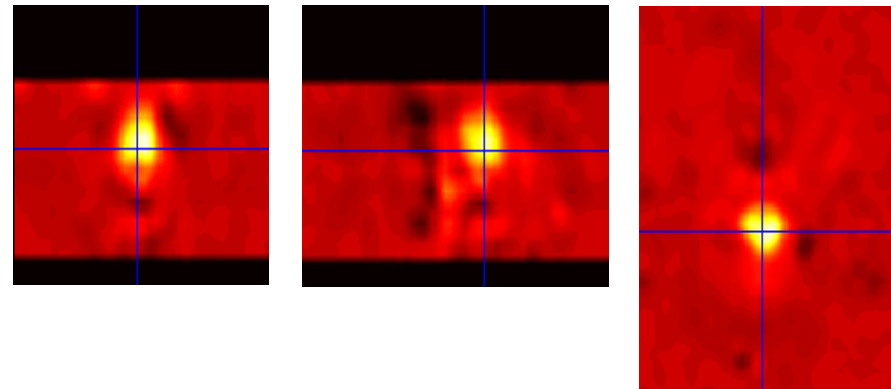
**Relevant IC are component,
time course sof which are
correlated to the task time course**

IC visualization

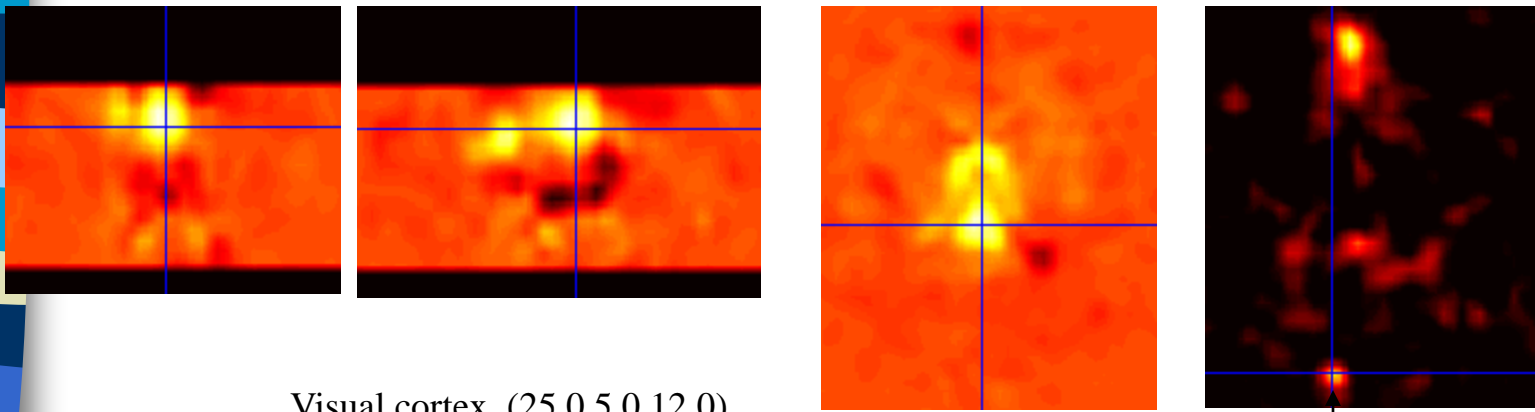
IC 8:



IC 1:



IC 2:



Visual cortex (25.0 5.0 12.0)

Course Campinas – July 20-29, 2010

9. Applications to Mars hyperspectral images analysis



Objectives: designing the separation method, modelization, IC interpretation, priors and beyond ICA

Reference: On the decomposition of Mars hyperspectral data by ICA and Bayesian positive source separation. Moussaoui S., Hauksdottir H., Schmidt F., Jutten C. Chanussot J., Brie D., Douté S., Benediksson J.A., Neurocomputing, 71(10-12), pp. 2194-2208, 2008



Contents

- ICA for hyperspectral images

- with H. Hauksdottir (MsSc thesis, Univ. of Iceland), Dr. J. Chanussot (LIS, Grenoble), Dr. S. Moussaoui (IRCCyN, Nantes), F. Schmidt and Dr. S. Douté (Planetology Lab., Grenoble)

- Discussion



1 - ICA for hyperspectral images:

1.1. The data

■ Observations

- OMEGA instrument: a spectrometer on board of Mars express
- 256 frequency bands in visible and IR, from 0.926 μm to 5.108 μm with a spectral resolution of 0.014 μm ,
- variable spatial resolution (elliptic orbit) from 300m to 4km,

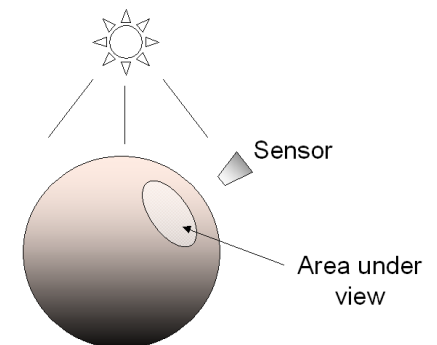
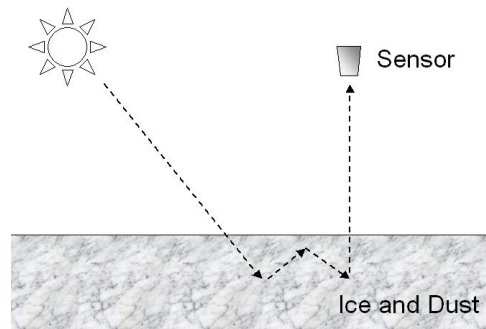
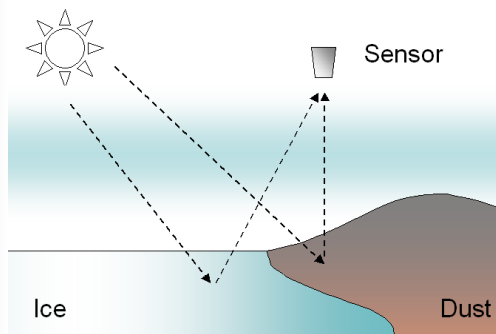
■ Data

- only 174 frequency bands (the other are too noisy),
- portion of image: about 256 x 256 pixels
- one hyperspectral image is a cube of 10,000,000 data (« pixels »)
- South Polar Cap of Mars mainly contains 3 endmembers: CO₂ ice, H₂O ice and Dust.

ICA for hyperspectral images: Physical properties

Physical model of observations

- reflected light of sun incident light according to ground reflectance,
- atmospheric attenuation and direct sensor illumination,
- **geometrical mixture** occurs when a few different chemicals reflect directly the sun light according to their local abundance,
- **intimate mixture** corresponds to a (NL) mixture at very small scale,
- solar position with respect to the Polar cap leads to **luminance gradient**.



ICA for hyperspectral images: A physical model

- The physical model of observations...

$$L(x, y, \lambda) = \Phi(\lambda) \left(L_a(\lambda) + \sum_{p=1}^P \alpha_p(x, y) L_p(\lambda) \right) \cos[\theta(x, y)]$$

... leads to the linear model:

$$L(x, y, \lambda) = \sum_{p=1}^P \alpha'_p(x, y) L'_p(\lambda) + E(x, y, \lambda) + \text{noise}$$

- With different endmembers, ICA seems a suitable approach

ICA for hyperspectral images: Spatial or spectral decomposition ?

ICA approximations: spatial or spectral decomposition ?

$N_f = 174$ "sensors"

$$I_{\lambda_k}(n) \approx \sum_{p=1}^{N_c} a_{kp} \Pi_p(n)$$

N_z "samples"

N_c "image ICs"

a_{1p}

\vdots spectrum ass. IC_p

$a_{N_f p}$

N_z "sensors"

N_c "spectrum ICs"

$$I_n(\lambda_k) \approx \sum_{p=1}^{N_c} a_{np} \psi_p(\lambda_k)$$

$N_f = 174$ "samples"

a_{1p}

\vdots image ass. IC_p

$a_{N_z p}$

ICA for hyperspectral images:

Parameter selection

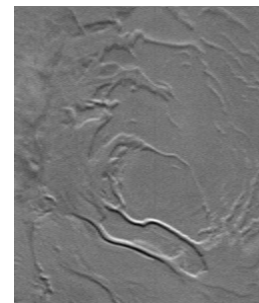
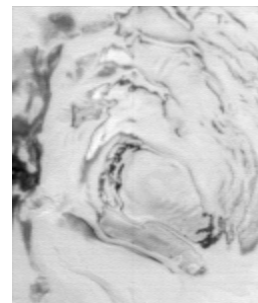
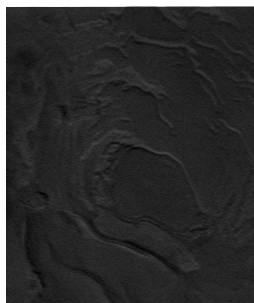
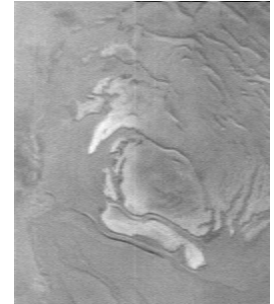
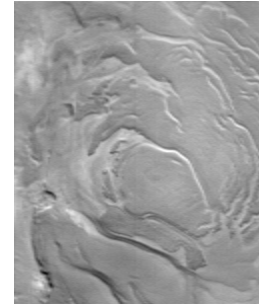
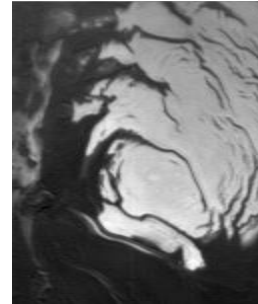
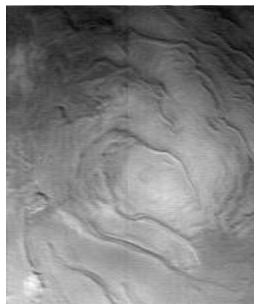
- Choosing the number of ICs ?
 - At least equal to the endmember number,
 - sufficient for insuring an accurate approximation.
- 3 endmembers: H₂O, CO₂ ices and Dust.
- Using PCA, with N_c = 7 components, one recovers 98% of the initial image power.

$$I_{\lambda_k}(n) \approx \sum_{p=1}^{N_c} a_{kp} \Pi_p(n)$$

Spatial ICA

ICA for hyperspectral images: ICA Results

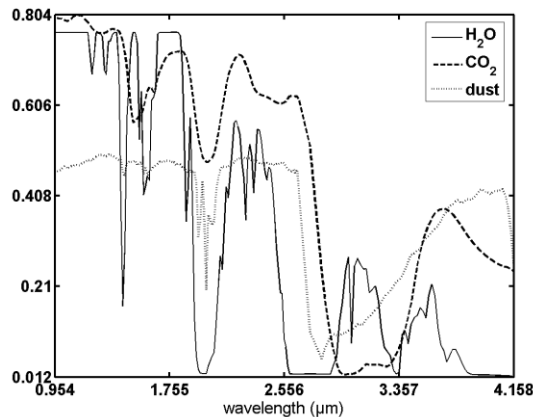
- After PCA, JADE gives these 7 ICs.
- How interpret ICs ?
- For endmembers, we have:
 - *Ground truth* with reference classification,
 - reference spectra.
- For the others ???



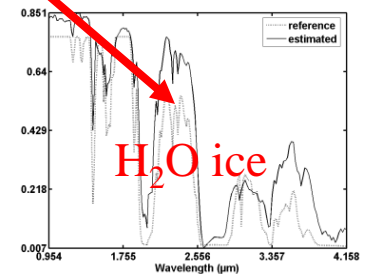
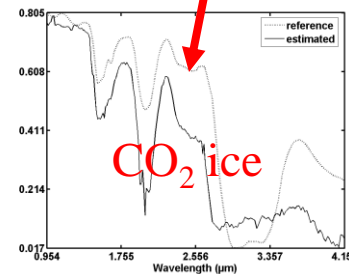
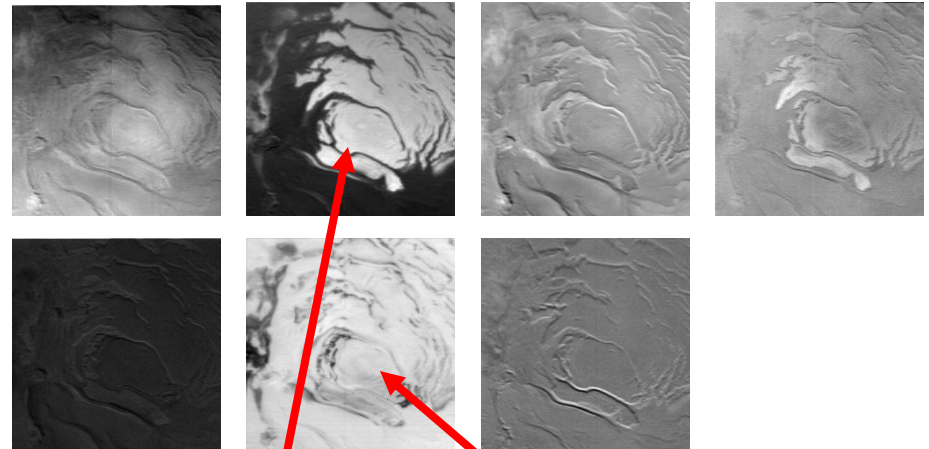
ICA for hyperspectral images: IC Interpretation

How interpret ICs ?

- reference spectra in Earth lab.



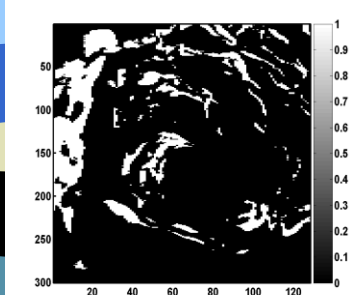
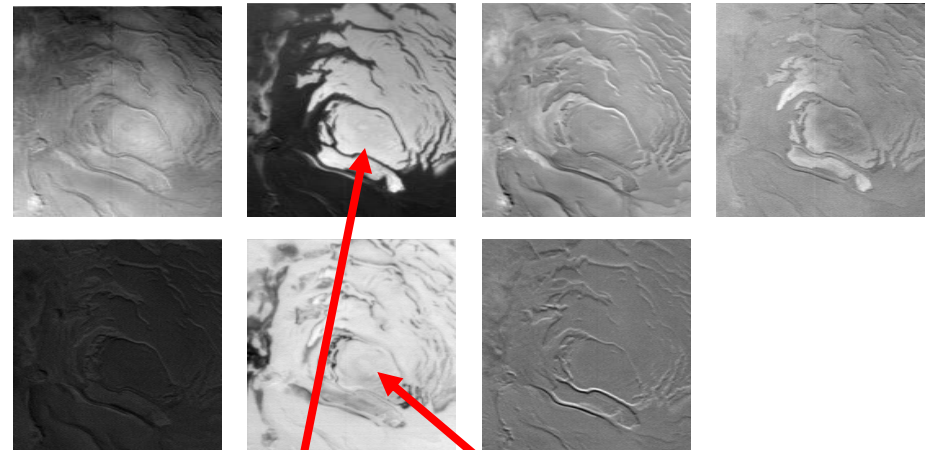
- Spectra associated to A column



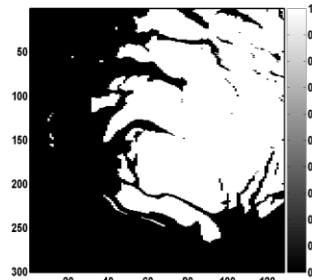
ICA for hyperspectral images: IC Interpretation

How interpret ICs ?

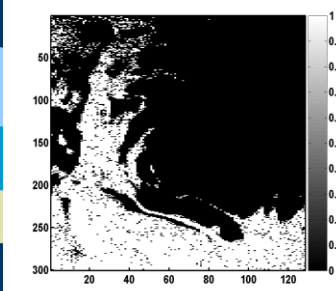
- reference classification



H₂O ice mask

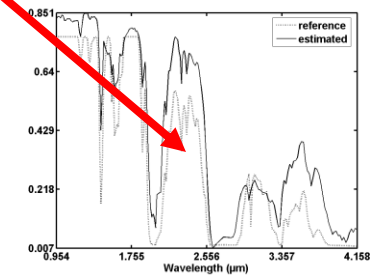
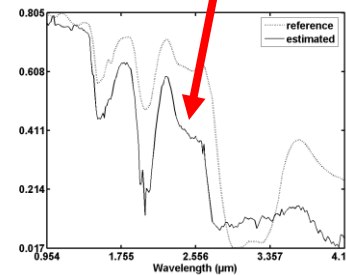


CO₂ ice mask



Dust

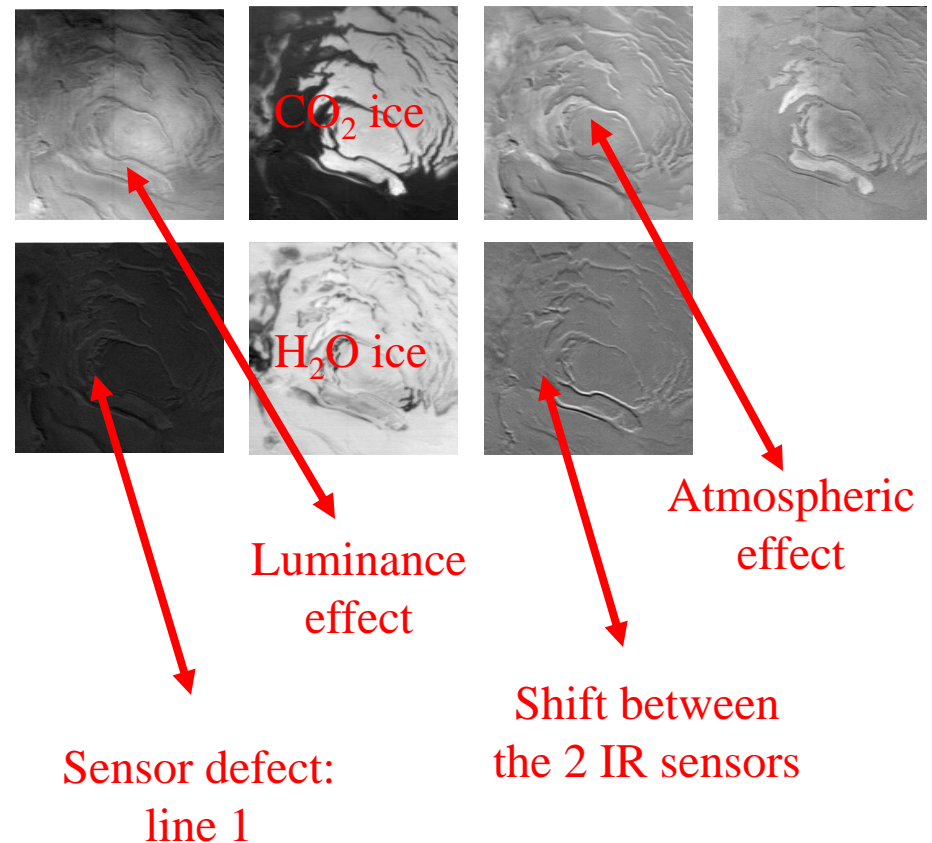
*CO₂ ice and dust are
strongly correlated !*



ICA for hyperspectral images: IC Interpretation

How interpret the other ICs ?

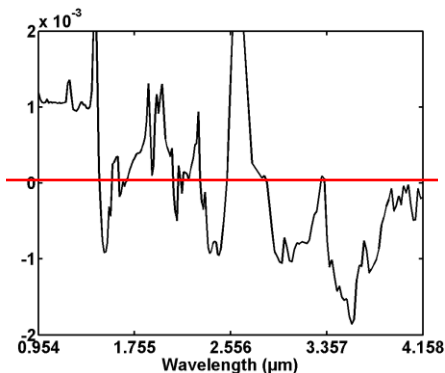
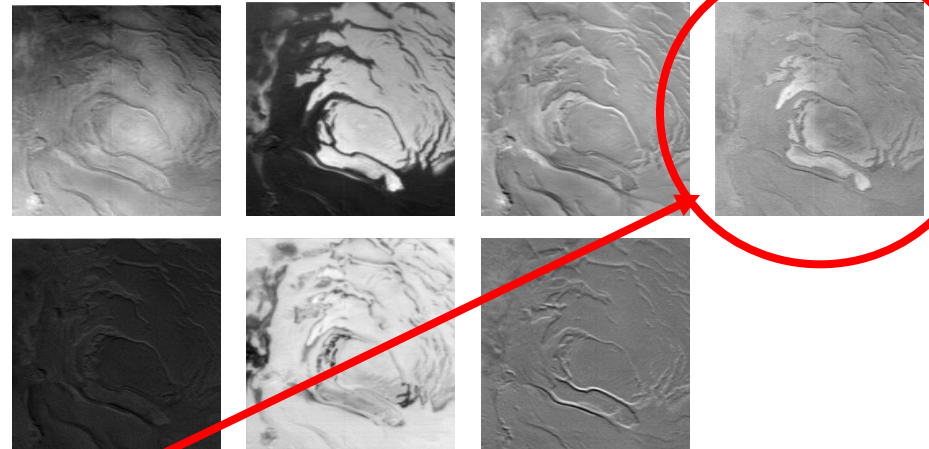
- Results with preprocessed data, with removal of luminance and atmospheric effects and defectuous sensors
- On these data, the power associated to IC1, IC3, IC4 and IC7 are very small
- We deduce that these ICs are related to effects removed by the preprocessing
- Spectra of these ICs are more or less flat



ICA for hyperspectral images: IC Interpretation

How interpret the last IC ?

- The spectrum looks like a nonlinear mixture of CO₂ ice and Dust spectra.
- Physicists suspect it could be associated to intimate mixtures.



Spectrum of IC4



ICA for hyperspectral images: Discussion

- Relevance of ICs
 - 5 ICs seems related to artefacts, and 2 like endmembers
 - Artefacts cannot be explained with endmembers, and appear like ICs. The initial model should be improved.
 - 2 endmembers are strongly correlated !
 - Spectra are sometimes negative !
- ICA is not suited to this problem !
- Classification cannot be done with these ICs.
- One should design a method based on true assumptions, like positivity...but it is another story !

10. Extraction of cardiac signals based on periodic component analysis

R. Sameni ^(1,3), Ch. Jutten ^(1,2), G. Clifford ⁽⁴⁾, M. Shamsollahi ⁽³⁾

(1) GIPSA-Lab, UMR CNRS 5216, Grenoble, France

(2) Institut Universitaire de France

(3) Sharif University of Technology, Tehran, Iran

(4) MIT, USA

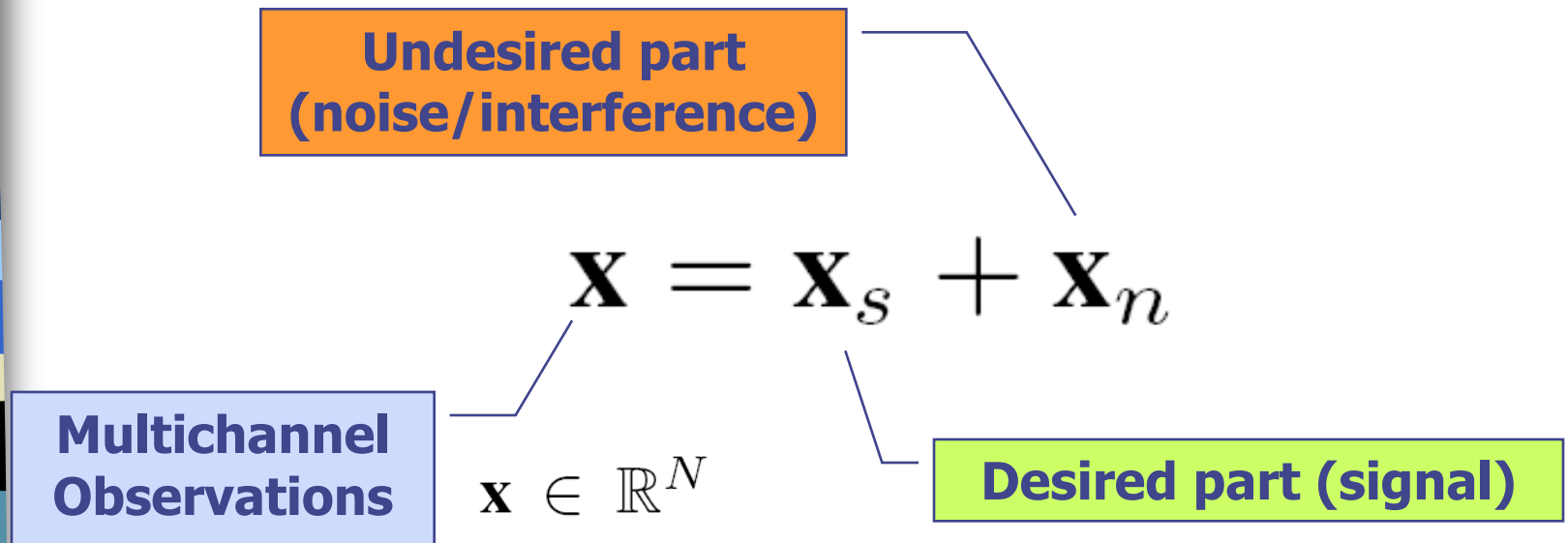
Overview

- Motivation
- Method
- Case Study
- Conclusion

Overview

- Motivation
- Method
- Case Study
- Conclusion

Data Model



Assumption1: The signal and noise parts are independent.

Assumption2: There is some **mutual information** within the signal parts of the observations, i.e., the signal parts of different channels are not **independent**.

Example: The latent variable model

$$\mathbf{x} = A\mathbf{s} + \mathbf{n}$$

$$\mathbf{x} \in \mathbb{R}^N \quad \mathbf{n} \in \mathbb{R}^N \quad A \in \mathbb{R}^{N \times M} \quad \mathbf{a}_i \in \text{span}\{A\}$$

$$\begin{aligned} \mathbf{x} &= \overset{\text{desired subspace}}{s_1 \mathbf{a}_1 + \dots + s_k \mathbf{a}_k} + \overset{\text{undesired subspace}}{\dots + s_M \mathbf{a}_M + \mathbf{n}} \\ &= \mathbf{x}_s + \mathbf{x}_n \end{aligned}$$

Limitations of linear transforms (e.g. PCA, ICA, ...)

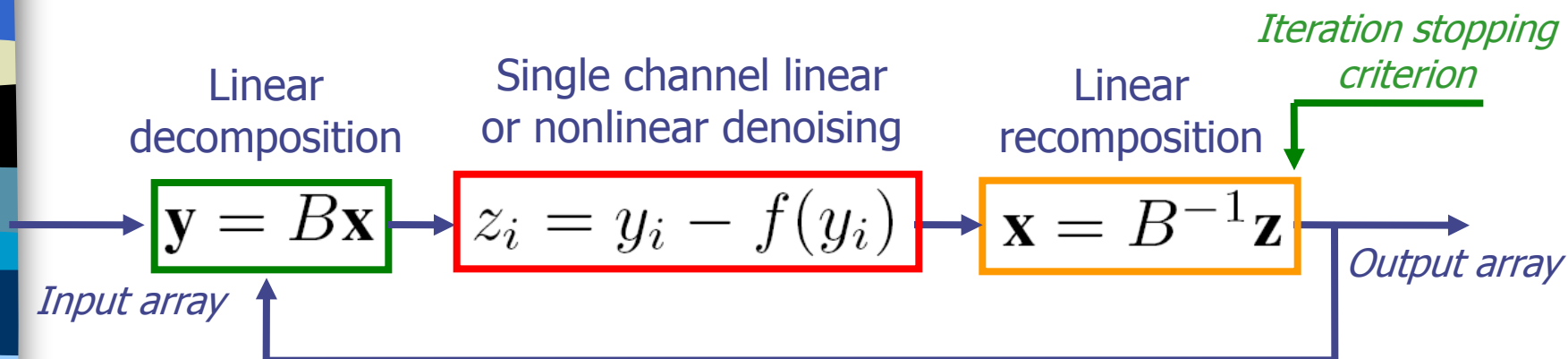
- Can not remove full-rank noise, and may even amplify them
- Can not generally decompose degenerate ($M > N$) mixtures
- Can not decompose coplanar (singular) mixtures
- Reduce the data dimensions for denoising
- Solution: Somehow break the linearity!

Overview

- Motivation
- **Method**
- Case Study
- Conclusion

Proposed method

Linear/nonlinear subspace removal by deflation



- In each iteration one of the dimensions of the desired (undesired) subspace are found and removed

Which linear transformation to use ?

$$\mathbf{y} = B\mathbf{x} = B(\mathbf{x}_s + \mathbf{x}_n) = \mathbf{y}_s + \mathbf{y}_n$$

- **PCA?** Decorrelates the output; but does not necessarily improve the signal/noise separability.
- **ICA?** Gives independent outputs; but again does not necessarily improve the signal/noise separability.

Proposed method

Which linear decomposition and denoising methods should we use?

There is no general answer; but

we can use *any *a priori** information of the signal and noise subspaces to design the required blocks

Which linear transformation to use ?

$$y = \mathbf{b}^T \mathbf{x} = \mathbf{b}^T \mathbf{x}_s + \mathbf{b}^T \mathbf{x}_n = y_s + y_n$$

■ SNR maximizer:

$$\text{SNR}(\mathbf{b}) = \frac{E\{y_s^2\}}{E\{y_n^2\}} = \frac{\mathbf{b}^T C_{\mathbf{x}_s} \mathbf{b}}{\mathbf{b}^T C_{\mathbf{x}_n} \mathbf{b}} \Rightarrow \mathbf{b} = \text{GEVD}(C_{\mathbf{x}_s}, C_{\mathbf{x}_n})$$

Generalized Eigenvalue
Decomposition

■ Periodicity maximizer: (for periodic or pseudo-periodic signals)

$$\epsilon(\mathbf{b}, \tau) = \frac{E_t\{(y(t+\tau) - y(t))^2\}}{E_t\{y(t)^2\}} \Rightarrow \mathbf{b} = \text{GEVD}(C_x(\tau), C_x(0))$$

Which linear transformation to use ?


$$y = \mathbf{b}^T \mathbf{x} = \mathbf{b}^T \mathbf{x}_s + \mathbf{b}^T \mathbf{x}_n = y_s + y_n$$

- **Nonstationary maximizer:** (for nonstationary signals)

$$\eta(\mathbf{b}) = \frac{E_{\theta}\{y(\theta)^2\}}{E_t\{y(t)^2\}} \Rightarrow \mathbf{b} = \text{GEVD}(C_{x(\theta)}, C_{x(t)})$$

- **Spectral-Contrast maximizer:** (for spectrally separable signals)

$$\sigma(\mathbf{b}) = \frac{E_{\nu}\{|Y(\nu)|^2\}}{E_f\{|Y(f)|^2\}} = \frac{\mathbf{b}^T S_{\mathbf{x}} \mathbf{b}}{\mathbf{b}^T C_{\mathbf{x}} \mathbf{b}} \Rightarrow \mathbf{b} = \text{GEVD}(S_{\mathbf{x}}, C_{\mathbf{x}})$$



$$Y(f) = \mathcal{F}\{y(t)\} = \mathbf{b}^T \mathcal{F}\{\mathbf{x}(t)\} = \mathbf{b}^T \mathbf{X}(f)$$

Which linear/nonlinear denoising to use ?

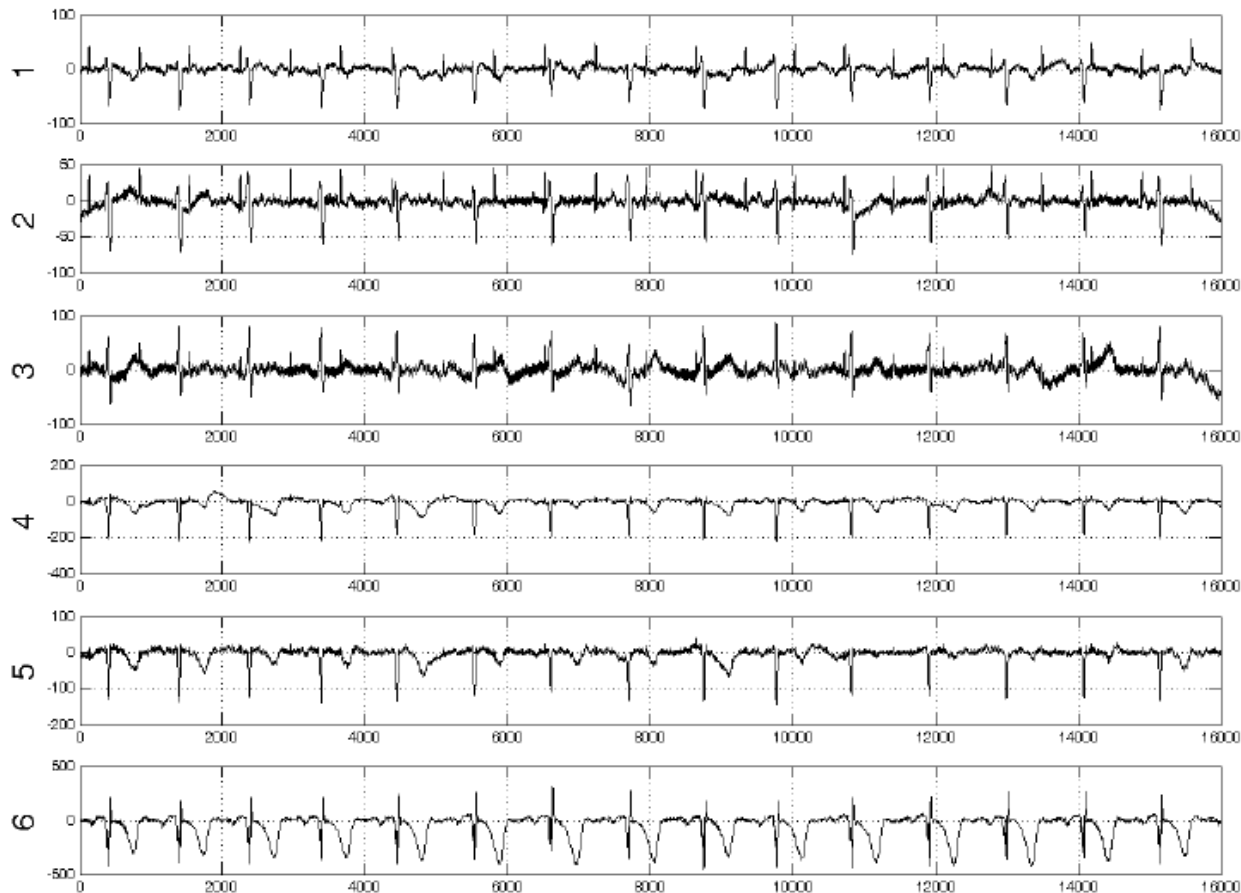
- Any transform that can (coarsely) separate the desired signal from noise, using temporal, frequency,... priors:
 - Wavelet decomposition
 - Wiener filter
 - Kalman filter
 - Time-frequency filter
 - ...

Overview

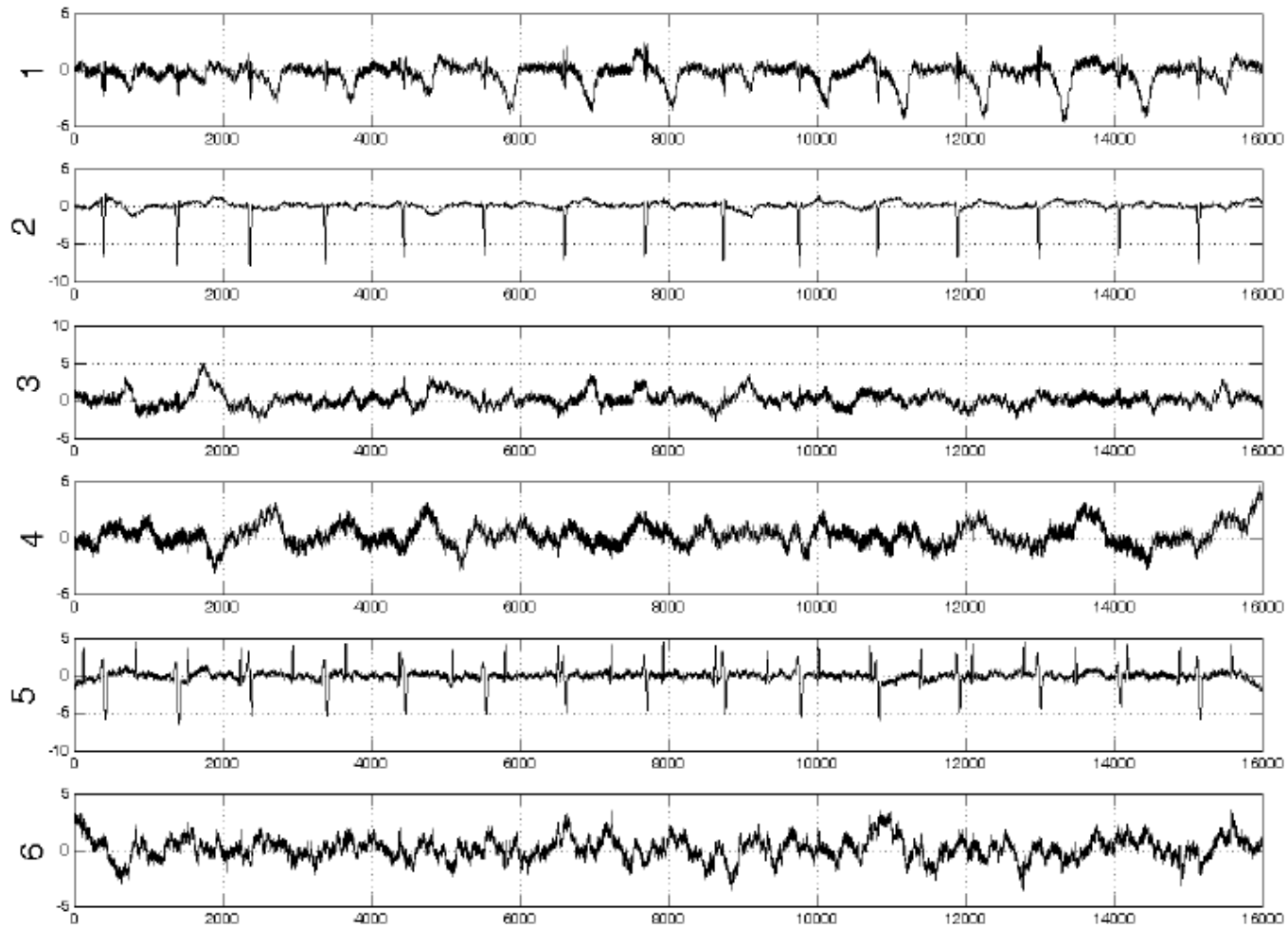
- Motivation
- Method
- Case Study
- Conclusion

Case Study

Removing maternal ECG signal from fetal ECG recordings

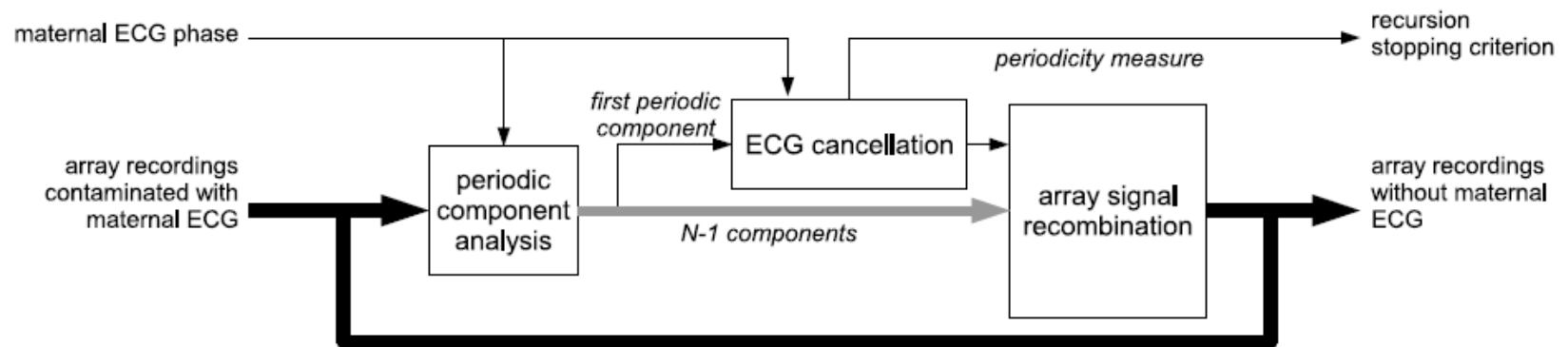


ICA Results (JADE)



Proposed method

- Linear transform: **Periodic Component Analysis (PCA)**
- Nonlinear transform: **Extended Kalman Filter (EKF)**

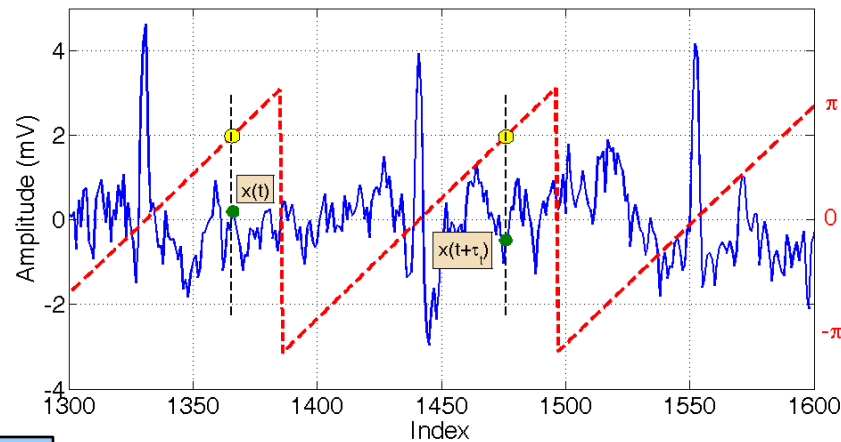


Periodic Component Analysis (PCA) Steps

- The cost function:

$$\epsilon(\mathbf{b}, \tau) = \frac{E_t\{(y(t + \tau) - y(t))^2\}}{E_t\{y(t)\}^2} \Rightarrow \text{GEVD}(C_x(\tau), C_x(0))$$

$$y = \mathbf{b}^T \mathbf{x}$$



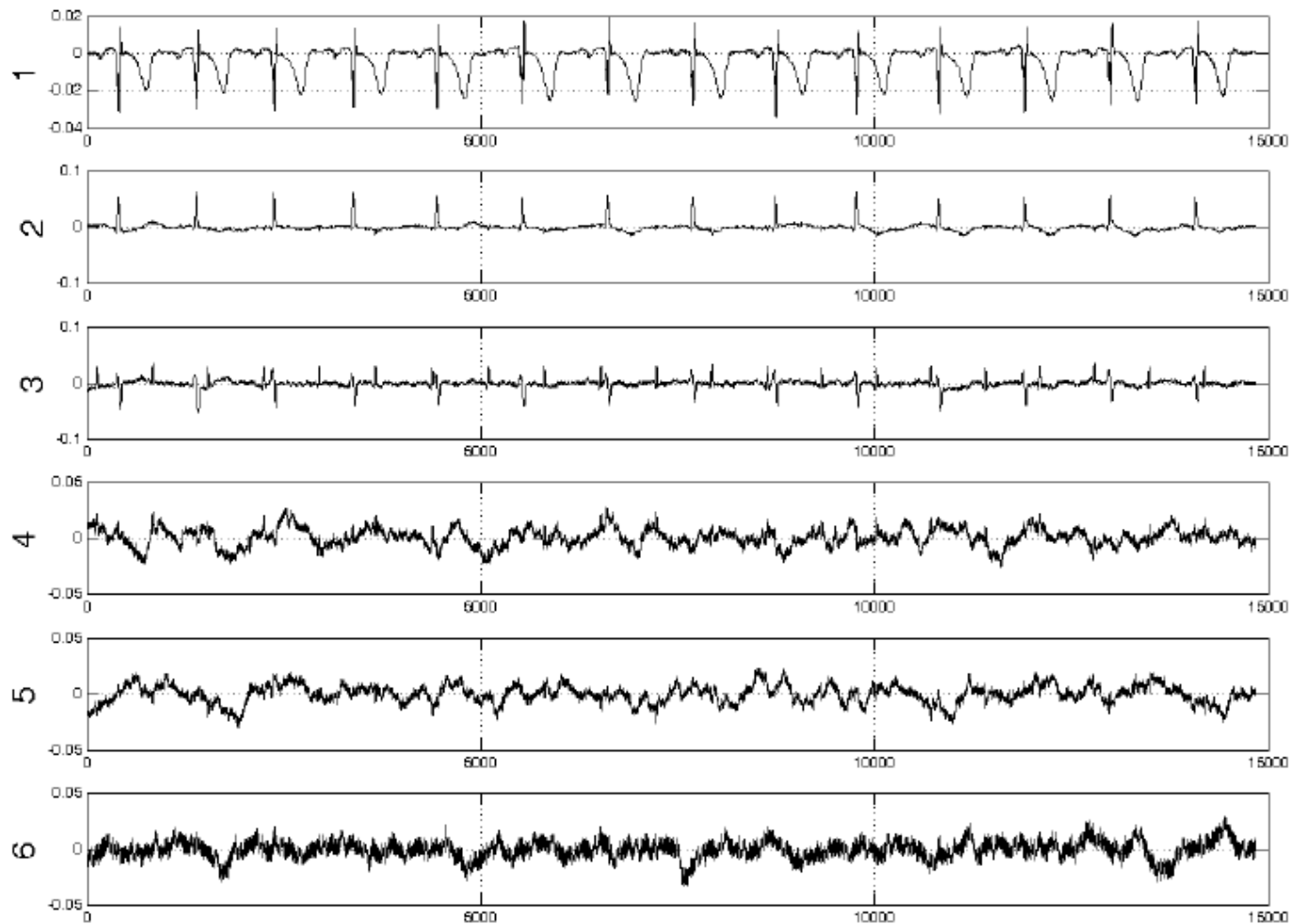
Using a time-varying lags:

$$\tau_t = \min\{\tau | \phi(t + \tau) = \phi(t), \tau > 0\}$$

$$\tilde{C}_x = E_t\{\mathbf{x}(t + \tau_t)\mathbf{x}(t)^T\}$$

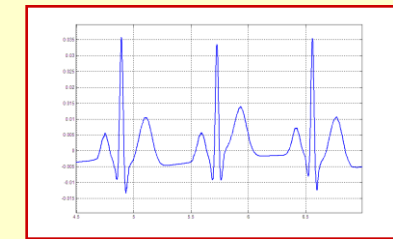
$$\text{GEVD}(\tilde{C}_x, C_x(0))$$

PCA Results

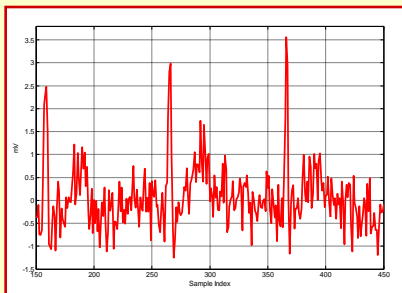


Extended Kalman Filter for ECG Denoising

$$\begin{cases} \mathbf{x}_{k+1} = f(\mathbf{x}_k, \mathbf{w}_k, k) \\ \mathbf{y}_k = g(\mathbf{x}_k, \mathbf{v}_k, k) \end{cases}$$



Dynamical ECG model



Noisy observations

Extended Kalman Filter

State equation

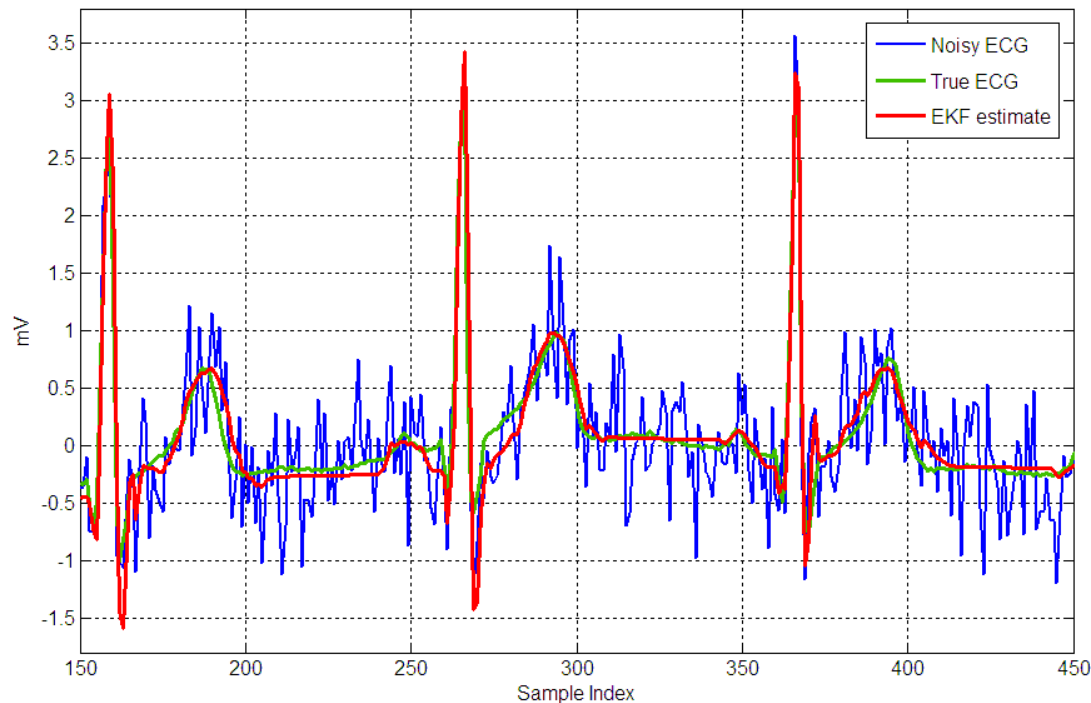
$$\theta_{k+1} = (\theta_k + \omega\delta) \bmod(2\pi)$$

$$z_{k+1} = - \sum_i \delta \frac{\alpha_i \omega}{b_i^2} \Delta\theta_i \exp(-\frac{\Delta\theta_i^2}{2b_i^2}) + z_k + \eta$$

Observation equation

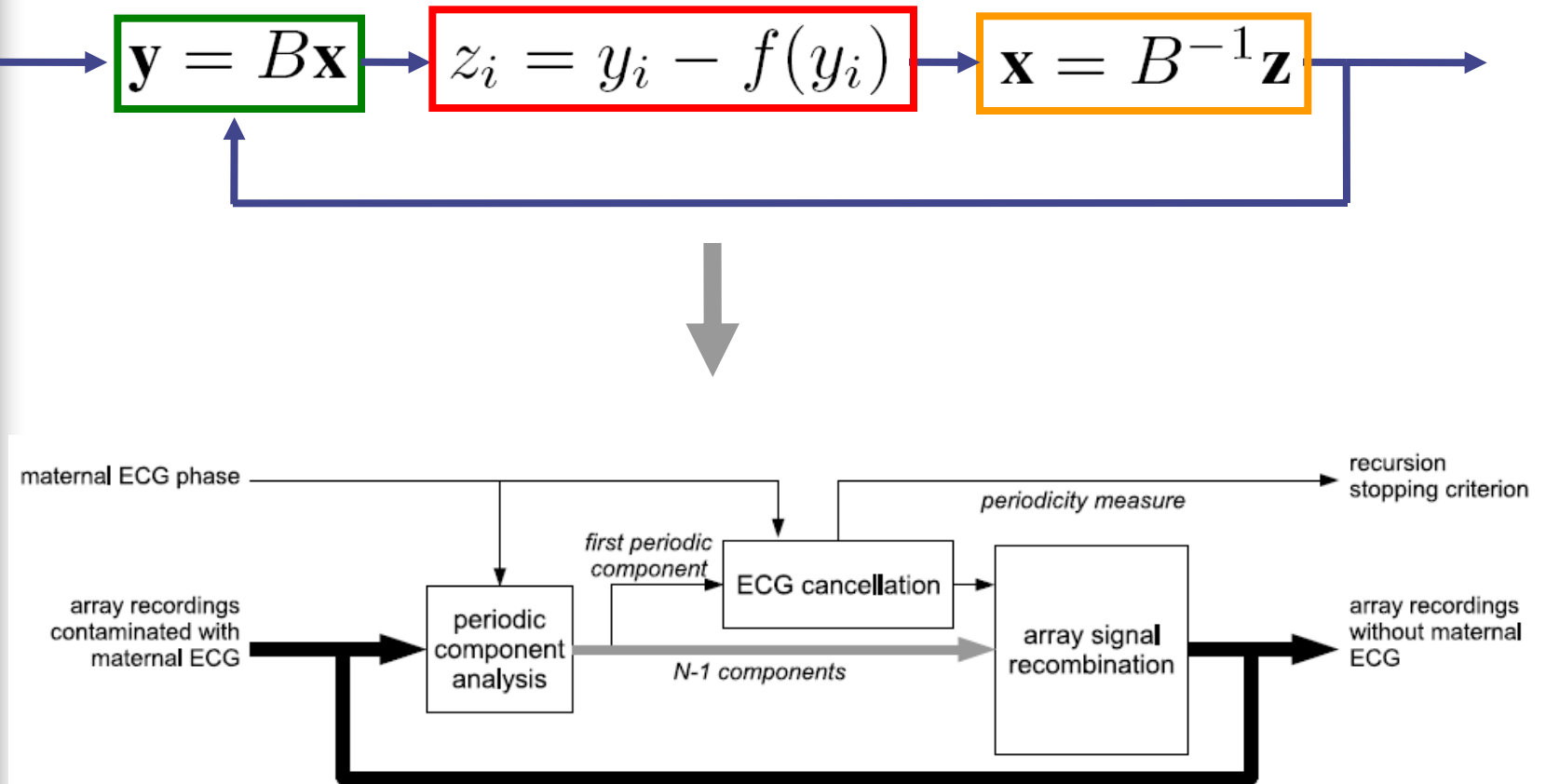
$$\begin{bmatrix} \phi_k \\ s_k \end{bmatrix} = \begin{bmatrix} 1 & 0 \\ 0 & 1 \end{bmatrix} \cdot \begin{bmatrix} \theta_k \\ z_k \end{bmatrix} + \begin{bmatrix} u_k \\ v_k \end{bmatrix}$$

Typical results of the EKF for ECG denoising

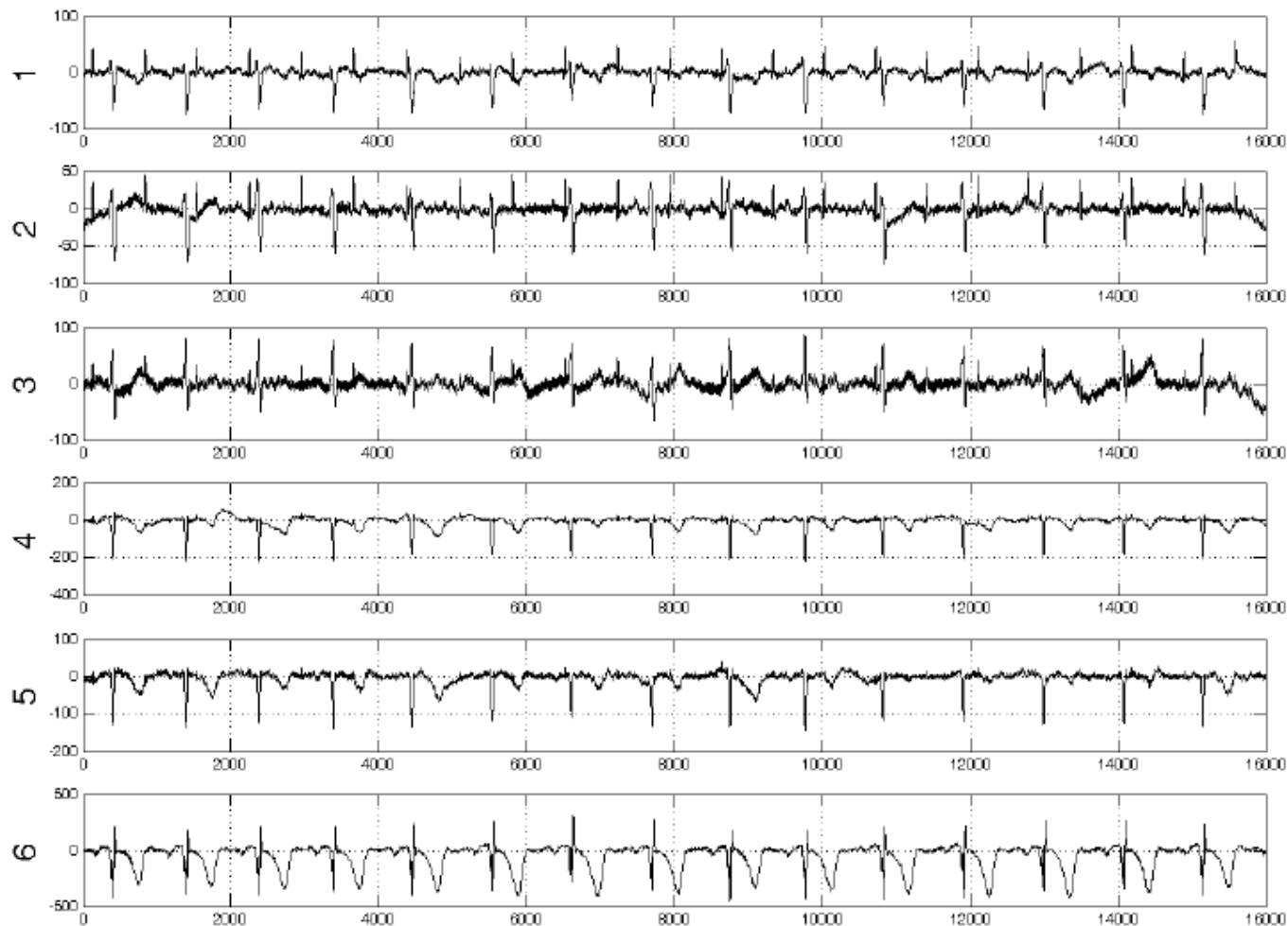


A typical result of the EKF performance for the input SNR of 5dB

Proposed method



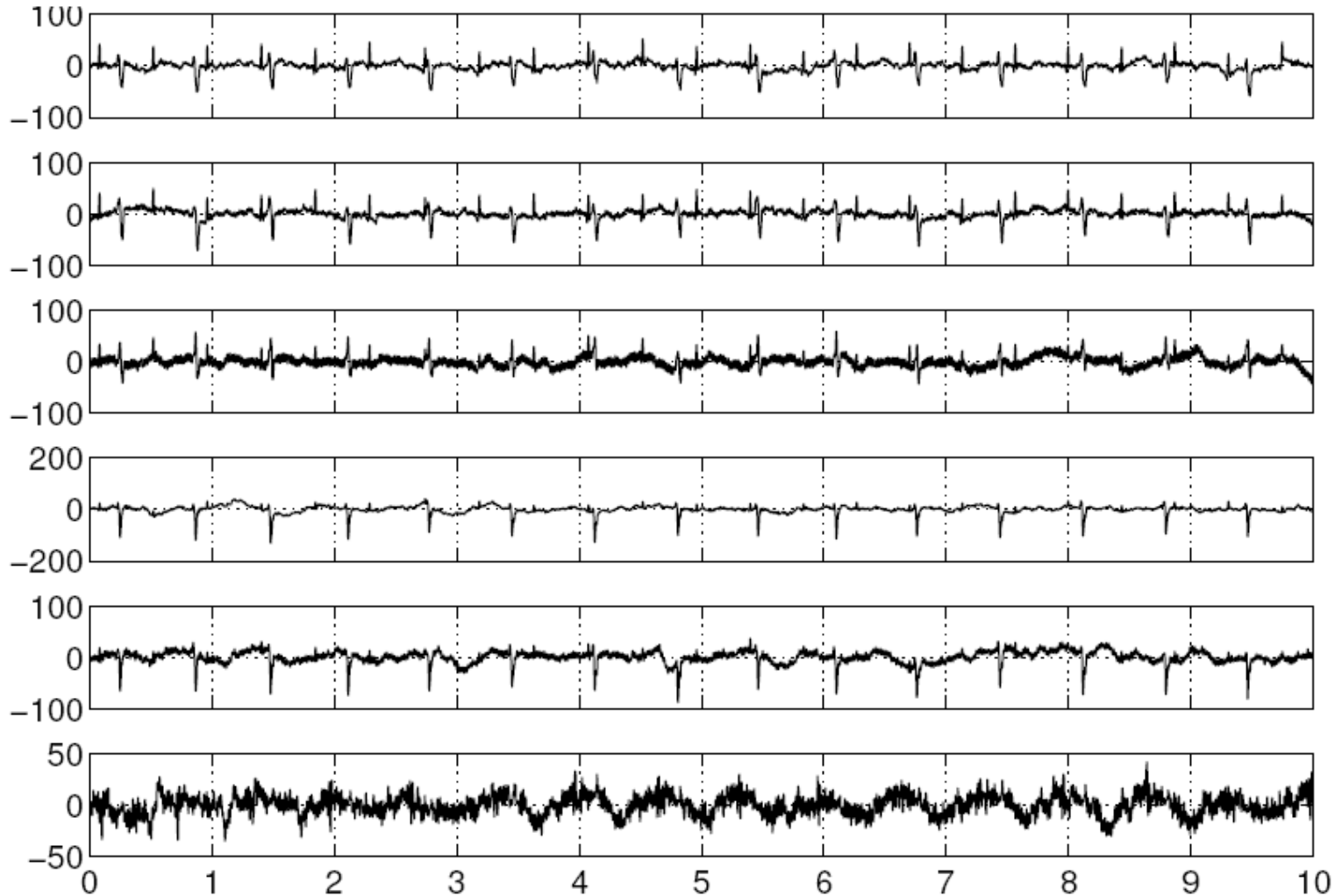
Proposed method: Original



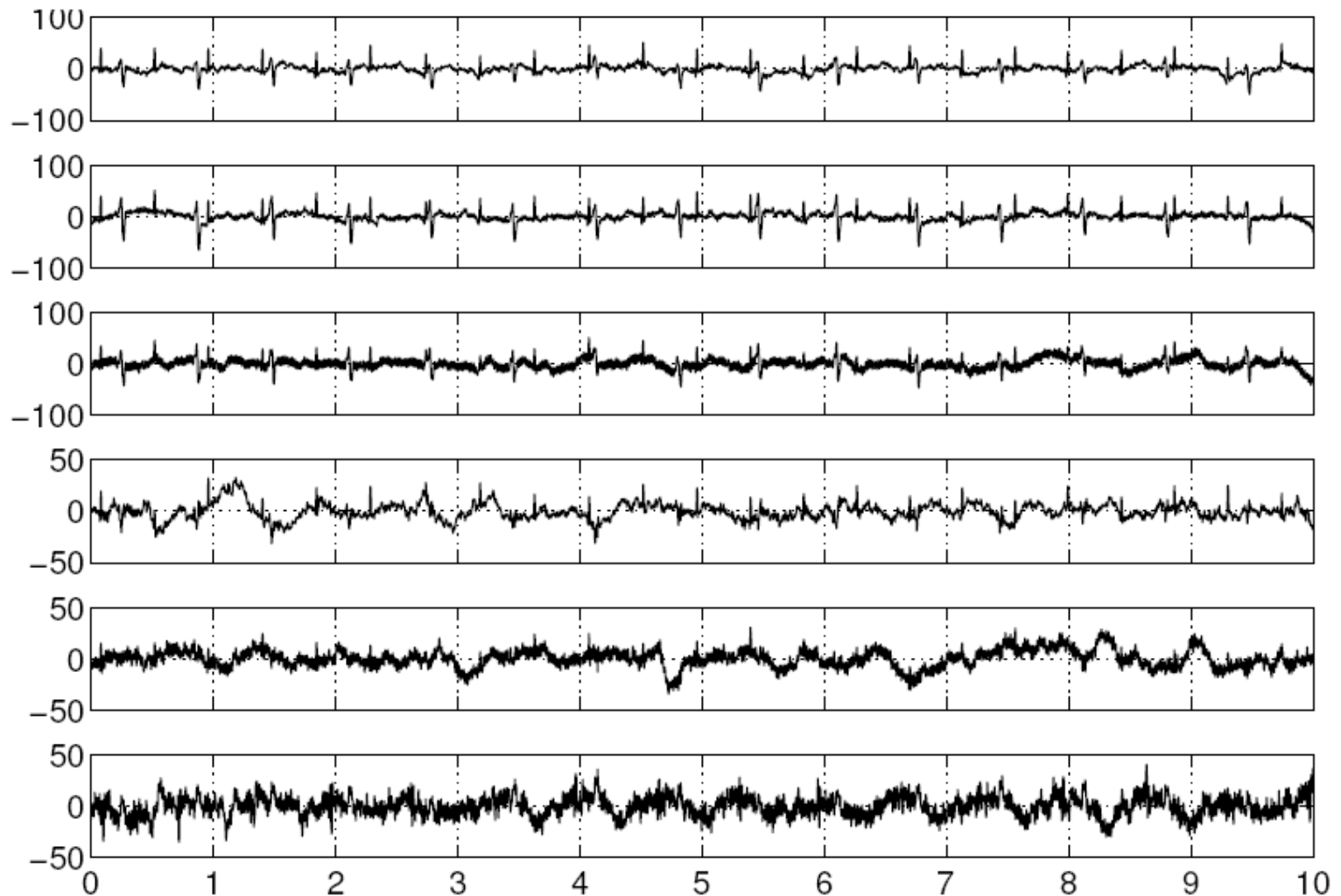
Proposed method: 1st iteration



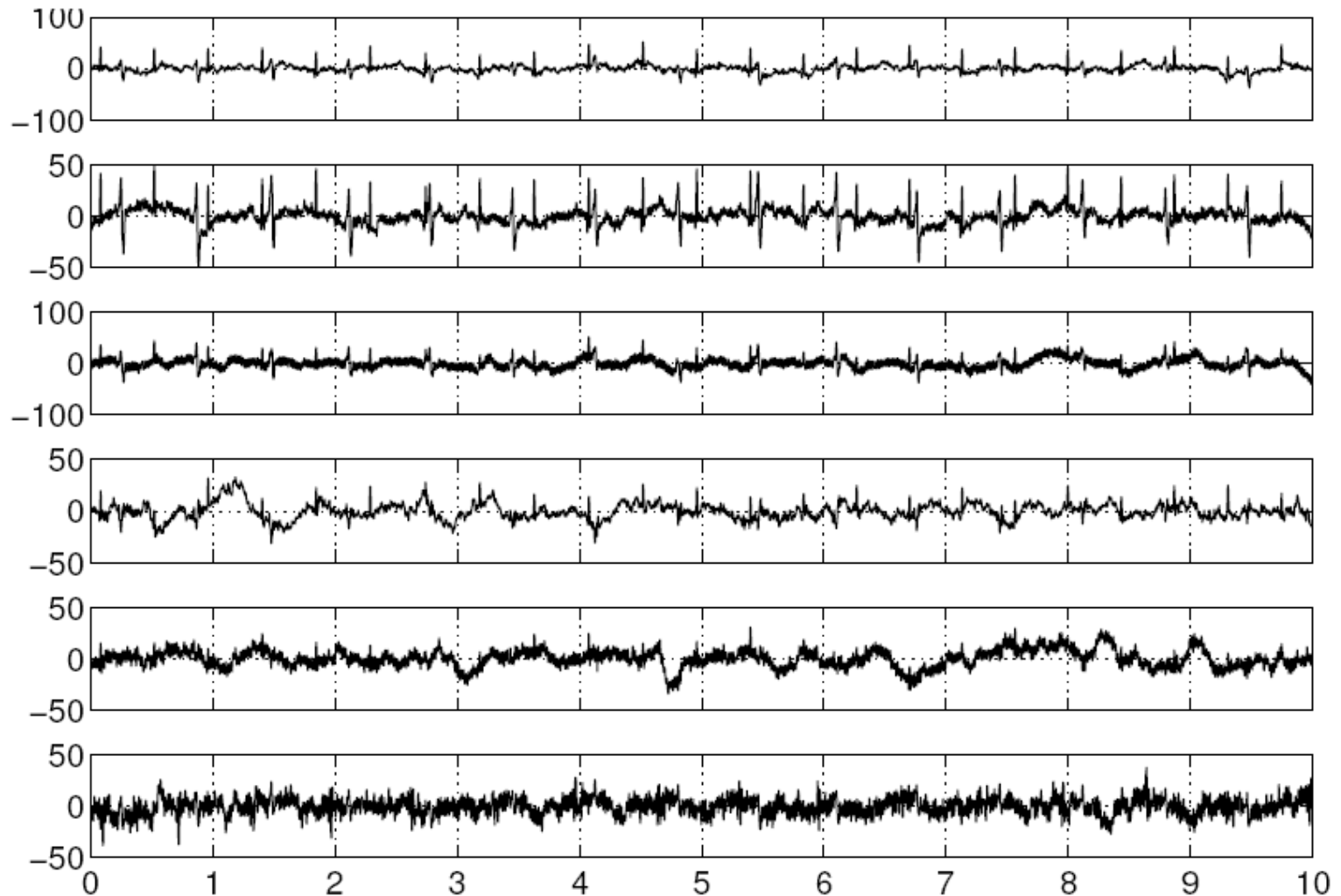
Proposed method: 2nd iteration



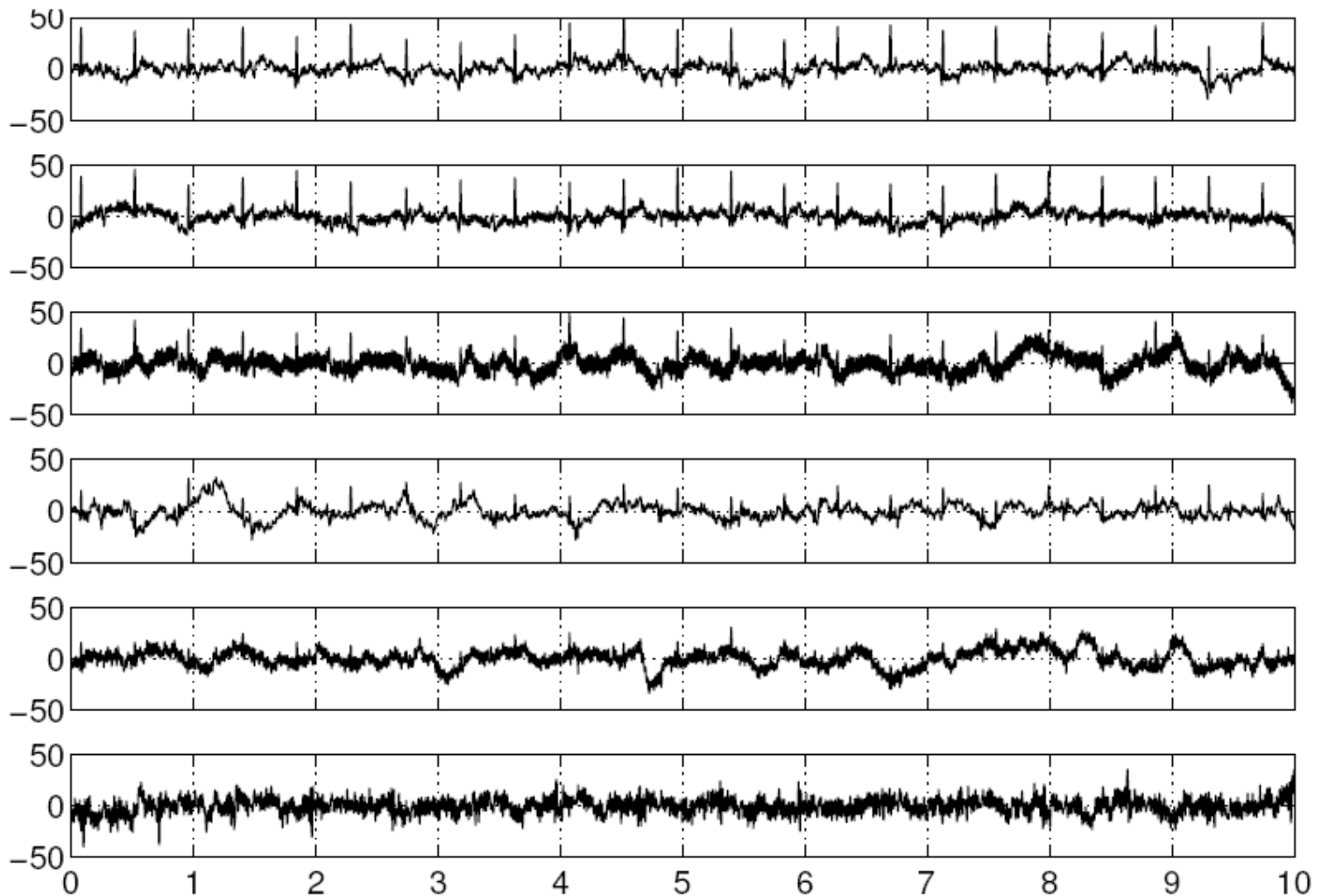
Proposed method: 3rd iteration



Proposed method: 4th iteration

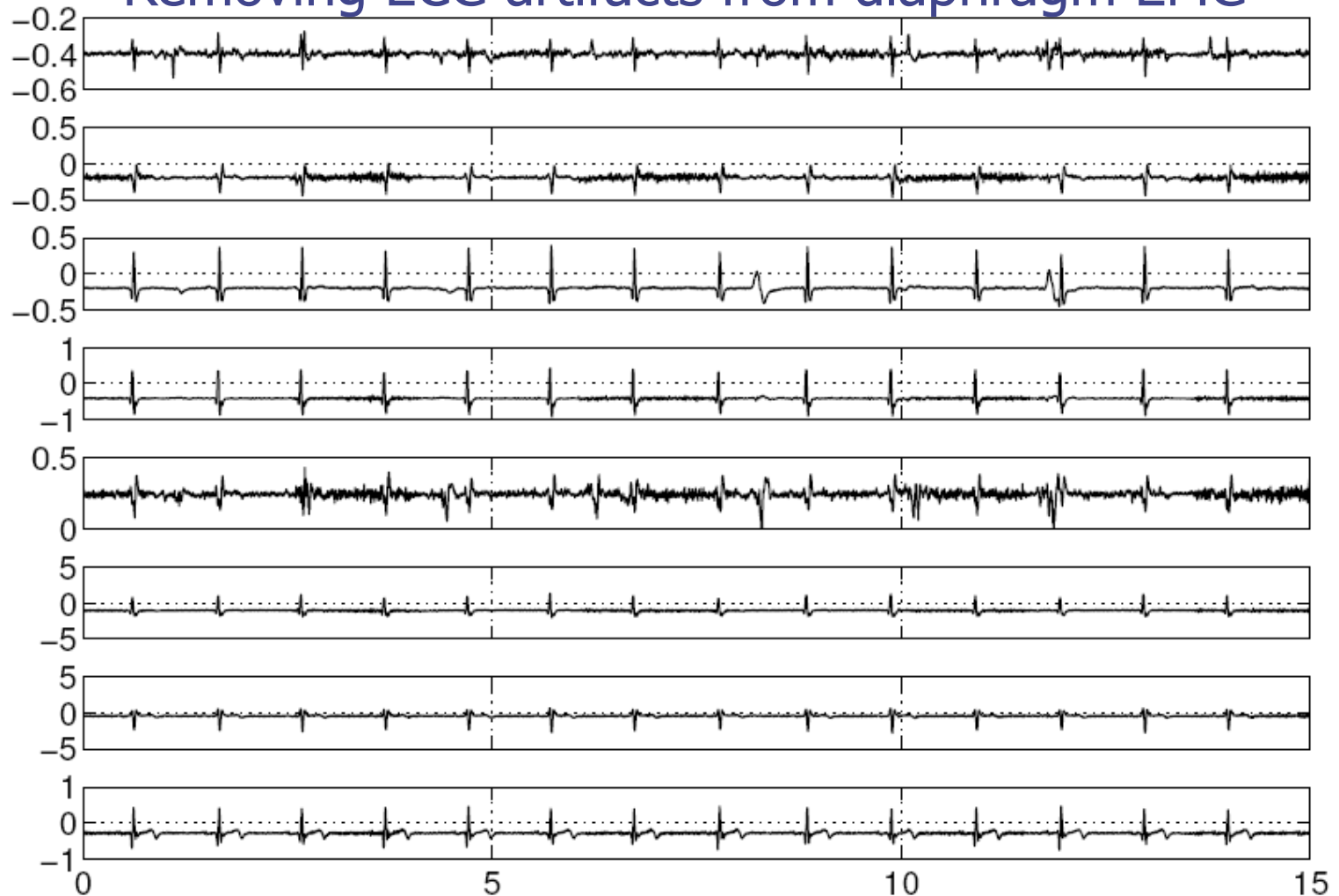


Proposed method: 5th iteration

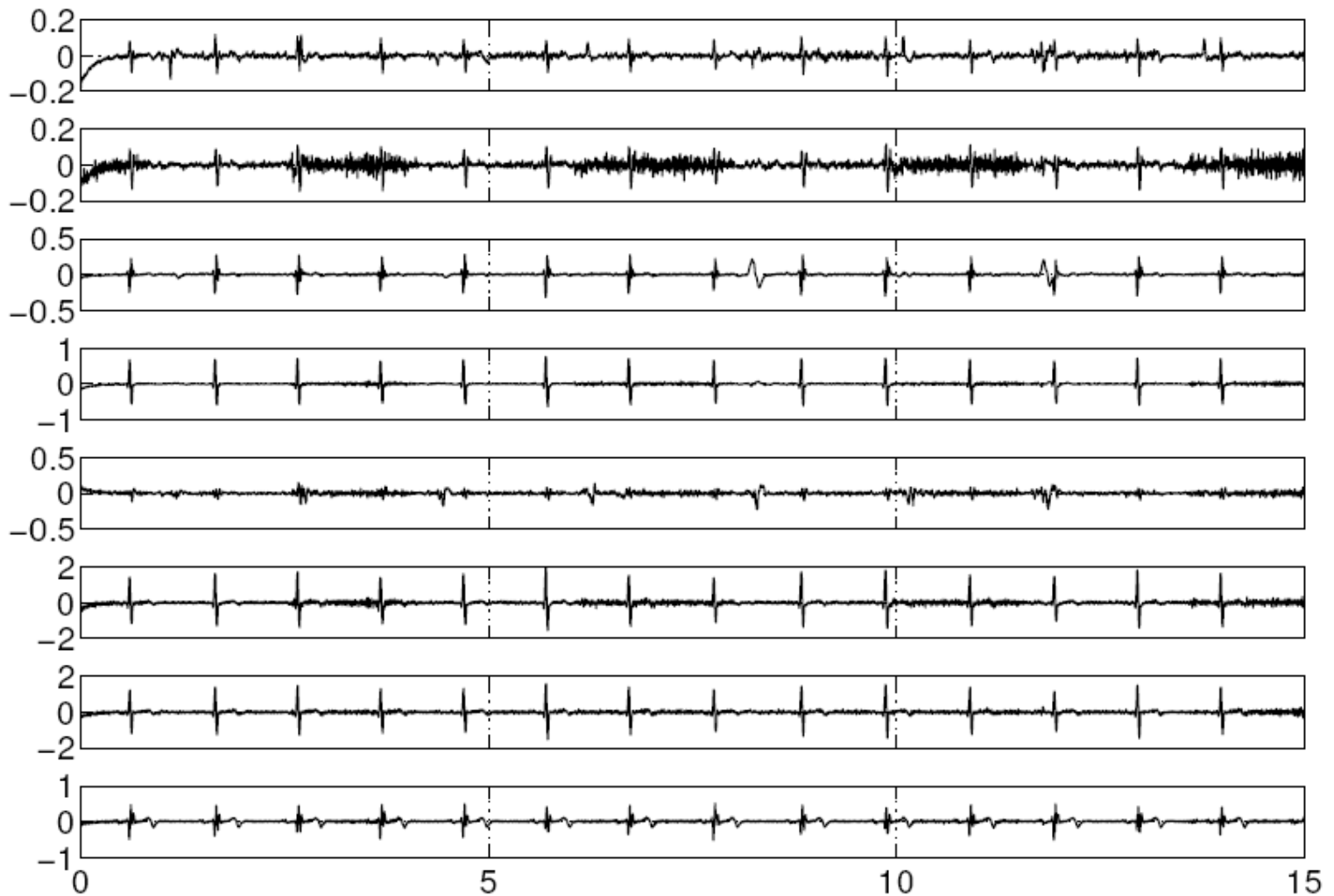


Case Study 2

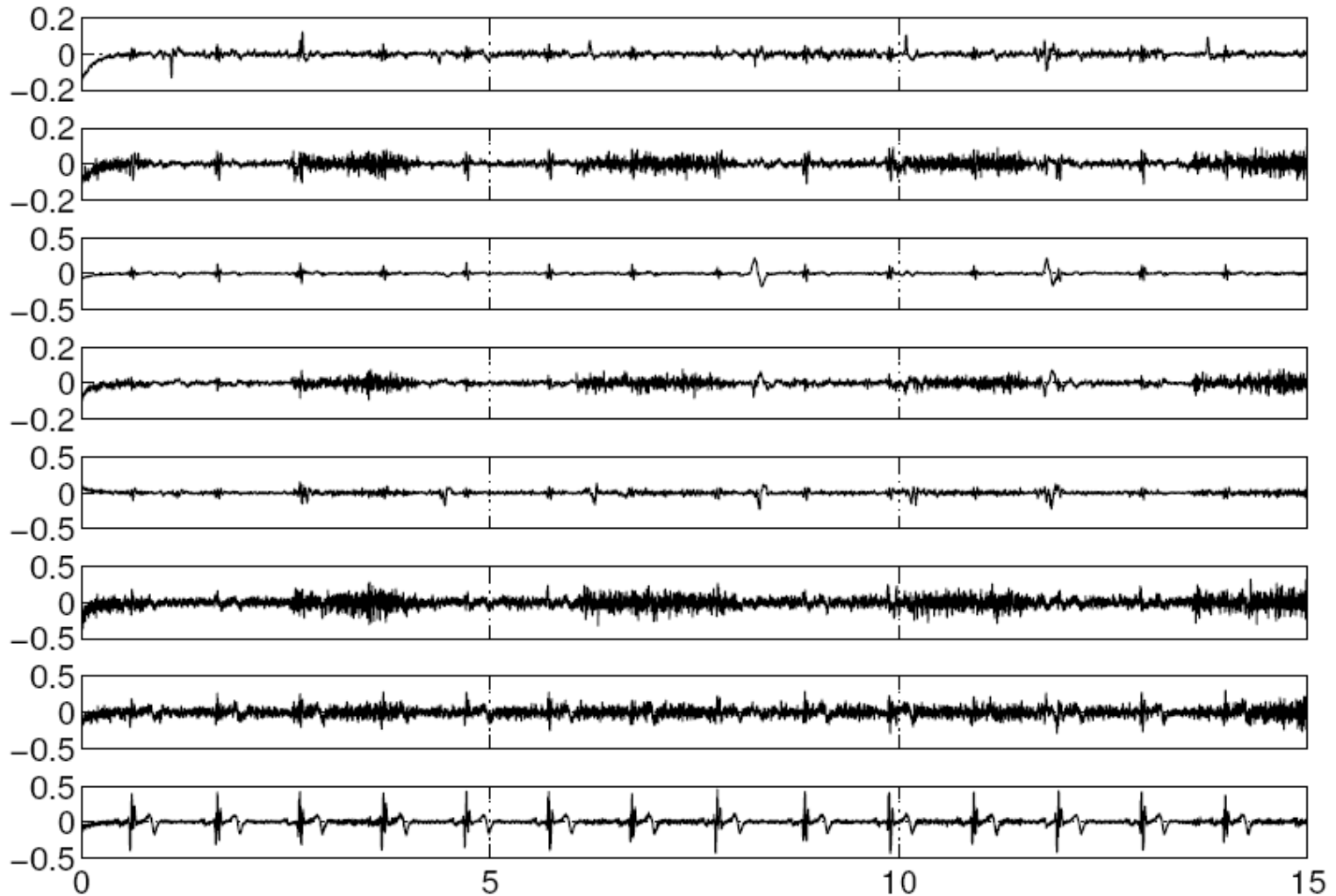
Removing ECG artifacts from diaphragm EMG



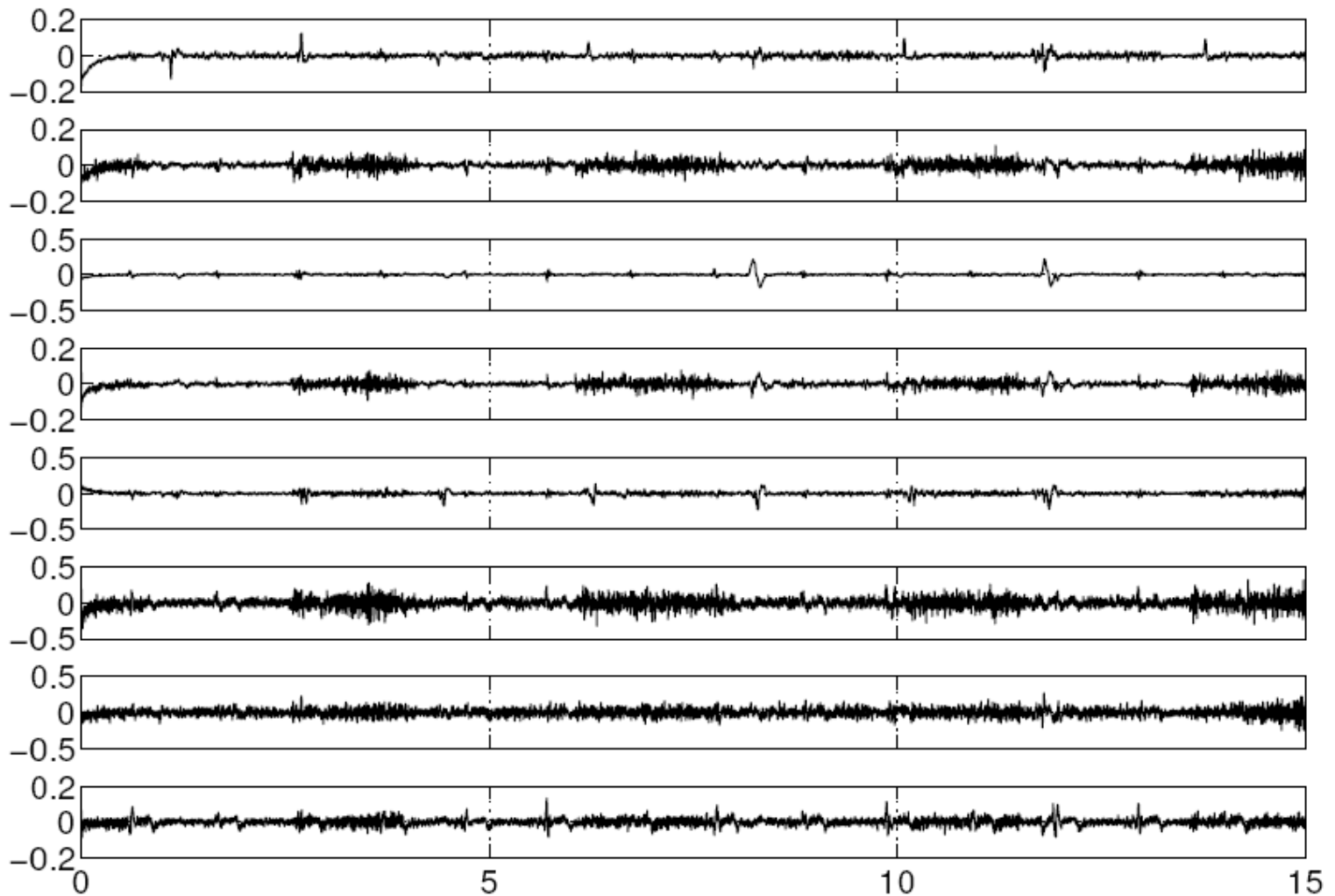
Proposed method: 1st iteration



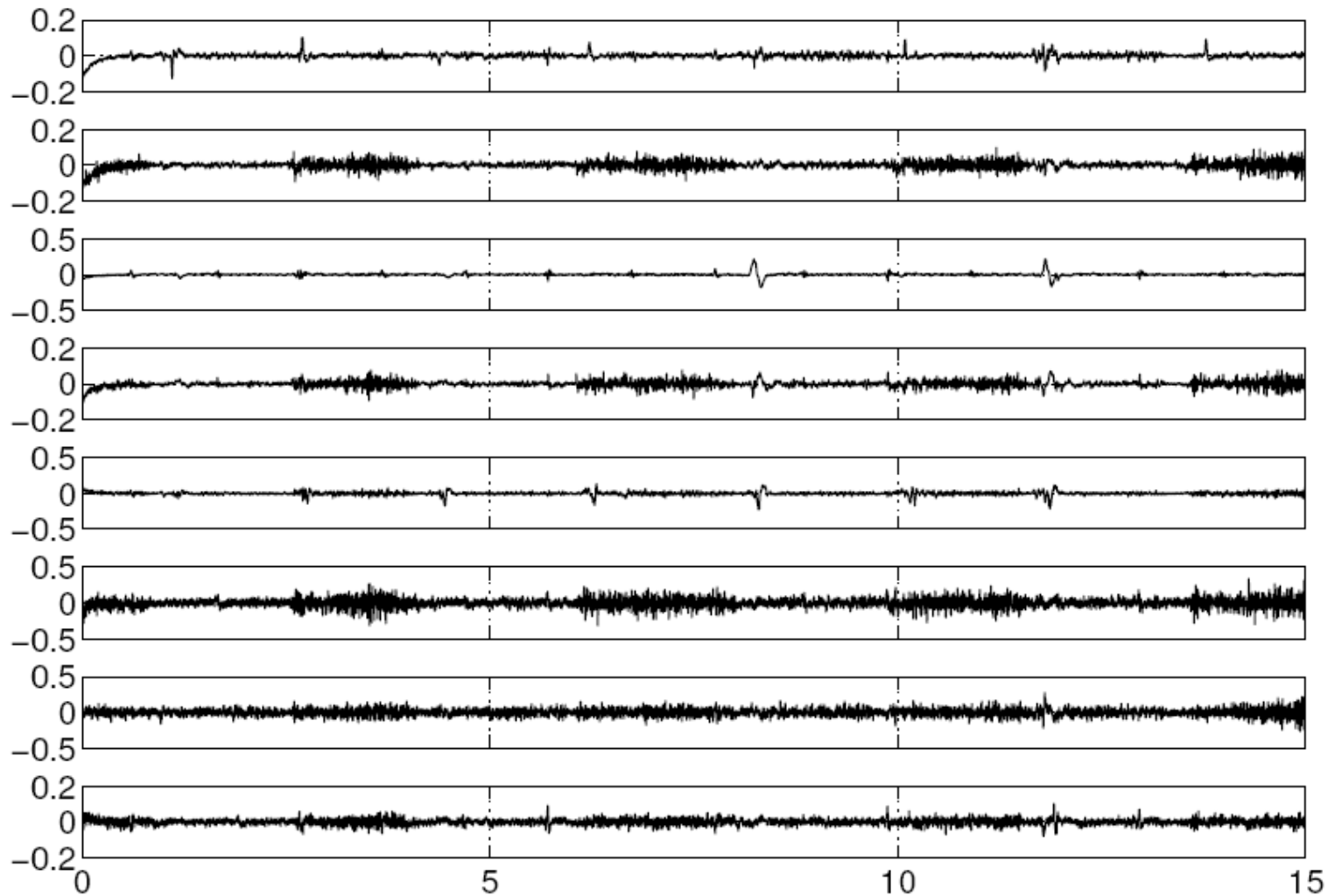
Proposed method: 2nd iteration



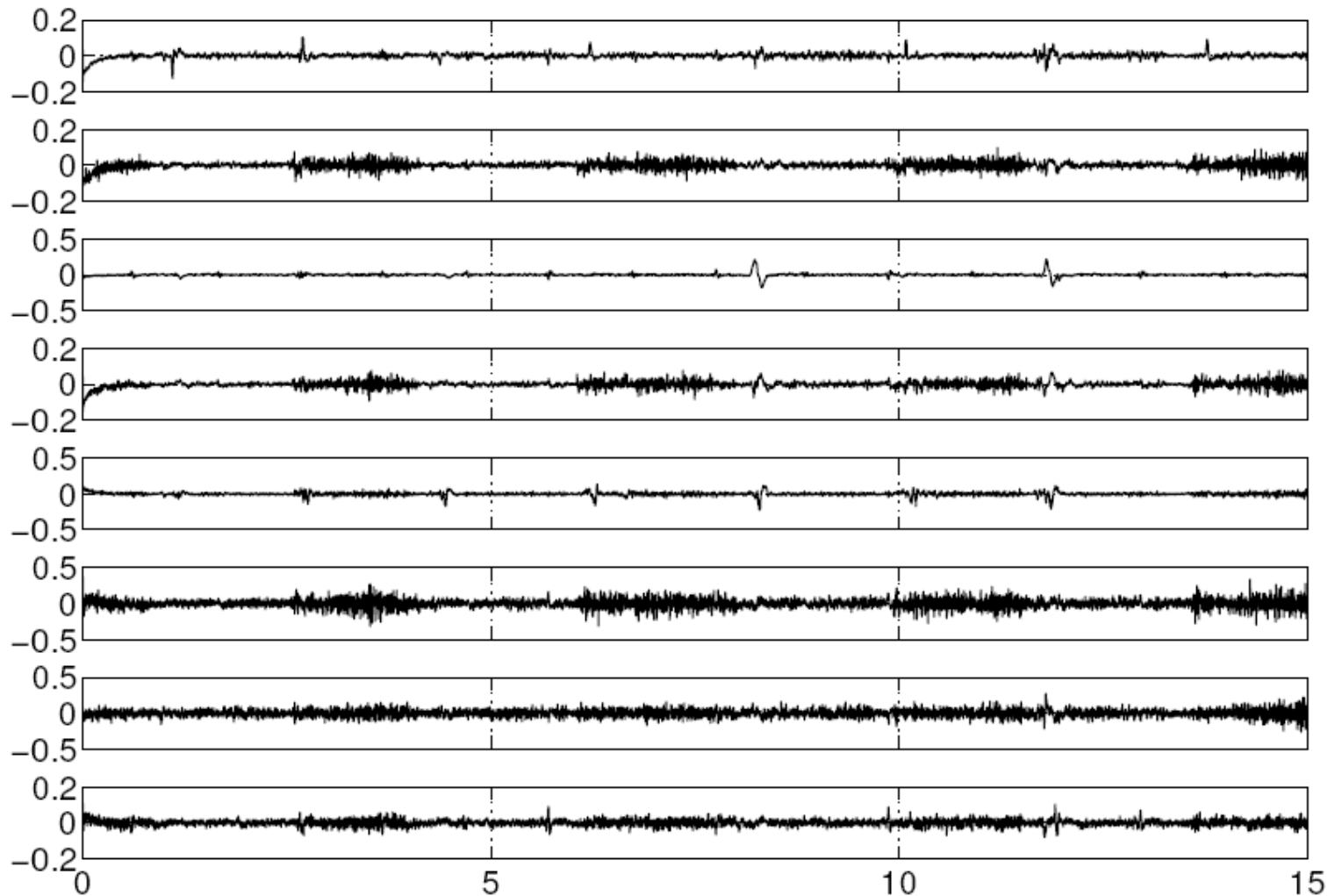
Proposed method: 3rd iteration



Proposed method: 4th iteration



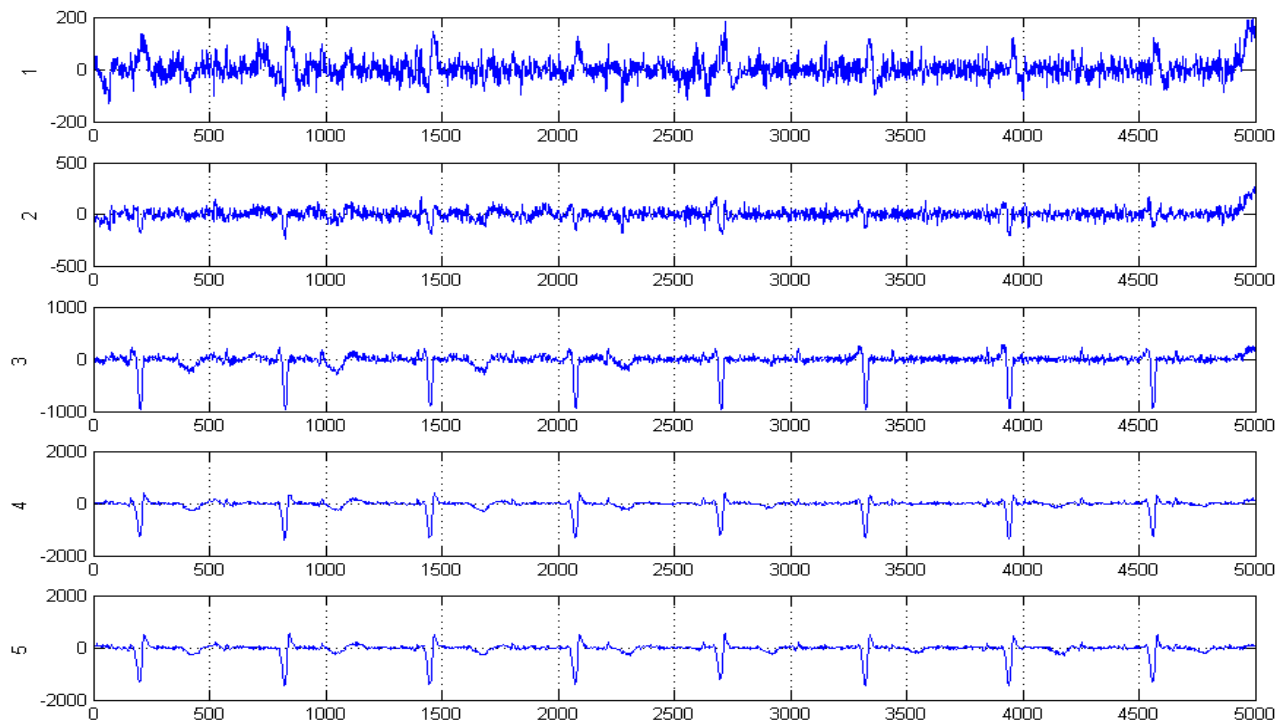
Proposed method: 5th iteration



Case Study 3

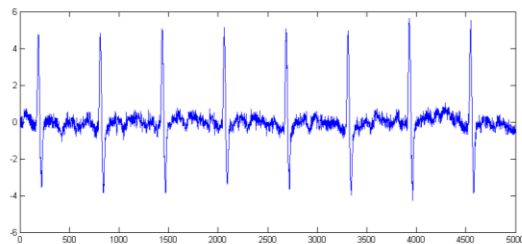
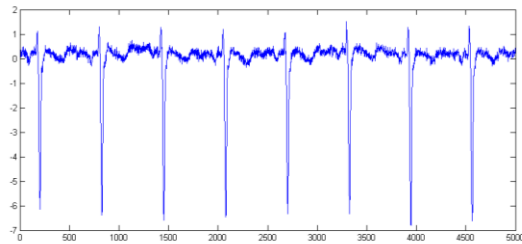
Extracting twin MCG signals from maternal MCG recordings

Typical Channels of the Original Data

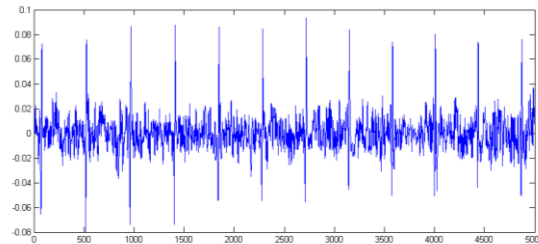


Case Study 3

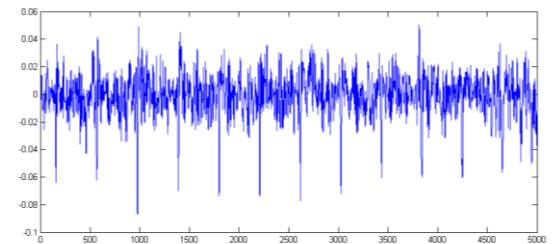
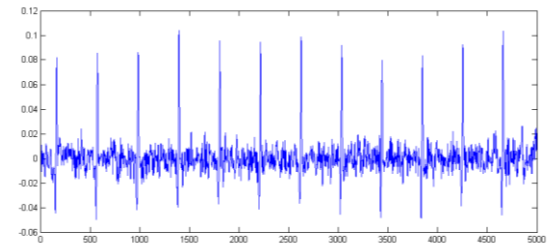
Maternal components



First fetus components

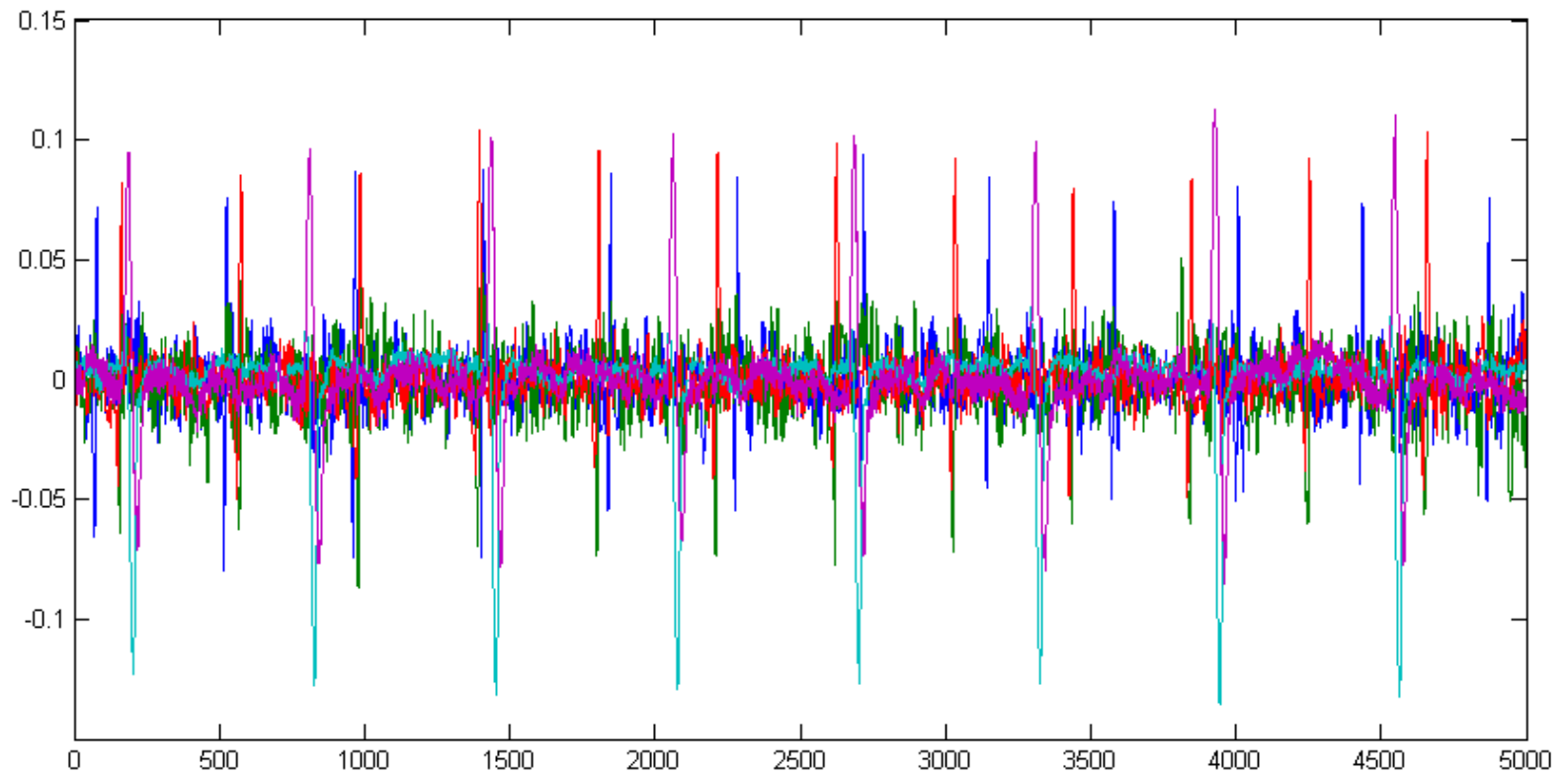


Second fetus components



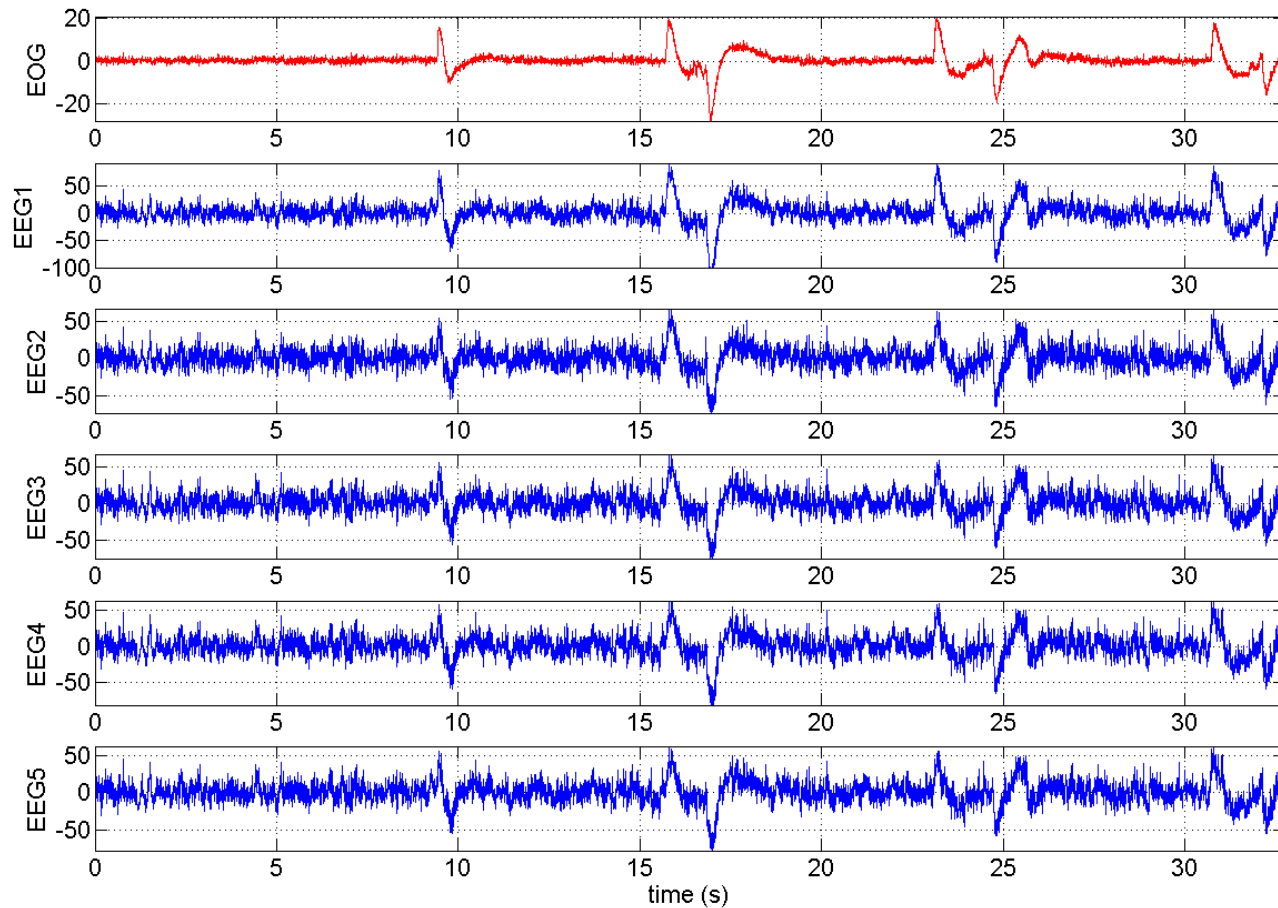
Case Study 3

All cardiac components



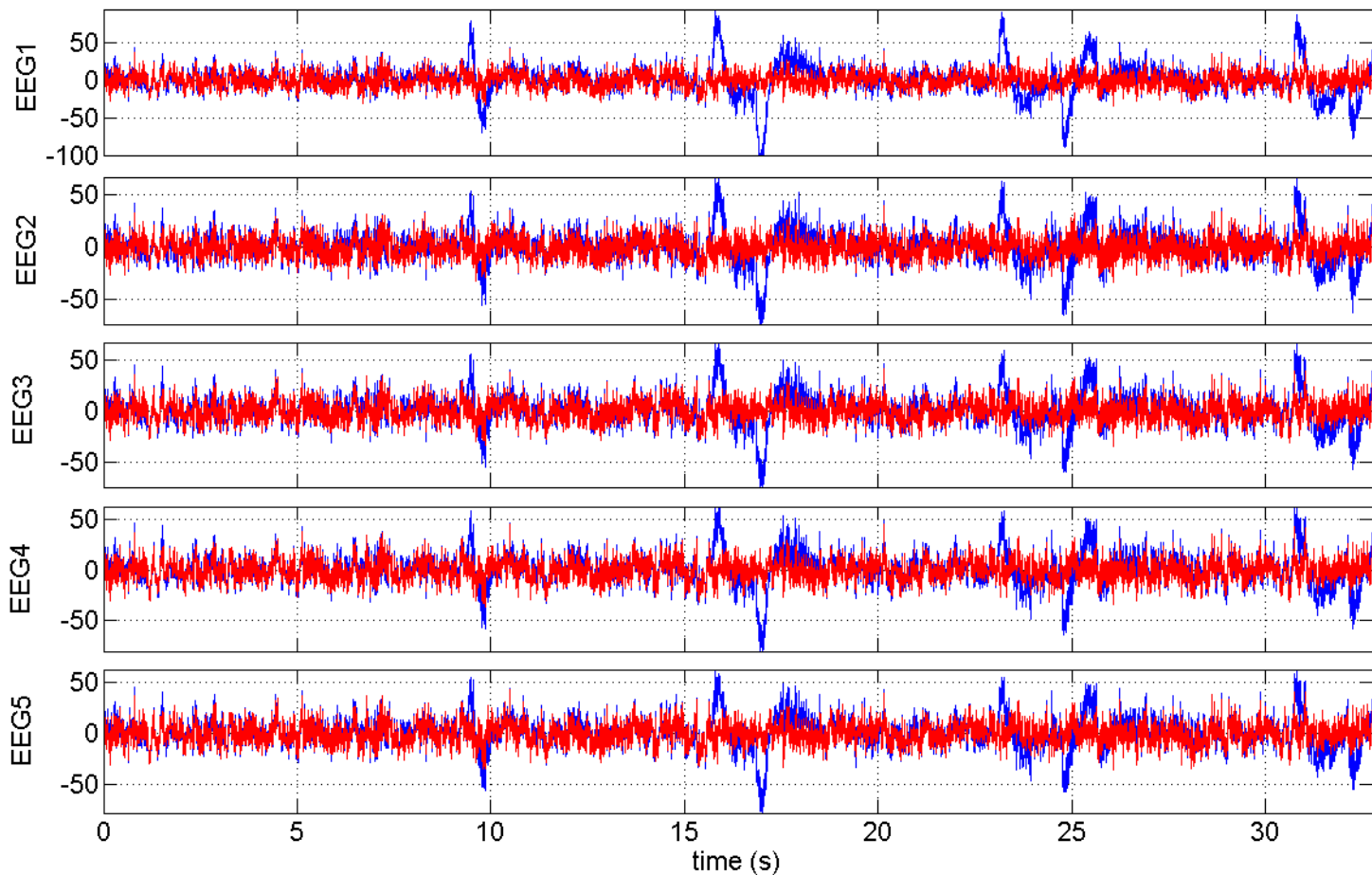
Case Study 4

Removing EOG artifacts from EEG recordings



Case Study 4

Using signal nonstationarity and wavelet denoising:



Overview

- Motivation
- Method
- Case Study
- Conclusion

Summary & Conclusions

- We proposed a method for the decomposition of signals within coplanar (intersecting) planes
- The method is a combination of linear and nonlinear methods
- The mutual information of the multichannels are gathered by the linear step, while the per-channel subspace separation is achieved by the nonlinear step
- The method does not have the limitations and drawbacks of linear decomposition methods
- It however requires *a priori* information about the nature of the desired and undesired subspaces

Periodic Component Analysis (PCA) Steps

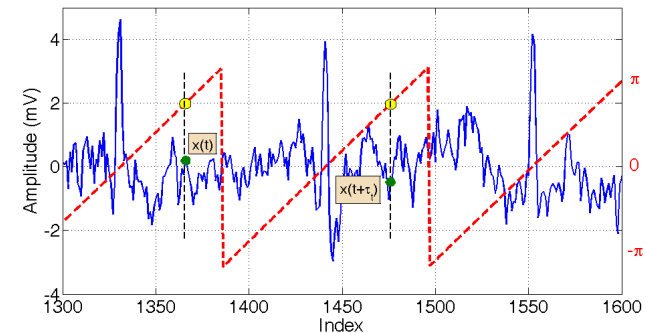
AMUSE ICA

- The cost function: $\epsilon(\mathbf{b}, \tau) = \frac{E_t\{(y(t + \tau) - y(t))^2\}}{E_t\{y(t)\}^2} \Rightarrow \text{GEVD}(C_x(\tau), C_x(0))$

Preprocessing (BW removal & denoising)

- R-peak detection

- Phase calculation



Time-varying cardiac period calculation

- Pseudo-covariance matrix calculation $\tau_t = \min\{\tau | \phi(t + \tau) = \phi(t), \tau > 0\}$

$$\tilde{C}_x = E_t\{\mathbf{x}(t + \tau_t)\mathbf{x}(t)^T\}$$

Generalized eigenvalue decomposition (GEVD)

$$\text{GEVD}(\tilde{C}_x, C_x(0))$$

11. Smart chemical sensor arrays



Objectives: modelization of a physical problem, NL models, priors

References: PhD dissertation and papers of Dr. Leonardo DUARTE, GIPSA-lab, Grenoble, Nov. 2009


11. Smart chemical sensor arrays



Part 1: Sparsity/nonstationary prior: one source is constant ([EUSIPCO 2008](#), Lausanne, Switzerland, Sept. 2008)

Part 2: Bayesian approach, with positivity prior ([ICA'2009](#), Paraty, Brasil, March 2009)

12. Removing showthrough in scanned images



Farnood Merrikh-Bayat, Massoud Babaie-Zadeh and Christian Jutten, *Adaptive Linear-quadratic Blind Source Separating Structure for Removing Show-through in Scanned Documents. To appear in 2010*

Removing show-through in scanned images

Problem

- Show-through, due to paper transparency and thickness,
- Pigment oil penetration,
- Vehicle oil component, due to loss of opacity,





Removing show-through in scanned images

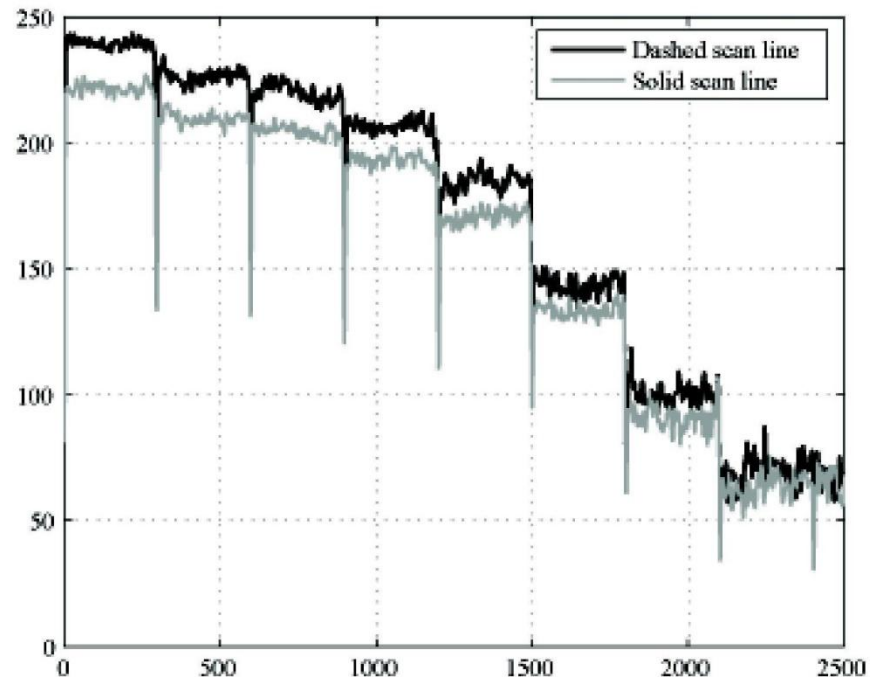
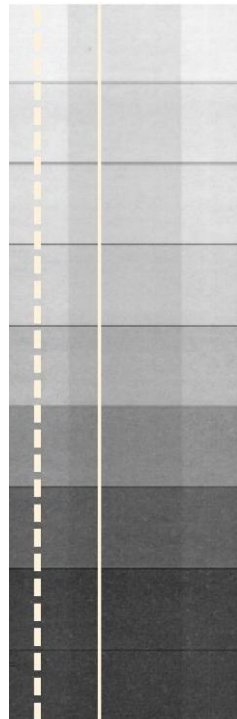
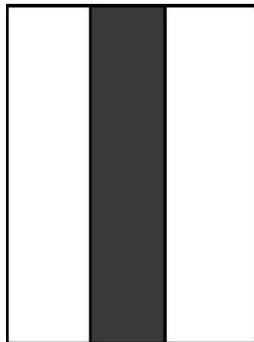
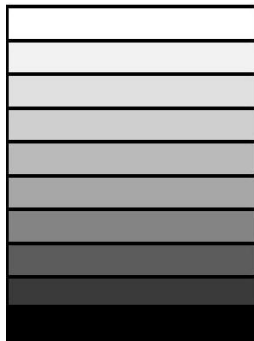
State-of-the-art

- Often applied for texts and handwriting documents,
- 1-side methods,
- 2-side methods,
- ICA assuming
 - Linear model of mixtures (Tonazzini et al., 2007 ; Ophir, Malah, 2007)
 - Nonlinear model of mixtures (Almeida, 2005 ; Sharma, 2001)
- In this work, we consider:
 - modelisation of the nonlinear mixture,
 - blurring effect.

Removing show-through in scanned images

Modeling the nonlinearity of show-through

- Evidence: sum of luminance is NL. Whiter the pixel, more important is show-through.



Removing show-through in scanned images

Modeling the nonlinearity of show-through

- Show-through has a gain which depends of the grayscale of the front image
- It leads to the model of mixtures:

$$\begin{cases} f_r^s(m,n) = a_1 f_r^i(m,n) + b_1 f_v^i(m,n) \times g_1(f_r^i(m,n)) \\ f_v^s(m,n) = a_2 f_v^i(m,n) + b_2 f_r^i(m,n) \times g_2(f_v^i(m,n)) \end{cases}$$

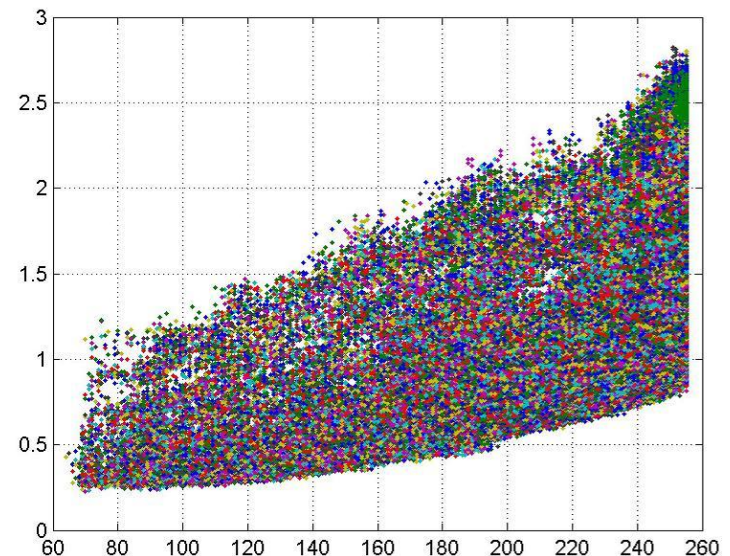
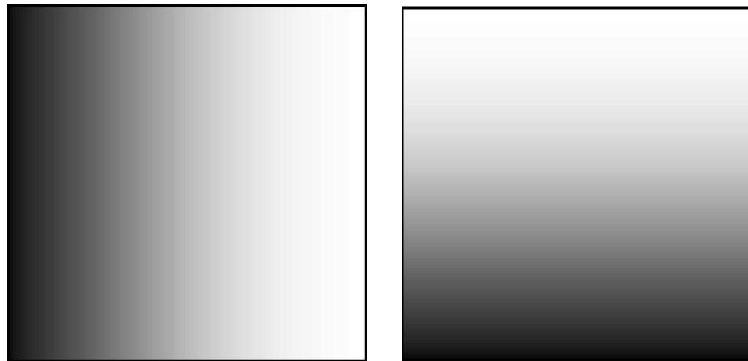
where i = initial, s = scanned, r = recto, v = verso, a_i, b_j are unknown mixing parameters, and g_k denote nonlinear gains

Removing show-through in scanned images

Shape of the nonlinear gain

- The gains can be estimated by drawing:

$$\begin{cases} g_1(f_r^i(m,n)) = [f_r^s(m,n) - a_1 f_r^i(m,n)] / b_1 f_v^i(m,n) \\ g_2(f_v^i(m,n)) = [f_v^s(m,n) - a_2 f_v^i(m,n)] / b_2 f_r^i(m,n) \end{cases}$$



Removing show-through in scanned images

Approximation of the nonlinear gain

- The gains can be approximated by and exponential:

$$\begin{cases} g_1(f_r^i(m, n)) = \gamma_1 \exp[\beta_1 f_r^s(m, n)] \approx \gamma_1 [1 + \beta_1 f_r^s(m, n)] \\ g_2(f_v^i(m, n)) = \gamma_2 \exp[\beta_2 f_v^s(m, n)] \approx \gamma_2 [1 + \beta_2 f_v^s(m, n)] \end{cases}$$

hence the following approximated mixing model:

$$\begin{cases} f_r^s(m, n) = a_1 f_r^i(m, n) + b'_1 f_v^i(m, n) [1 + \beta_1 f_r^i(m, n)] \\ f_v^s(m, n) = a_2 f_v^i(m, n) + b'_2 f_r^i(m, n) [1 + \beta_2 f_v^i(m, n)] \end{cases}$$

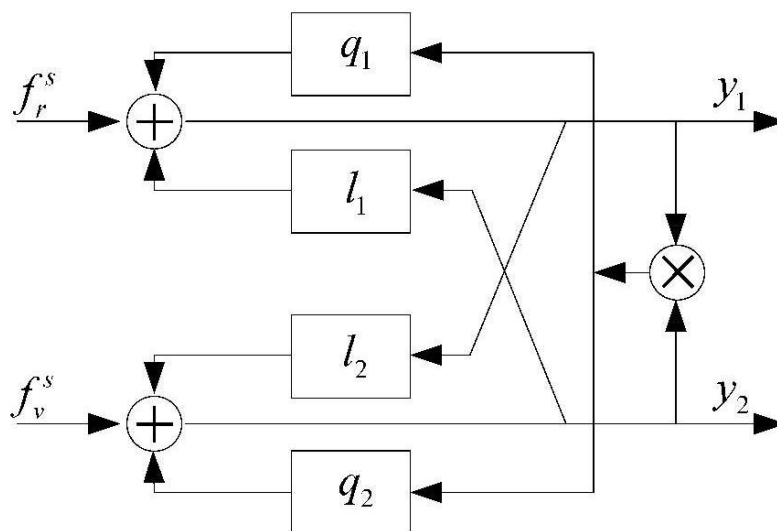
which can be written as a bilinear model:

$$\begin{cases} f_r^s(m, n) = a_1 f_r^i(m, n) - l_1 f_v^i(m, n) - q_1 f_v^i(m, n) f_r^i(m, n) \\ f_v^s(m, n) = a_2 f_v^i(m, n) - l_2 f_r^i(m, n) - q_2 f_r^i(m, n) f_v^i(m, n) \end{cases}$$

Removing show-through in scanned images

Recursive separation structure

- The bilinear mixture model has been studied by Deville and Hosseini (IWANN'03, ICA'04)

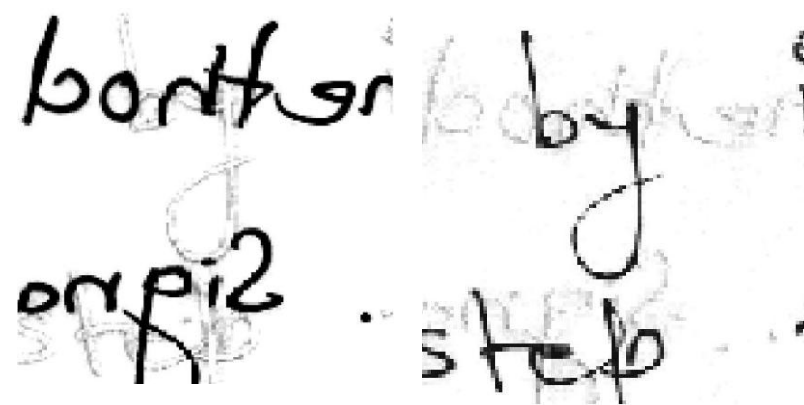
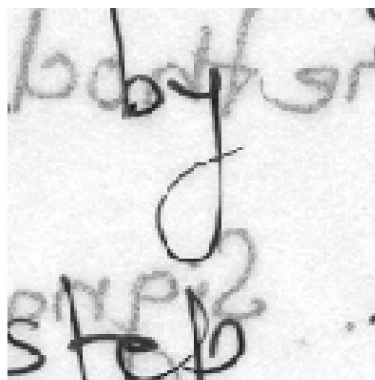
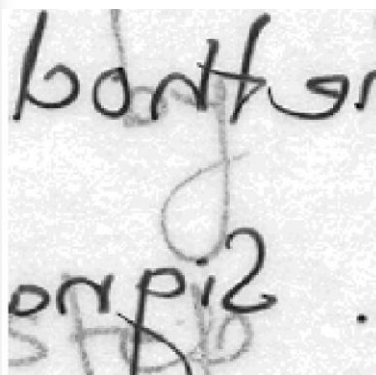
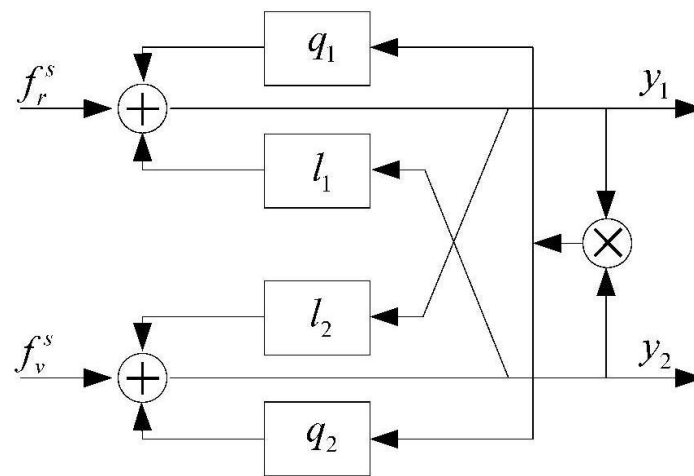


$$\begin{cases} f_r^s(m,n) = a_1 f_r^i(m,n) - l_1 f_v^i(m,n) - q_1 f_v^i(m,n) f_r^i(m,n) \\ f_v^s(m,n) = a_2 f_v^i(m,n) - l_2 f_r^i(m,n) - q_2 f_r^i(m,n) f_v^i(m,n) \end{cases}$$

Removing show-through in scanned images

Recursive separation structure

- The bilinear mixture model is:
 - Not always invertible,
 - Not always stable.
- Parameters are estimated by ML approach and lead to the following results





Removing show-through in scanned images

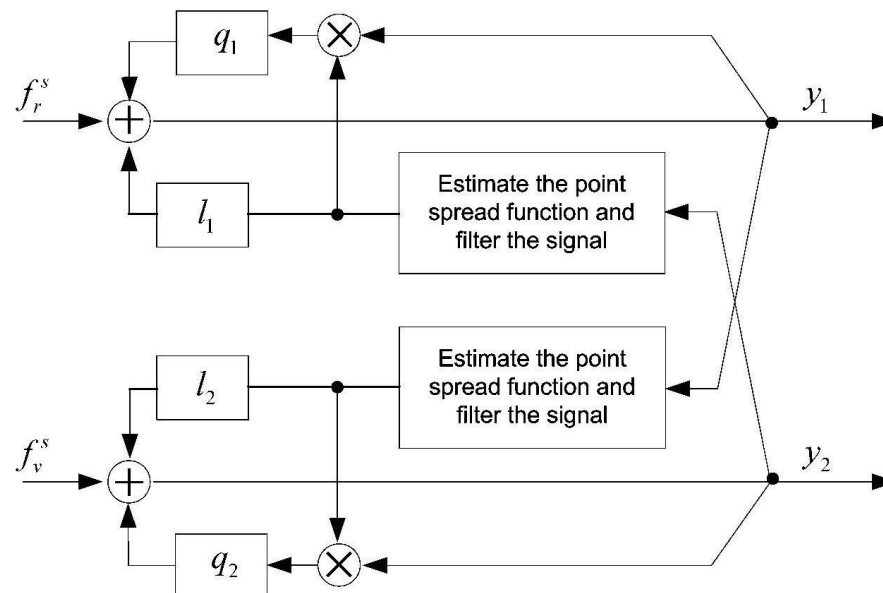
Recursive separation structure

- The results are not perfect: the other side image is never perfectly removed, especially where there is no superimposition.
- This means that, even without superimposition, difference between verso image and recto image is not a simple gain
- We assume that due to diffusion in the paper, there is a blurring effect, which can be modelled by a 2D filter

Removing show-through in scanned images

Final recursive separation structure

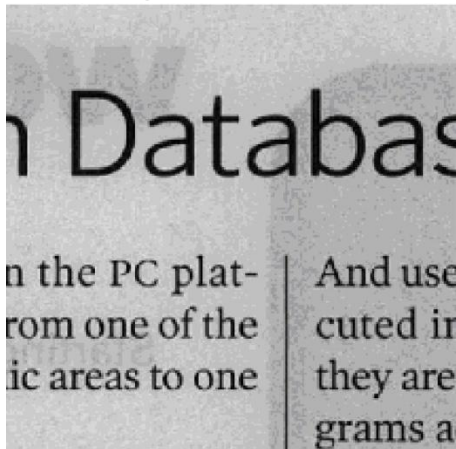
- The mixture is not the nonlinear superimposition of the recto image with the verso image, but with a **FILTERED** version of the verso image, hence the final separation structure



Removing show-through in scanned images

Results

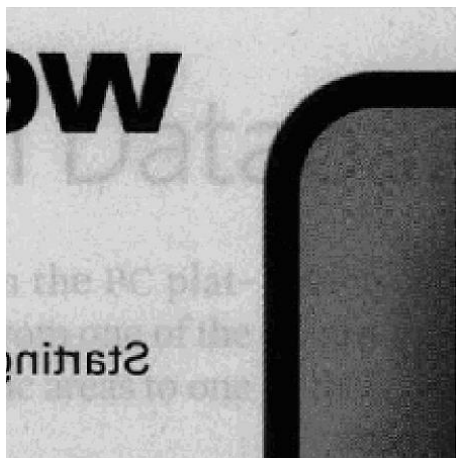
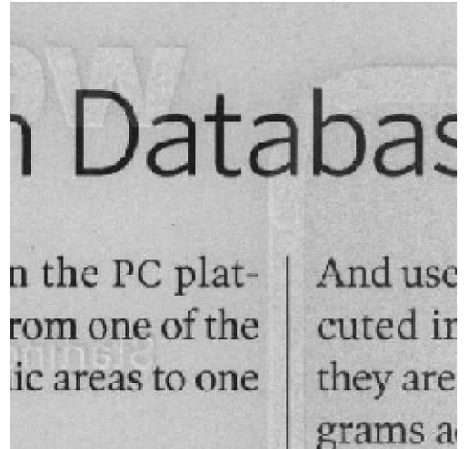
Images scannées



Estimées avec filtre



Estimées sans filtre





Scanned images: Conclusion and perspectives

- Show-through is a NL phenomenon which can be modeled by bilinear mixtures ;
- In addition, it is necessary to consider the blurring effect, which can be viewed as a 2-D filtering effect.
- Experimental results show the mixture model has to take into account both NL and convolutive effects.
- For avoiding registration due to the 2-side scanning, one can explore if two scans of the same side provide sufficient diversity
- Other priors, like positivity of images, and of the coefficients could be exploited, e.g. by NMF or Bayesian approaches



Final conclusion

- Blind source separation

- requires a few sensors (spatial diversity)
- required a relevant model of mixtures (linear, convolutive, nonlinear)

Without priors, source statistical independence is required: ICA

- Semi-blind separation

- *weak prior* (only qualitative) : source sparsity, coloration or non stationarity,
- other diversity: frequential (in frequencial bins), temporal or time-frequency

In that case, independence is not nécessaire: decorrelation is sufficient, and Gaussian source can be separated

- Applications in many domains

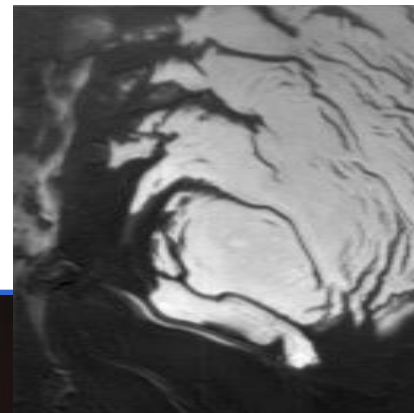
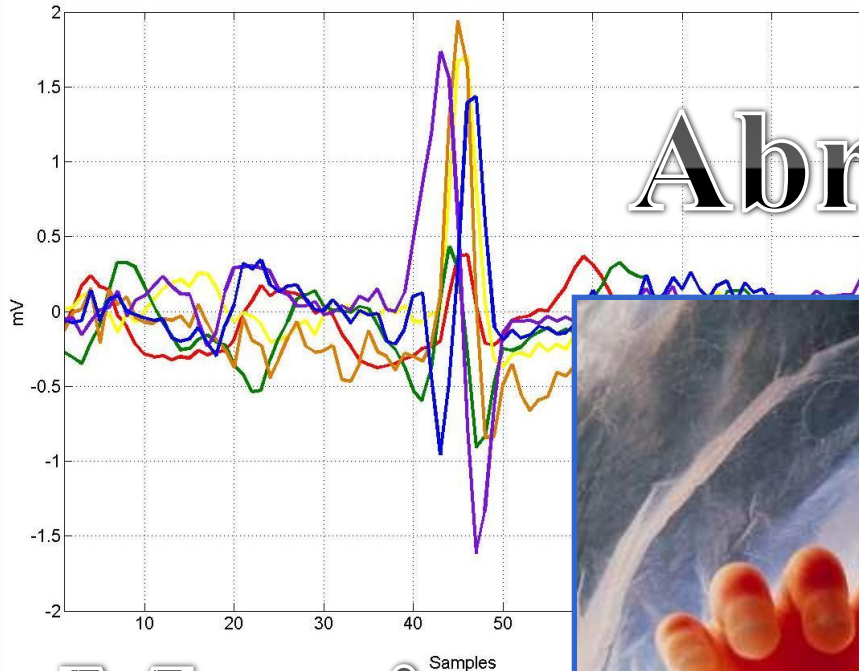
Play with source separation

- **ICA server:** <http://sig.enst.fr/~cardoso/icacentral/>
- **Demos and softwares:**
 - Linear and PNL mixtures, Deconvolution and Wiener systems:
http://www.lis.inpg.fr/demos/sep_sourc/ICAdemo/index.html
 - FastICA: <http://www.cis.hut.fi/projects/ica/fastica/>
 - Jade: <http://www.tsi.enst.fr/icacentral/Algos/cardoso/>
 - Comon's page: <http://www.i3s.unice.fr/~comon/>
 - Makeig's demos: <http://www.sccn.ucsd.edu/~scott/index.html>
 - T.W. Lee's demo: <http://www.sn1.salk.edu/~tewon/>

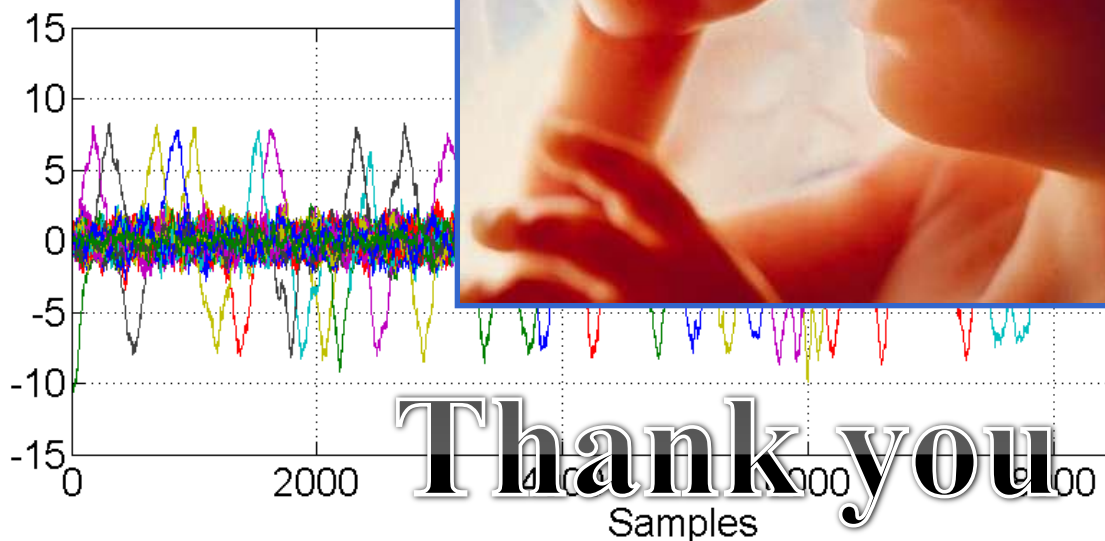
- **Books**

P. Comon, C. Jutten (Eds.) Handbook of blind source separation. Independent Component Analysis and Applications. Academic Press, Feb. 2010

Abrigado



Merci



Thank you

christian.jutten@gipsa-lab.grenoble-inp.fr

bonjour
on p12